

Cost Analysis of PEM Fuel Cell Systems for Transportation

September 30, 2005

E.J. Carlson, P. Kopf, J. Sinha, S. Sriramulu,
and Y. Yang
TIAX LLC
Cambridge, Massachusetts

Subcontract Report
NREL/SR-560-39104
December 2005

NREL is operated by Midwest Research Institute • Battelle Contract No. DE-AC36-99-GO10337



Cost Analysis of PEM Fuel Cell Systems for Transportation

September 30, 2005

E.J. Carlson, P. Kopf, J. Sinha, S. Sriramulu,
and Y. Yang

TIAX LLC

Cambridge, Massachusetts

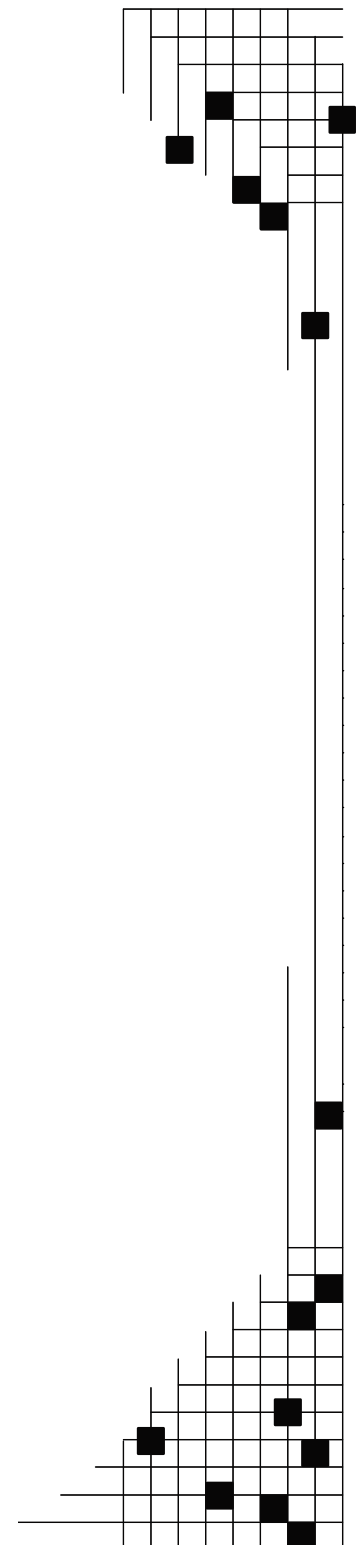
NREL Technical Monitor: K. Wipke

Prepared under Subcontract No. KACX-5-44452-01

Subcontract Report

NREL/SR-560-39104

December 2005



National Renewable Energy Laboratory

1617 Cole Boulevard, Golden, Colorado 80401-3393
303-275-3000 • www.nrel.gov

Operated for the U.S. Department of Energy
Office of Energy Efficiency and Renewable Energy
by Midwest Research Institute • Battelle

Contract No. DE-AC36-99-GO10337

**This publication was reproduced from the best available copy
Submitted by the subcontractor and received no editorial review at NREL**

NOTICE

This report was prepared as an account of work sponsored by an agency of the United States government. Neither the United States government nor any agency thereof, nor any of their employees, makes any warranty, express or implied, or assumes any legal liability or responsibility for the accuracy, completeness, or usefulness of any information, apparatus, product, or process disclosed, or represents that its use would not infringe privately owned rights. Reference herein to any specific commercial product, process, or service by trade name, trademark, manufacturer, or otherwise does not necessarily constitute or imply its endorsement, recommendation, or favoring by the United States government or any agency thereof. The views and opinions of authors expressed herein do not necessarily state or reflect those of the United States government or any agency thereof.

Available electronically at <http://www.osti.gov/bridge>

Available for a processing fee to U.S. Department of Energy
and its contractors, in paper, from:

U.S. Department of Energy
Office of Scientific and Technical Information
P.O. Box 62
Oak Ridge, TN 37831-0062
phone: 865.576.8401
fax: 865.576.5728
email: <mailto:reports@adonis.osti.gov>

Available for sale to the public, in paper, from:

U.S. Department of Commerce
National Technical Information Service
5285 Port Royal Road
Springfield, VA 22161
phone: 800.553.6847
fax: 703.605.6900
email: orders@ntis.fedworld.gov
online ordering: <http://www.ntis.gov/ordering.htm>



Table of Contents

TABLE OF CONTENTS	III
LIST OF TABLES	V
LIST OF FIGURES	VII
1. ABSTRACT	1
2. SUMMARY	2
3. INTRODUCTION	10
4. SUMMARY OF COST PROJECT RESULTS (1998-2004)	11
4.1. REFORMER BASED SYSTEM (2001)	11
4.2. SUMMARY OF KEY COST DRIVERS (2001 – 2004)	22
5. PROJECT OBJECTIVE, SCOPE, AND APPROACH	23
5.1. OBJECTIVE	23
5.2. SCOPE	23
5.3. APPROACH	24
6. MANUFACTURING COST MODEL DESCRIPTION	25
6.1. TECHNOLOGY-BASED COSTING METHODOLOGY	25
6.2. PEM FUEL CELL MANUFACTURING COST MODEL.....	26
6.2.1. <i>Overview</i>	26
6.2.2. <i>Cost Definition</i>	27
6.2.3. <i>Baseline Cost Model Description</i>	27
6.2.3.1. Definition of System Operating Parameters.....	28
6.2.3.2. Development of Subsystem and Component Design	28
6.2.3.3. Cost Analysis	29
6.2.4. <i>Sensitivity Analyses</i>	29
6.2.5. <i>Supply Chain Analysis</i>	31
7. DOE FUEL CELL SYSTEM TARGETS	33
8. SYSTEM ANALYSIS	34
8.1. INTRODUCTION.....	34
8.2. SYSTEM DESCRIPTION	34
8.3. SYSTEM PERFORMANCE RESULTS	36
8.3.1. <i>Stack Efficiency</i>	36
8.3.2. <i>System Parasitic Power Consumption</i>	38
8.4. SYSTEM EFFICIENCY	39
8.5. SYSTEM COMPONENT SIZING	39
8.5.1. <i>PEMFC Stack</i>	39
8.5.2. <i>Power Density Assessment</i>	39
9. COST ANALYSIS	41
9.1. INTRODUCTION.....	41
9.2. STACK.....	41
9.2.1. <i>Membrane</i>	43
9.2.1.1. Description.....	43
9.2.1.2. Manufacturing Process.....	45
9.2.1.3. Membrane Costing.....	49

9.2.2.	<i>Gas Diffusion Layer (GDL)</i>	52
9.2.2.1.	Description	52
9.2.2.2.	Manufacturing Process	52
9.2.2.3.	Costing	53
9.2.3.	<i>Bipolar plates</i>	54
9.2.3.1.	Description	54
9.2.3.2.	Manufacturing Process	55
9.2.3.3.	Costing	58
9.2.4.	<i>MEA</i>	60
9.2.4.1.	Description	60
9.2.4.2.	Manufacturing Process	61
9.2.4.3.	Costing	63
9.2.5.	<i>Gasket</i>	64
9.2.5.1.	Description	64
9.2.5.2.	Manufacturing Process	65
9.2.5.3.	Costing	66
9.2.6.	<i>Stack Assembly</i>	66
9.2.7.	<i>Stack Cost</i>	67
9.2.7.1.	Baseline Cost	67
9.2.7.2.	Single Variable Sensitivity Analysis	67
9.2.7.3.	Monte Carlo Simulation	69
9.2.7.4.	Stack Cost Comparison – 2004 vs. 2005	70
9.3.	QC AND STACK BURN-IN	71
9.4.	BOP	72
9.4.1.	<i>Air Management</i>	72
9.4.1.1.	Air Filtration	72
9.4.1.2.	Compressor-Expander	73
9.4.2.	<i>Water Management</i>	74
9.4.2.1.	Enthalpy Wheel Humidifier	75
9.4.2.2.	Membrane Humidifier	76
9.4.3.	<i>Thermal Management</i>	78
9.4.4.	<i>Fuel Management</i>	81
9.5.	SYSTEM COST	85
9.6.	SCENARIOS	88
9.6.1.	<i>Lower Platinum Price</i>	88
9.6.2.	<i>Inclusion of Value Chain Costs</i>	88
9.7.	STUDY RESULTS RELATIVE TO DOE TARGETS	89
10.	CONCLUSIONS AND RECOMMENDATIONS	91
10.1.	KEY DRIVERS	91
10.2.	OTHER FACTORS	92
10.3.	RECOMMENDATIONS	92
11.	ACKNOWLEDGEMENTS	94
12.	APPENDIX	95
12.1.	\$450/TROZ BASELINE COST SCENARIO	95
13.	REFERENCES	98

List of Tables

Table 1. Key Model Parameters.....	4
Table 2. Changes in Stack Materials Cost on an Area Basis from 2004 to 2005	7
Table 3. System Metrics Relative to DOE 2005 Targets.....	8
Table 4. Component List and Allocation to Subsystems.....	12
Table 5. 2001 Assumptions for the Reformer and Fuel Cell Stack	13
Table 6. Comparison of Hybridization Scenarios with a 120 kW ICE Base Case	17
Table 7. 2004 Stack Parameters Compared to 2001 Values.....	18
Table 8. Comparison of Cost of Reformate and Direct Hydrogen Systems.....	19
Table 9. Comparison of 50 kW and 80 kW Costs for the 2004 Systems	19
Table 10. DOE Targets	33
Table 11. Summary of the Stack Operating Conditions that Influence the System Design and Configuration of the 80 kWe PEMFC System.....	34
Table 12. Parameters Influencing the Stack Efficiency Estimation	37
Table 13. Parasitic Power Consumption in the System.....	38
Table 14. Stack Specifications and Performance Assumptions.....	42
Table 15. Stack Material Assumptions	42
Table 16. Stack Component Weight and Dimensions	43
Table 17. Membrane Material Parameters.....	48
Table 18. Membrane Process Parameters	48
Table 19. Membrane Material and Process Cost (on an active area basis).....	49
Table 20. Membrane Single Variable Sensitivity Analysis Data Range Table	50
Table 21. GDL Material Parameters.....	52
Table 22. GDL Process Parameters	53
Table 23. Material and Process Costs (on an active area basis)	54
Table 24. Bipolar Plate Material and Process Comparisons.....	54
Table 25. Graphite Foil Bipolar Plate Material Parameters.....	58
Table 26. Graphite Foil Bipolar Plate Process Parameters.....	58
Table 27. Graphite Foil Bipolar Plate Cost Break Down	59
Table 28. Compression Molded Bipolar Plate Cost.....	60
Table 29. Anode Material Parameters	63
Table 30. Cathode Material Parameters.....	63
Table 31. MEA Process Parameters.....	63
Table 32. MEA Cost Break Down.....	64
Table 33. Seal Material Parameters	66
Table 34. Gasket Molding Process Parameters.....	66
Table 35. Gasket Cost Break Down.....	66
Table 36. Stack Sensitivity Analysis Variable Ranges.....	68
Table 37. Stack Cost Comparison 2004 vs. 2005 (\$/m ²).....	70
Table 38. Stack Cost Comparison 2004 vs. 2005 (\$/kW).....	71
Table 39. Conditioning & QC Cost	71
Table 40. Key Characteristics of Honeywell CEM	73
Table 41. Comparison between Honeywell and TIAX Estimates for CEM Cost	74
Table 42. Weight/Volume Parameters of Enthalpy Wheel Humidifier	76
Table 43. Materials, Processes, and Costs for Humidicore Enthalpy Wheel	76

Table 44. Weight/Volume Parameters for Membrane Humidifier	77
Table 45. Comparison of TIAX and PermaPure Cost Estimate for Membrane Humidifier.....	78
Table 46. Key Characteristics of Thermal Management System	79
Table 47. Technical Specifications of High-Temperature Radiators.....	80
Table 48. Cost of High-Temperature Radiators for 40°C Ambient Temperature	80
Table 49. Characteristics of H ₂ Ejector.....	83
Table 50. Characteristics of Recirculating Blower Assembly.....	84
Table 51. Comparison Between 2004 and 2005 System Costs	85
Table 52. Parameter Values for the System Cost Sensitivity Analysis	86
Table 53. Low Platinum Price Scenario	88
Table 54. Value Chain Cost Calculation.....	89
Table 55. Summary of 2005 PEMFC System Results.....	90

List of Figures

Figure 1. Overall System Configuration with Major Components.....	4
Figure 2. Breakdown of System Cost for an 80 kW Direct Hydrogen Fuel Cell System (\$108/kW, \$8,640) Produced at 500,000 Units per Year	5
Figure 3. Breakdown in Stack and BOP Component Cost Contributions for an 80 kW Direct Hydrogen Fuel Cell System (\$108/kW, \$8,640)	5
Figure 4. Cost Breakdown for a 2005 80 kW Direct Hydrogen Stack (\$67/kW, \$5,360). 6	
Figure 5. Range in System Cost due to Uncertainty in Input Parameters.....	7
Figure 6. System Configuration Used in 2001 Reformer – Fuel Cell System Cost Projection.....	11
Figure 7. Thermally integrated reformer design used to cost the fuel processor including ATR, high and low temperature shift beds, burner and steam generation tubes	12
Figure 8. 2001 Reformer Based System Cost Breakdown (system cost of \$324/kW)....	14
Figure 9. 2001 Fuel Cell System Cost Breakdown.....	15
Figure 10. Stack and MEA Cost Breakdown for the 2001 System Configuration.....	15
Figure 11. Direct Hydrogen System for 2004 Cost Update.....	16
Figure 12. Cost of Compressed Hydrogen Storage Scenarios.....	17
Figure 13. Stack Cost Versus Platinum Loading for Reformate and Direct Hydrogen Stacks	21
Figure 14. Stack Cost versus Ohmic Resistance.....	22
Figure 15. Scope of 2005 PEMFC Costing	24
Figure 16. 2005 Cost Project Approach.....	24
Figure 17. Manufacturing Cost Model Schematic.....	26
Figure 18. Cost Elements of Detailed Cost Build-up	27
Figure 19. Approach to PEMFC System Cost Model.....	28
Figure 20. Graphite Foil Bipolar Plate Manufacturing Flow Chart.....	29
Figure 21. Example of Single Variable Sensitivity Analysis	30
Figure 22. Example of Monte Carlo Sensitivity Analysis	31
Figure 23. Illustrative Automotive PEMFC Supply Chain.....	32
Figure 24. PEMFC System Layout.....	35
Figure 25. Comparison of the Required Flow from the Ejector versus the Actual Flow Estimated for the Chosen Ejector Design.....	36
Figure 26. Stack Efficiency as a function of the purge rate from the anode recycle loop for single cell operating voltage of 0.7 V. Comparable results are obtained for 0.65 V operation.	37
Figure 27. Nitrogen concentration in the anode stream as a function of the stack power output (which is given as a fraction of the rated power). S1 corresponds to 0.7 V single cell voltage and S3 to 0.65 V.....	38
Figure 28. Efficiency of the 80 kW PEMFC system as a function of the rated power. S1 corresponds to 0.7 V single cell voltage, S2 to 0.65 V (base case) and S3 to 0.6 V.	39
Figure 29. 2005 Stack Design.....	43
Figure 30. Nafion Membranes Structure	46
Figure 31. Membrane Manufacturing Process Flow.....	47
Figure 32. Membrane Cost Breakdown Pie Chart	49
Figure 33. Membrane Single Variable Sensitivity Analysis Tornado Chart	50
Figure 34. DuPont, GM, and TIAX Membrane Cost Comparison.....	51
Figure 35. GDL Manufacturing Process Flow Chart.....	52

Figure 36. Grafcell [®] Production Process from GrafTech Website	55
Figure 37. U.S. Patent 3,404,061 Flexible Graphite Web Process	56
Figure 38. Embossing a Sheet of Flexible Graphite Material.....	56
Figure 39. Graphite Foil Bipolar Plate Process Flow	57
Figure 40. Graphite Foil Process Cost Bar Chart	59
Figure 41. Compression Molded Bipolar Plate Process Flow	60
Figure 42. Framing Seal Structure (U.S. Patent No. 6,716,550)	61
Figure 43. Framing Seals Layout (U.S. Patent No. 6,716,550).....	61
Figure 44. MEA Structure.....	61
Figure 45. MEA with Frame Seals Manufacturing Process Flow	62
Figure 46. U.S. Patent 5,284,718, A Top View of Gasket Grooves in Bipolar Plate.....	65
Figure 47. U.S. Patent 5,284,718, A Top View of a Sealing Gasket.....	65
Figure 48. Stack Assembly Flow Chart	67
Figure 49. Stack Baseline Cost (\$/kW).....	67
Figure 50. Single Variable Sensitivity Analysis Tornado Chart.....	68
Figure 51. Stack Cost Monte Carlo Simulation Sensitivity Chart	69
Figure 52. Stack Cost Monte Carlo Simulation Frequency Chart	69
Figure 53. Fuel Cell Stack and BOP	72
Figure 54. (a) Honeywell Fuel Cell Turbo-Compressor with Mixed-Flow Compressor and VNT [®] Variable Nozzle Turbine, (b) Honeywell Fuel Cell Turbo-Compressor Motor Controller	73
Figure 55. Humidicore Enthalpy Wheel Humidifier from Emprise	75
Figure 56. Membrane Humidifier from PermaPure.....	77
Figure 57. Typical Arrangement of Radiators in Fuel Cell Vehicle.....	79
Figure 58. Fuel Management System	81
Figure 59. Zones of Operation of the Blower and Ejector.....	81
Figure 60. Optimum Purge Rate for Cell Voltage of 0.7 V	82
Figure 61. Ejector-Venturi Operating Principle.....	83
Figure 62. (a) Croll-Reynolds' Schematic of Multiple Ejectors in Series, (b) Ejector from Elmridge.....	83
Figure 63. Hydrogen Recirculating Blower from H ₂ Systems, Inc.	84
Figure 64. Stack and BOP Contributions to System Cost	85
Figure 65. Detailed Breakout of System Cost	86
Figure 66. Parametric Studies on System Cost.....	87
Figure 67. Monte Carlo Analysis on System Cost.....	87
Figure 68. Illustrative Automotive PEMFC Supply Chain.....	89
Figure 69. Breakdown of System Cost for an 80 kW Direct Hydrogen Fuel Cell System (88 \$/kW, \$450/troz platinum price) Produced at 500,000 Units per Year	95
Figure 70. Breakdown in Stack and BOP Component Cost Contributions for an 80 kW Direct Hydrogen Fuel Cell System (\$88/kW, \$450/troz platinum price).....	95
Figure 71. Cost Breakdown for 2005 80 kW Direct Hydrogen Stack (\$48/kW, \$450/troz platinum price).....	96
Figure 72. Range in Stack Cost due to Uncertainty in Input Parameters (\$450/troz platinum price).....	96
Figure 73. Range in System Cost due to Uncertainty in Input Parameters (\$450/troz platinum price).....	97

1. Abstract

The successful commercialization of PEM fuel cells in transportation markets requires that the technology be competitive with internal combustion engine powertrains with regard to performance and cost, while meeting efficiency and emissions targets. TIAX has been working with the U.S. Department of Energy (DOE) since the late 1990s to assess the cost of PEM fuel cell systems using near-term technology as a basis, but cost modeled at high-production volumes. Integral to this effort has been the development of a system configuration in conjunction with Argonne National Laboratories (ANL), the specification of performance parameters and catalyst requirements, the development of representative component designs and manufacturing processes for these components, and the development of a comprehensive bill of materials and list of purchased components. The model, data, component designs, and results have been refined on the basis of comments from the FreedomCAR Technical Team and fuel cell system and component developers.

In 2005, the cost of an 80 kW direct hydrogen fuel cell system was assessed relative to the DOE 2005 target of \$125/kW. This system includes the fuel cell stack and balance-of-plant (BOP) components for water, thermal, and fuel management. Hydrogen storage is not included in this target. In this report, we provide a comprehensive description of the assumptions, approach, and final results of the 2005 PEMFC costing effort. The results of sensitivity and Monte Carlo analyses on components and the overall system are presented including the most important cost factors and the uncertainty in the fuel cell system cost projection given the model assumptions. The effects of selected scenarios on the fuel cell system cost (\$/kW) were assessed, including the effect of platinum price and the effect of individual component markups on overall system cost. The results of these analyses are presented and their implications discussed.

2. Summary

Background

The critical role that performance and cost play in the commercialization of fuel cell powertrains led DOE to initiate several studies beginning in 1998 to develop projections of fuel cell technology costs at high production volumes. The results of these assessments would provide DOE with:

- Metrics to track the status of current technology and project the impact of future developments on system cost
- A quantitative cost and technology framework supported by well documented design, performance, and material cost assumptions with which to conduct discussions with car makers and component developers on cost and performance targets
- Insights into gaps in available technology and into areas in need of cost reduction for R&D portfolio planning

This report presents the 2005 results and provides a high-level summary of TIAX's findings since the project inception.

Objective

In 2005, the focus of the project was to update the cost projection and compare it with the DOE target of \$125/kW for the fuel cell subsystem and BOP systems for air, water, thermal, and fuel management. Hydrogen storage, power electronics, electric drive motor, and hybrid batteries were excluded from the scope of this project.

Approach

The approach starts with a technology assessment of the system configuration and component technologies, leading to a bill-of-materials (BOM) for the system. For the stack components, bottom-up, activities-based costing methods were used to develop high-level cost projections for the material and process costs. For the BOP components, we worked with suppliers to obtain cost projections, which were then calibrated against our experience with similar technologies. Our preliminary estimates for the cost and system configuration, along with key design, cost, and process assumptions, were then presented to the car companies and material developers for their feedback. Sensitivity and Monte Carlo methods were used to identify key cost drivers and estimate the uncertainty in the results.

Critical Factors

Cell Voltage

As in any analysis with a large number of parameters and design options, the assessment involved a number of design decisions relative to tradeoffs among performance, cost, and efficiency. For purposes of cost reduction and integration of the fuel cell system into the vehicle, the designer needs to minimize the size, weight, and cost of the system, while for fuel conservation one needs to maximize efficiency. Unfortunately, these goals are in conflict. Increasing the cell voltage at rated power, e.g., to 0.8 volts, increases efficiency but also increases the stack size, weight, and cost. Designing for long life may also increase system cost through increased loadings of valuable materials such as platinum.

In the 2005 project, the Fuel Cell Tech Team recommended the use of 0.65 volts for the cell voltage at rated power to reduce stack size and cost.

Platinum Price

We were also faced with the selection of a platinum price for the baseline analysis. A dilemma arises from the current high in platinum prices (\$900/troz) relative to the historically constant price of \$450/troz. Use of the lower value allows easier comparison with the results of previous projections, while use of the current price allows one to see the impact of high prices. We have used today's price for the baseline case while using the sensitivity analysis to capture the impact of uncertainty in these values.

Power Density and Platinum Loading

Power density on an active area basis and platinum loading are additional key parameters that drive the cost and size of the stack. We searched the literature and approached the industry for comments to identify the most likely values for the baseline case and reasonable upper and lower limits. The literature provides single cell results but little information on values for current stack designs with reasonable lifer, for example, power density without platinum loading. For the baseline costs, we assumed a total platinum loading of 0.75 mg/cm² and a power density of 600 mW/cm² at 0.65 volts.

Vertically Integrated Process vs. Outsourcing of Stack Components

We continued to use a vertically integrated process for the manufacture of the stack components; however because the component markups over manufacturing cost in the value chain are not captured in this approach it led to a minimum cost estimate. In the case of the stack, with the integrator purchasing most of the components (membrane electrode assemblies (MEAs), gas diffusion layers, and bipolar plates), the markup could increase the projected cost of the stack by 20 percent to 50 percent. In our model, we treat the BOP components as purchased items and include markups in their cost contribution.

Quality Control

We have not included the cost of quality control into the current projection, partly because effective QC metrics are still under development and because current manufacturing processes are highly proprietary. High-level estimates were made for the impact of stack burn-in and performance characterization. For example, a 2 hour burn-in could raise the stack cost by 3%.

All these factors will clearly increase the manufacturing cost of the system. As production volumes increase and component manufacturers accumulate experience, the cost of items, such as quality control, will decline.

System Description

When this project started in 1998 the baseline system was a 50 kW net electric PEMFC system with a fuel flexible reformer. With the transition from the Partnership for a New Generation of Vehicles (PNGV) to the FreedomCAR program, the focus shifted to direct hydrogen fueled systems and the rated power of the fuel cell system increased to 80 kW to better reflect the current practice of car companies. The peak and transient power of this system may be further enhanced by hybridization with batteries. Similar to earlier

work, a PEMFC stack operating at 80°C and 2.5 atm at rated power is used. In addition to the stack, the system includes components to humidify the anode and cathode streams, heat exchangers to cool the stack, and a blower to recirculate hydrogen in the anode loop. Figure 1 shows the overall system. Unlike earlier work, our cost assessment of the system does not include any fuel storage or fuel generation components.

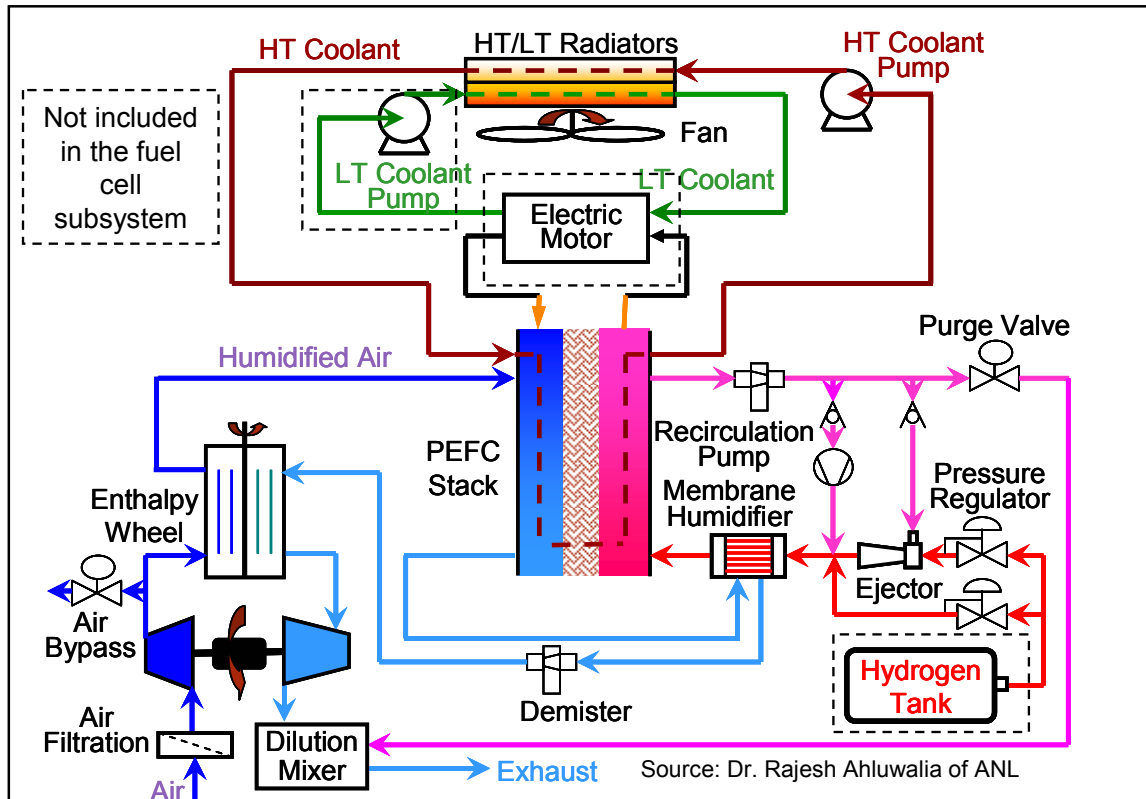


Figure 1. Overall System Configuration with Major Components

Key Findings

A PEMFC for transportation produced at high volume but based on today's technology has a projected manufactured cost below the \$125/kW target. Figure 2 shows the breakdown of the total cost of \$108/kW between the stack, BOP, and assembly. All \$/kW costs are given on a dollar per net power basis. Key assumptions in this projection are summarized in Table 1.

Table 1. Key Model Parameters

Parameter	Units	2005	2004
Power Density	mW/cm ²	600	350
Cell Voltage	Volts	0.65	0.7
Net Power	kW	80	80
Gross Power	kW	90	88
Production Volume	Units/year	500,000	500,000
Platinum Loading	mg/cm ²	0.75	0.3
Platinum Cost	\$/troz	900	450

Significant changes in parameter values included an increase in power density due to performance improvements and a decrease in the design cell voltage, an increase in platinum loading to represent current practice in stacks, and an increase in platinum cost to reflect current pricing.

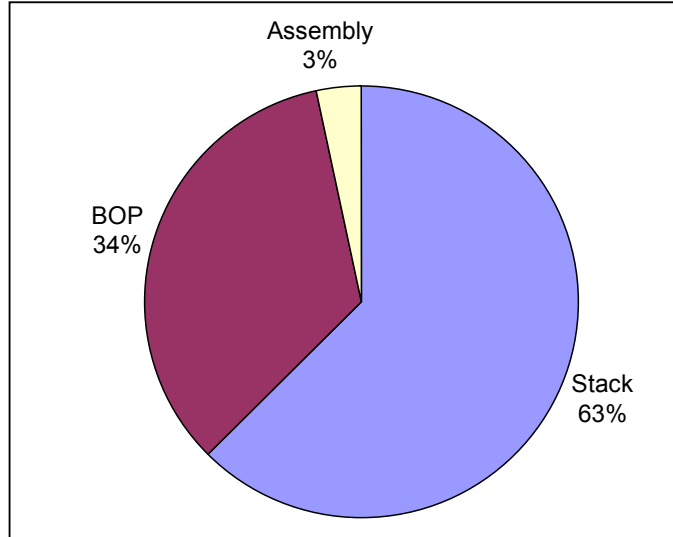


Figure 2. Breakdown of System Cost for an 80 kW Direct Hydrogen Fuel Cell System (\$108/kW, \$8,640) Produced at 500,000 Units per Year

Figure 3 shows the split between the stack and BOP costs with the stack contributing approximately 63 percent. After the stack, the compressor-expander module (CEM), membrane humidifier, and carbon materials are the most important cost contributors.

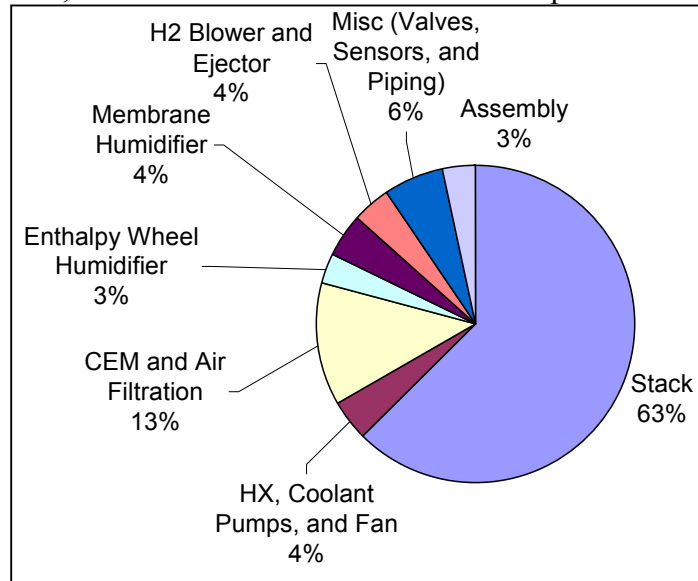


Figure 3. Breakdown in Stack and BOP Component Cost Contributions for an 80 kW Direct Hydrogen Fuel Cell System (\$108/kW, \$8,640)

Figure 4 shows the breakdown in the stack costs for 2005. The electrode contribution dominates because of the increased platinum loading and price, while the other components decreased in percent contribution and in cost per area because of reductions in material costs and the amount of material (thinner layers). The report details these changes. The top three cost drivers for the stack and the system are:

- Power density
- Platinum cost
- Platinum loading

Power density drives the size of the overall stack, while the product of platinum cost and loading determines the cost of the electrodes, the largest stack cost. Single cell power densities in the literature are higher than the selected value, but these values are derated in the stack to minimize hot spots and degradation. Increases in platinum cost and loading offset the decreases in other cell components and the increase in power density.

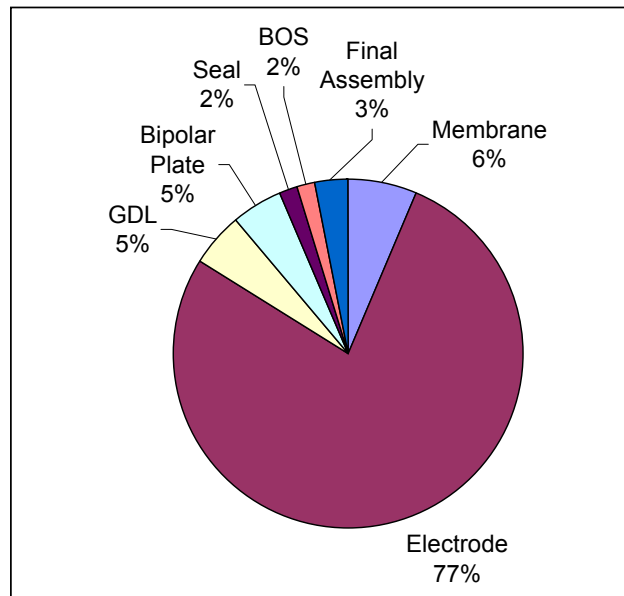


Figure 4. Cost Breakdown for a 2005 80 kW Direct Hydrogen Stack (\$67/kW, \$5,360)

A number of factors contribute to the system cost and Figure 5 shows the results of a Monte Carlo simulation to assess the effect of uncertainty in these parameters. The minimum, maximum, and most likely values are contained in the body of the report. For the range of input parameters considered, the analysis shows 98% certainty that the mean system cost is below the DOE target of \$125/kW.

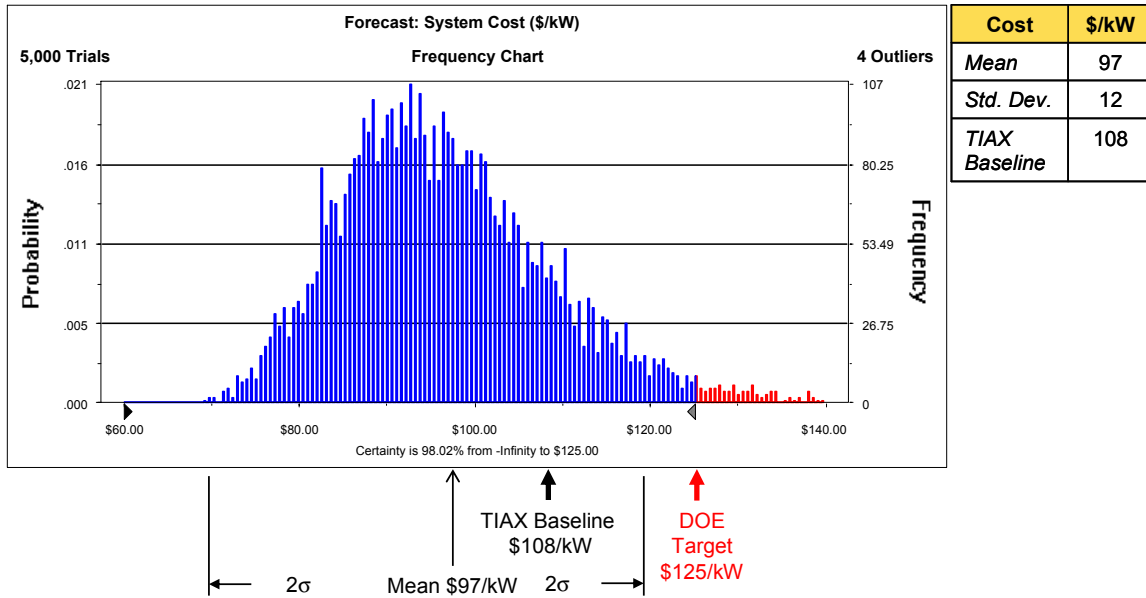


Figure 5. Range in System Cost due to Uncertainty in Input Parameters

Table 2 summarizes the key changes in stack material cost for 2005. A high-level assessment of the membrane cost resulted in a lowering of the perfluoro-sulfonic acid membrane cost. A decrease in thickness and cost of the gas diffusion layer and bipolar plate lowered these stack component costs. To achieve the thinner bipolar plates, this component was changed from a molded graphite resin composite to a molded/stamped expanded graphite part.

Table 2. Changes in Stack Materials Cost on an Area Basis from 2004 to 2005

Component	2004 Cost ¹ (\$/m ²)	2005 Cost ¹ (\$/m ²)	% Change	Cost Drivers / Comments
Membrane	48.85 ²	23.38	-52%	TIAX bottom-up costing, 2 mil unsupported membrane
Electrode	67.19	279.02	315%	Platinum cost increased from \$450/troz to \$900/troz, platinum loading increased from 0.3 mg/cm ² to 0.75 mg/cm ² , platinum process markup is 20% which is same as 2004
GDL	32.00	18.40	-43%	GDL thickness decreased from 350 μm to 260 μm thickness (\$8.50/m ² on actual area)
Bipolar plate	28.10	N/A	N/A	All plates have cooling channels

Bipolar plate with cooling	27.45	17.38	-37%	Material changed from molded graphite to expanded graphite. Every plate is a cooling plate. Thinner plate with less material
Seal	7.25	6.08	-15%	Increased amount of material, but switched from fluoropolymer to nitrile rubber (\$5/lb)
BOS	6.91	6.03	-13%	Larger active area and same cost of components
Final Assembly	8.14	10.53	29%	Increased number of cells due to lower cell voltage. Does not include stack conditioning and QC
Total	225.88	360.81	60%	

¹ m² of active area

² \$40/m² membrane purchased, plus \$8.85/m² to condition membrane to fuel cell use

For the system configuration used in the baseline assessment, Table 3 shows various system metrics relative to DOE targets for 2005. The stack cost is slightly higher than the target, due to the high assumed platinum price and the high platinum loading. Decreasing the thickness of the bipolar plates and increasing the area power density led to stack power densities close to the DOE target, while on a system level both power densities satisfy the targets. The volumetric density does not include allowance for a packing factor and might not satisfy the target in product form. Both efficiencies (rated and 25 percent of rated power) are about 5 percent lower than the DOE targets as a result of designing at 0.65 volts. The baseline system contains 1.4 grams platinum per kilowatt. FreedomCAR and DOE roadmaps show values of 1.1 and 1.3 g Pt/kW respectively for the 2004 stack status similar to the baseline value from this study.

Table 3. System Metrics Relative to DOE 2005 Targets

Metric	Units	Value	DOE 2005 Target
Stack volume	L	51	
Stack weight	kg	58	
Stack cost	\$/kW _e	67	\$65
Stack power density	W _e /L	1569	1500
Stack specific power	W _e /kg	1379	1500
Fuel cell system (FCS) volume¹	L	131	
FCS weight	kg	138	
FCS cost	\$/kW _e	108	\$125
FCS power density¹	W _e /L	610	500
FCS specific power	W _e /kg	580	500
FCS efficiency @ rated power	%	46	50
FCS efficiency @ 25% rated power	%	55	60

¹ Does not include packing factor, which would lower system power density

Technology has progressed relative to the systems used in earlier analyses, leading to the reduction in cost and increases in power density. Discussions with MEA developers revealed that single cell performance of new products are significantly better with much lower platinum loadings, while providing longer life. When these improvements are realized at the stack level, the costs are further reduced.

The issue of platinum pricing has a significant effect on stack and system cost. However, reductions in platinum loading will reduce the impact if prices remain at high-levels. In the longer term, the balance between supply and demand will determine whether platinum prices return to historic values.

With increasing stack performance, lower platinum loadings, and lower platinum prices, BOP components will become more important cost contributors. More attention to BOP components and simplification of the system will be necessary to satisfy longer term fuel cell subsystem targets.

3. Introduction

Every new technology faces substantial barriers to commercialization; however, transportation markets present unique challenges including the size of the market, cost drivers, consumer expectations, product requirements (e.g., performance, safety, and reliability), well-entrenched technologies and emerging alternative technologies, fuel infrastructure issues, OEM profits, and societal (government) requirements. The latter includes emissions of pollutants and greenhouse gases, efficiency goals, and energy policy. Within this array of challenges, developers and automotive companies are attempting to develop cost-effective electric fuel cell powertrains for passenger vehicles. The current DOE goal for a fuel cell powertrain cost is \$30/kW_e (2015). Starting in the mid-1970s, the battery electric vehicle (BEV) story vividly illustrates the significant hurdles that radical new powertrains face in passenger vehicles. Even though the most recent industry/government BEV initiative, the U.S. Automotive Battery Consortium (USABC), failed to produce a viable mass-market EV battery, it led to significant advances in powertrain components, including electric motors and power electronics, that have benefited the fuel cell and hybrid electric vehicle efforts.

Fuel cells have the potential to provide a clean power source for powering automobiles of the future. While there are many technical challenges facing fuel cells (such as cold start, durability, etc.), there are also major challenges relating to the economic viability of the technologies in the marketplace. Fuel cells and the hydrogen fuel must be cost-competitive with current gasoline and internal combustion technologies for fuel cell powertrains to enter the market place.

Starting in 1998, the Technology & Innovation group of Arthur D. Little, Inc. (now TIAX LLC) began a five-year program (1) to model and project fuel cell system costs for the DOE, Office of Advanced Automotive Technologies (now Hydrogen FCIT). The project started with the characterization of the status of fuel cell system technology, development of a system layout and thermodynamic model, and development of an activities-based cost model for production of this system at high production volumes. The initial cost results for an on-board, fuel-flexible, reformer-based fuel cell system were presented at the first Future Car Congress (2) and are summarized in Section 4, “Summary of Cost Projection Results,” along with the results of more recent analyses. The model and supporting databases have evolved. The efforts of this project were extended in 2005 through a project with NREL.

4. Summary of Cost Project Results (1998-2004)

Earlier cost projections from this project are presented to provide a historical perspective on how the projected cost of fuel cell systems has changed as the technology and system specifications have evolved. We also provide the results of several analyses to address questions such as the trade-offs among efficiency, cost, and weight when operating at high and lower voltage and how stack cost might change as platinum loading is decreased. The earlier analyses provide insights into key cost drivers. The following results are summarized:

- Cost projection for fuel flexible reformer based system (2001)
- Impact of lowering platinum loading on fuel cell cost
- Impact of cell voltage on weight, system efficiency, and cost
- Cost projection for compressed hydrogen storage
- Cost projection for direct hydrogen based system (2004)

We will also provide a summary of critical assumptions and how these may have changed over time.

4.1. Reformer Based System (2001)

The reformer system configuration shown in Figure 6 was developed in concert with ANL using a thermally integrated auto-thermal reformer with shift beds.

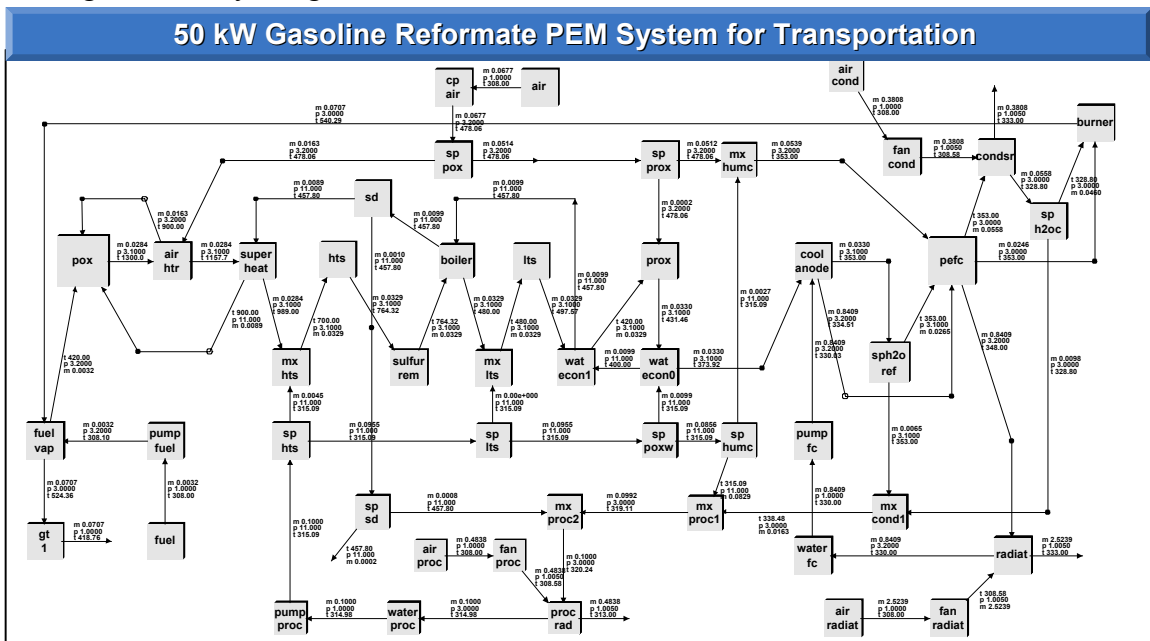


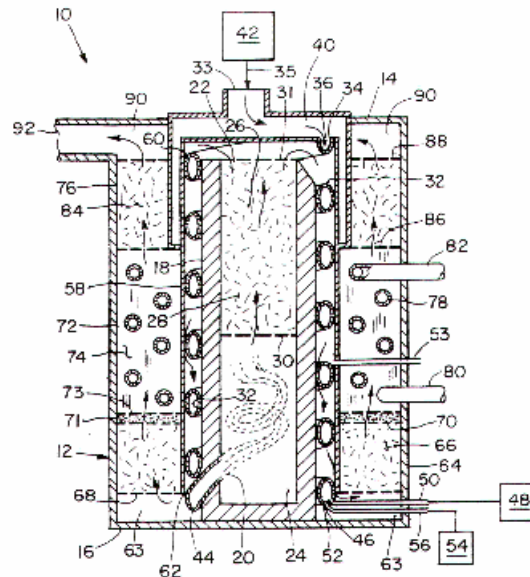
Figure 6. System Configuration Used in 2001 Reformer – Fuel Cell System Cost Projection

When the program started, the system included both the hydrogen supply and the stack subsystems. The system in Figure 6 translates into the component list shown in Table 4 with the allocation of components between subsystems dictated by the PNGV program definitions.

Table 4. Component List and Allocation to Subsystems

Fuel Processor Sub-System		Fuel Cell Sub-System	Balance-of-Plant
<ul style="list-style-type: none"> ◆ Reformate Generator ◆ ATR ◆ HTS ◆ Sulfur Removal ◆ LTS ◆ Steam Generator ◆ Air Preheater ◆ Steam Superheater ◆ Reformate Humidifier 	<ul style="list-style-type: none"> ◆ Fuel Supply ◆ Fuel Pump ◆ Fuel Vaporizer 	<ul style="list-style-type: none"> ◆ Fuel Cell Stack (Unit Cells) ◆ Stack Hardware ◆ Fuel Cell Heat Exchanger ◆ Compressor/Expander ◆ Anode Tailgas Burner ◆ Sensors & Control Valves 	<ul style="list-style-type: none"> ◆ Startup Battery ◆ System Controller ◆ System Packaging ◆ Electrical ◆ Safety
<ul style="list-style-type: none"> ◆ Reformate Conditioner ◆ NH₃ Removal ◆ PROX ◆ Anode Gas Cooler ◆ Economizers (2) ◆ Anode Inlet Knockout Drum 	<ul style="list-style-type: none"> ◆ Water Supply ◆ Water Separators (2) ◆ Heat Exchanger ◆ Steam Drum ◆ Process Water Reservoir 		
<ul style="list-style-type: none"> ◆ Sensors & Control Valves for each section 			

The cost of the reformer was based on a design similar to one in the patent literature from Arthur D. Little as shown in Figure 7.



Source: Arthur D. Little patent (US 6,126,908)

Figure 7. Thermally integrated reformer design used to cost the fuel processor including ATR, high and low temperature shift beds, burner and steam generation tubes

In 2001, the assumptions shown in Table 5 were used to scale the reformer beds and the stack. The selection of 0.8 volts for the fuel cell voltage at rated power was driven by overall system-efficiency targets rather than trying to minimize system size by operation of the stack at or near its high power point.

Table 5. 2001 Assumptions for the Reformer and Fuel Cell Stack

Reformer

Parameter	Catalyst Beds				Clean-up Beds	
	ATR	HTS	LTS	PROX	Sulfur Removal	NH ₃ Removal
Temperature (°C)	1030	430	230	205	490	80
Catalyst	Pt/Ni	Fe ₃ O ₄ / CrO ₃	Cu/ZnO	Pt	ZnO	Activated Carbon
Support	Alumina	Alumina	Alumina	Alumina	None	None
GSHV (1/hours)	15,000	10,000	5,000	10,000	N/A	None

Fuel Cell Stack

Fuel Cell Operating Assumption	Units	2000/2001 Baseline
Unit Cell Voltage	Volts	0.8 ¹
Power Density	mW/cm ²	250 ²
Fuel Utilization	%	85
Cathode Stoichiometry		1.0
Operating Temperature	°C	80
Percent Anode Air Bleed	%	1

¹ This cell voltage was specified to satisfy overall system efficiency goals.

² A current density of 310 mA/cm² at 0.8 volts (250 mW/cm²) was selected on the basis of near term projections of available stack and unit cell data.

Figure 8 shows how the \$324/kW cost of the 2001 system was allocated among the subsystems. The contributions to the fuel cell subsystem are broken down further in Figure 9 and Figure 10. At this time, the fuel cell stack cost was \$180/kW with major contributions from the electrodes (high platinum loading of 0.8 mg/cm² total plus 0.2 mg/cm² ruthenium and low power density of 250 mW/cm²) and the membrane (\$100/m²). Older electrode technology and reformate, rather than hydrogen fuel, resulted in the low power density. Bipolar plates and the gas diffusion layers represented approximately 20% of the stack cost. The fuel cell subsystem also included a tailgas burner to burn unused fuel and a high-temperature expander to recover this energy. The expander was integral to the turbo compressor-expander module.

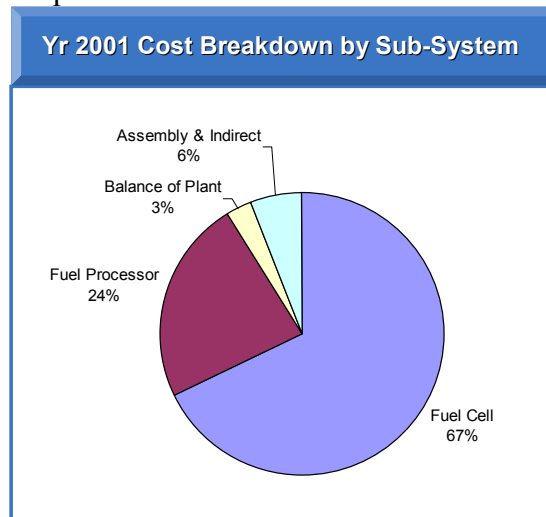


Figure 8. 2001 Reformer Based System Cost Breakdown (system cost of \$324/kW)

Fuel Cell Sub-System	Factory Cost	
	Yr 2001 Estimate*	
	(\$)	(\$/kW)
Fuel Cell Stack	9,035	181
Tailgas Burner	358	7
Air Supply	992	20
Cooling System	587	12
Total	11,000	220

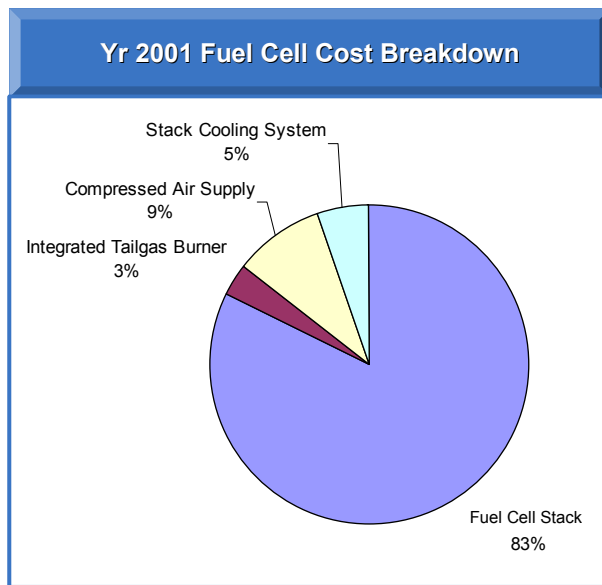


Figure 9. 2001 Fuel Cell System Cost Breakdown

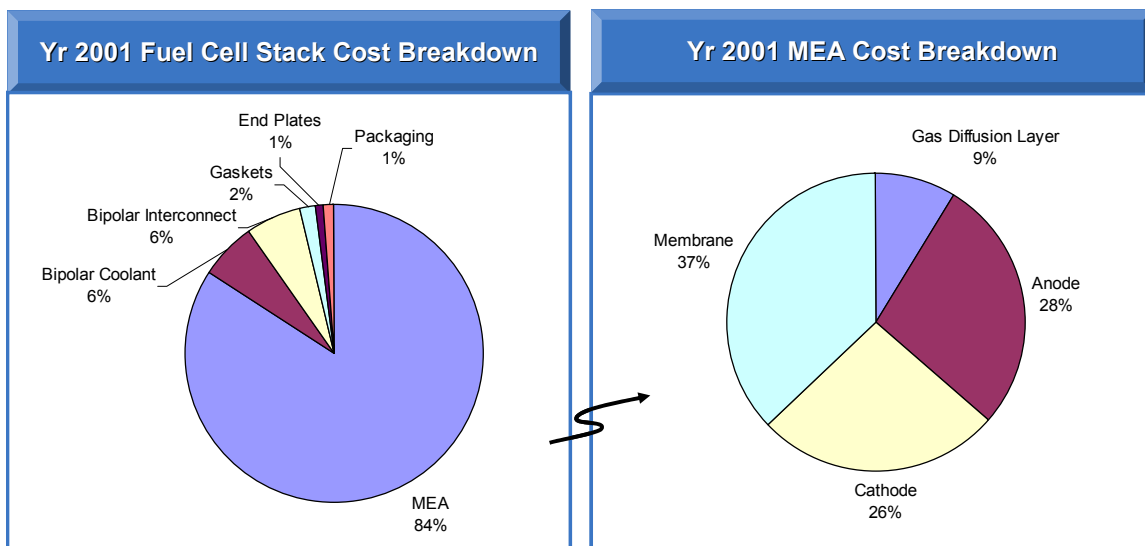


Figure 10. Stack and MEA Cost Breakdown for the 2001 System Configuration

In 2001, the top four cost drivers for the stack were:

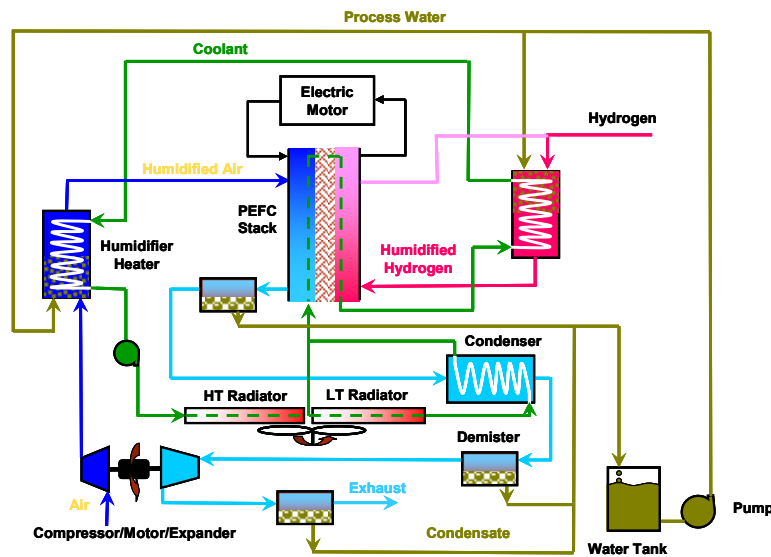
- Power density
- Nafion cost
- Platinum loading
- Platinum price

Low power density and high platinum loadings combined to produce a high overall platinum content, 3.62 g Pt/kW in the stack and a total of 4 g PGM/kW for the system (reformer catalysts and ruthenium in the anode for CO tolerance).

During this period, the impact of operation at a high power point, i.e., 0.65 volts, on cost, efficiency, and weight was evaluated. Consideration of the high power point operation yielded mixed results. Operation at 0.65 volts doubled the assumed power of the stack (500 mW/cm^2) and lowered the system cost by approximately 20%. However, system weight increased slightly because of larger heat exchange requirements and a larger reformer. At rated power, the overall system efficiency decreased from 37% to 29% (LHV). The efficiency for this powertrain would be higher if calculated on the basis of a typical driving cycle in which a vehicle operates much of the time at fractions of the rated power, i.e., 25% to 30%.

2004

In 2004, a bottom-up cost analysis of compressed hydrogen was conducted and then combined with an updated stack cost based on pure hydrogen. We again worked with ANL to develop a system configuration and specifications for sizing the hydrogen storage capacity. In this analysis the system configuration shown in Figure 11 was used as a basis for calculating the efficiency of various hybridization options for a mid-size sedan (e.g., Ford Taurus) with a 370 mile range on a combined urban/highway drive cycle.



Source: Dr. Rajesh Ahluwalia of ANL

Source: Dr. Rajesh Ahluwalia of ANL

Figure 11. Direct Hydrogen System for 2004 Cost Update

A peak power of approximately 120 kW was selected for the different hybridization scenarios. Analysis of the system by ANL (3, 4) led to an 80kW fuel cell with 40 kW battery (peak). As shown in Table 6, this 80/40 system had a fuel economy of 68 mpgge and a hydrogen requirement of 5.6 kg for a range of 370 miles in a combined urban/highway drive cycle.

Table 6. Comparison of Hybridization Scenarios with a 120 kW ICE Base Case

ANL Results	ICEV 120 kW	FC EV 120 kW	FC HEV 100 kW	FC HEV 80 kW	FC HEV 60 kW
Engine/Fuel Cell Power, kW peak	114	120	100	80	60
Battery Power, kW peak	0	0	20	40	55
Fuel Economy, mpgge	23	59	65	68	69
Hydrogen Required	N/A	6.3	5.9	5.6	5.6

A Type IV carbon fiber wound tank with a polymer liner was used as the basis of the hydrogen storage tank cost analysis. The tank had metal bosses at each end, an outer layer of damage-resistant glass fiber, and impact-resistant foam end domes. BOP components in the hydrogen supply subsystem included an internal regulator, pressure relief components, valves, sensors, fill port, and piping. Figure 12 shows the cost results for different scenarios, including 5,000 and 10,000 psi storage pressures, single versus multiple tanks, and two fiber types (strength and cost). M30S is higher tensile strength, higher tensile modulus and higher cost, aerospace grade carbon fiber compared to T700S.

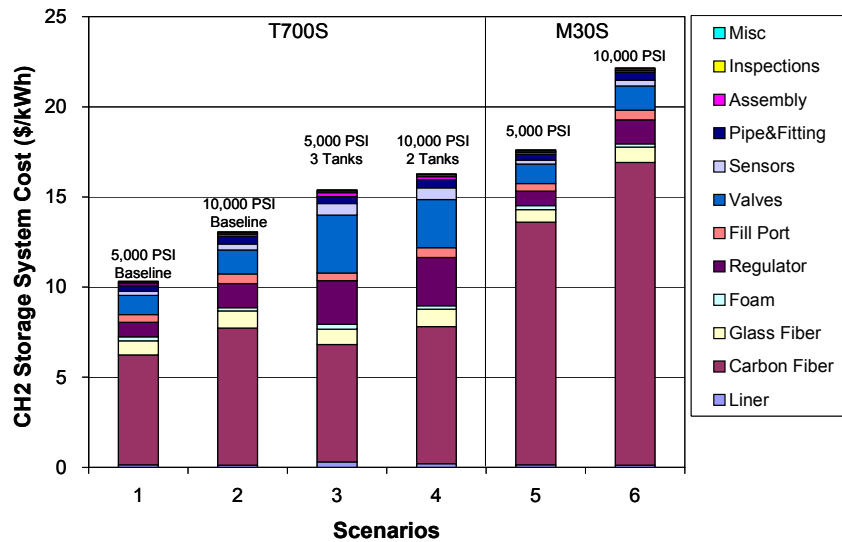


Figure 12. Cost of Compressed Hydrogen Storage Scenarios

The leading cost drivers for the storage subsystem were the cost and weight of the carbon fiber followed by the fill port and regulator costs. Multiple tank scenarios were considered to lower the profile of the system for vehicle integration, while higher strength fibers were looked at to reduce system weight. The storage system was found to satisfy the DOE mid-term specific energy target, but failed to meet volume and cost targets. The results of this analysis were then used to estimate an overall system cost.

Table 7 compares the fuel cell system design assumptions for the 2001 reformat system and the 2004 direct hydrogen case. Overall, changing to direct hydrogen increased the power density of the stack and fuel utilization leading to reductions in stack size and cost and increases in efficiency. Calculation of the system efficiency on a drive-cycle basis allowed the stack to be designed at a lower cell voltage (higher area power density) while satisfying efficiency targets. Presentations by DuPont (5) discussed pathways to lower membrane costs, i.e., on the order of \$40/m². For these assumptions, Table 8 contains a comparison of the 2001 and 2004 system cost estimate metrics. The latter is reported on a 50 kW basis for consistency with the reformat values. In the 2004 hydrogen system the fuel loop has a simple design and does not contain a provision for purging nitrogen, circulation to minimize transport limitations at high power, or a tailgas burner. The increases in power density, reduction in platinum loading, and decrease in membrane cost were the primary drivers in lowering the cost of the stack and the system. Changing to compressed hydrogen lowers the cost of the fuel source, but only incrementally reduces the overall system cost.

Table 7. 2004 Stack Parameters Compared to 2001 Values

Parameter	Units	2001	2004	Comments
System Power	kW	50	80	Change to mid-size sedan with hybridization
Cell Voltage	V	0.8	0.69	Efficiency calculated on a drive-cycle basis
Power Density	mW/cm ²	250	450	Increase due to lower voltage and direct hydrogen
Total Pt Loading	mg/cm ²	0.8	0.3	Technology improvements and direct hydrogen
Fuel Utilization	%	85	100	Reformat to direct hydrogen
Electrolyte Cost	\$/m ²	100	40	Industry feedback

Table 8. Comparison of Cost of Reformate and Direct Hydrogen Systems

Component	2001 Reformate System (\$50/kW basis)	2004 Direct Hydrogen (\$50/kW basis)
Fuel Cell SS	221	104
Stack	181	73
TGB	7	0
Air Supply	20	20
Cooling	12	11
Fuel Supply	76	58
BOP	10	5
Assembly and Indirect	17	8
Total	324	176

For purposes of comparison with the 2005 assessment, Table 9 presents the 2004 results on an 80 kW basis. Increasing the power rating of the system decreases the \$/kW value to \$145/kW because a number of the components (i.e., controllers, sensors) do not change in scale with power and because we did not vary the size of the hydrogen storage system. As a result, the fuel cell system changed by approximately 5% while the fuel supply decreased by approximately 30%.

Table 9. Comparison of 50 kW and 80 kW Costs for the 2004 Systems

Component	50 kW Basis	80 kW Basis
Fuel Cell SS	104	97
Stack	73	72
TGB	0	0
Air Supply	20	13
Cooling	11	12
Fuel Supply	58	38
BOP	5	4
Assembly and Indirect	8	6
Total	176	145

Platinum Loading Analysis

Electrode cost is a major cost driver of the stack and the system. As part of our 2002 effort, the factors influencing platinum loadings were assessed to develop an estimate of future fuel cell stack cost for reformate and hydrogen systems. Platinum loading per kilowatt is a critical issue as indicated by the cost contribution of the electrodes to the stack (Figure 10) and by the DOE funding resources allocated to platinum reduction and performance improvements.

Projections of minimum platinum requirements were estimated based on an analysis that considered:

- Impact of catalyst particle size and catalyst activity on kinetics
- Impact of electrolyte anion adsorption on catalyst kinetics
- Development of polarization curves based on electrochemical kinetics
- Impact of ohmic resistance losses on polarization curve

An overview of this work was presented at the Future Car Congress in 2002 (2). This analysis was based on the assumption that the fuel cell would be operating at relatively high unit cell voltages (e.g., 0.8 volts) to achieve overall system efficiency targets. However, analyses that consider overall vehicle efficiency and reward higher fuel cell system power density will allow some relaxation of this stack efficiency target. At high cell voltages, cathode kinetics control the current flow and Tafel kinetics can be used to assess the effect of operating conditions and cathode voltage losses. Voltage drops were then assigned to the anode and resistive components on the basis of experimental data. Analysis of a series of scenarios involving catalyst loadings, pressure, and temperature led to the conclusion that the stack would have to operate at high temperature (e.g., 160°C) and elevated pressure (e.g., 3 atm) to satisfy long-term DOE fuel cell power density (milliwatt/cm²) goals.

The polarization curves and functional relationships between platinum loading and performance were then combined with the stack cost model to assess the relationship between platinum loading and materials cost. Several overall assumptions are important to understanding the basis of the analysis.

- First, we assumed the performance of the catalyst is not limited by diffusion, the structure of the electrode, or the dispersion of the catalyst. In the early days of PEM fuel cell development, significant performance gains were made while appreciably decreasing the catalyst loadings. In our analysis, reduction in platinum loading leads to lower power density.
- Second, introduction of resistance losses to the analysis reduces the power density that can be achieved by increasing catalyst loading or by decreasing the cell voltage. Voltage losses across resistances (I^2R) in the system reduce the voltage available to perform useful work at the electrodes.
- Third, in the baseline cost estimate, the fuel cell stack materials represent over 90% of the stack cost. Consequently, in this following analysis, only material costs were considered (i.e., MEA, gas diffusion layer, and bipolar plate).

Figure 13 shows the material cost (\$/kW_e) versus cathode platinum loading for stacks operating at 3 atm, 160°C, and 0.8 volts with direct hydrogen and reformat. Assumptions in this analysis include the use of an alloy catalyst with kinetic activity two times that of platinum, a unit cell resistance of 0.1 ohm/cm², and an anode catalyst loading of one half the cathode loading.

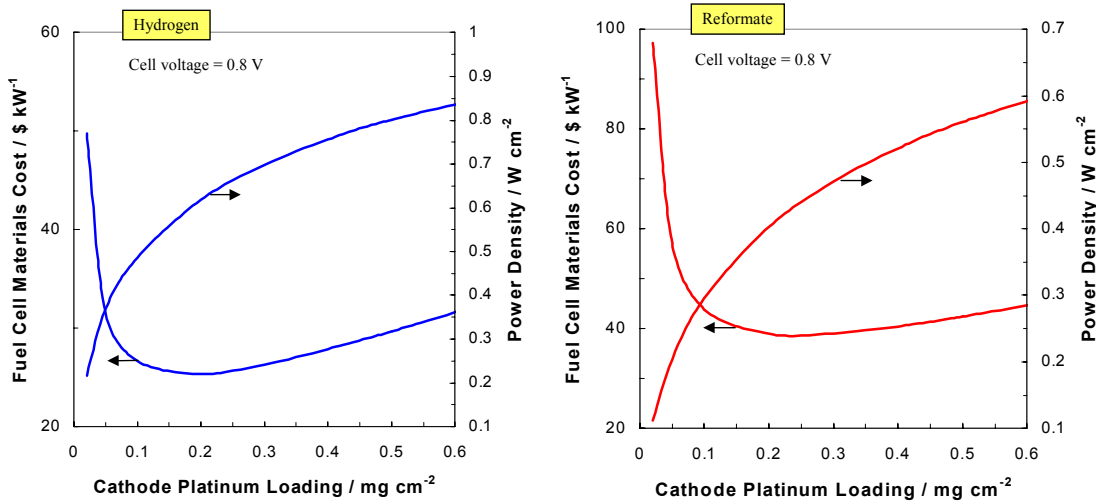


Figure 13. Stack Cost Versus Platinum Loading for Reformate and Direct Hydrogen Stacks

The analysis produced an “L” shaped curve where material costs rise sharply at low platinum loadings (low power density) and then show weak dependence with increasing platinum loading. Figure 14 shows the flat portion of the curve for various values of resistance. Independent of the resistance value, all the curves have a minimum cost in the platinum loading region of 0.1 to 0.3 mg/cm². Insights into the factors influencing minimum platinum loading in addition to the value (mg/cm²) and the resulting “L” shaped curve include:

- Reduction of platinum loadings beyond some minimum value negatively impacts cost. First, on an area basis, the non-platinum material cost increases relative to the catalyst cost. Second, more materials are used due to a larger stack resulting from lower power density.
- Cost goes through a minimum with increasing platinum loading due to the negative impact of resistance on power density. The kinetic benefit of the increased platinum loading is not realized due to the voltage losses arising from ohmic losses.
- This analysis shows the critical cost implications of high ohmic losses within the stack.

Assumption of different material costs will shift the curves but not change their nature or general shape.

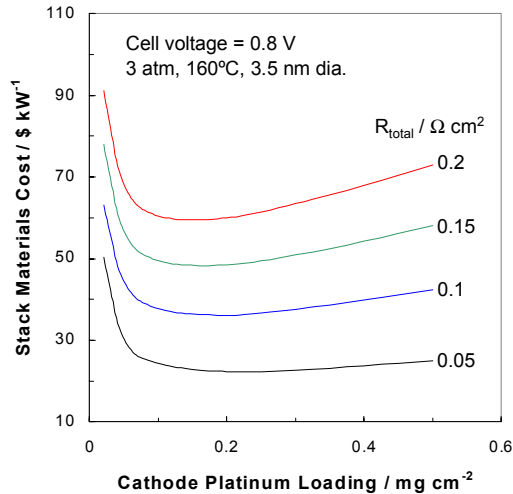


Figure 14. Stack Cost versus Ohmic Resistance

4.2. Summary of Key Cost Drivers (2001 – 2004)

The stack contributes the largest percentage of cost to the fuel cell subsystem. In discussing the stack parameters that influence cost, one must consider performance metrics, material/component costs, material loadings, and the interaction between these factors. The following points highlight the key drivers and illustrate the interactions.

- The cost and size of the stack scale inversely with power density. The power density of the stack will depend on the polarization (iV) curve of the MEA in the stack, the cell voltage selected for operation at rated power, and the ohmic losses within the stack. MEA developers provide single cell iV curves for their products, however, the need to avoid hotspots in the stack and the presence of ohmic losses between the bipolar plates and the MEA result in lower performance in the stack.
- System designers must then make trade-offs between power density and efficiency when selecting a design cell voltage. For example, at this stage of development, the car companies may prefer to have smaller stacks rather than the highest efficiency for the sake of integrating the stack into the vehicle.
- A key driver of power density will be platinum loading; however, the costs of other stack materials (i.e., membrane, bipolar plates, and GDLs) set lower limits on platinum loading while ohmic losses limit the benefits of increasing Pt loading. The potential improvements in power at high loadings are offset by the voltage losses from contact and electrolyte resistances at high currents.
- At high production volumes, material costs represent 70% to 80% of the system cost. Consequently, reduction of the amount of material (kg/kW) and cost of materials (\$/kg) is critical to lowering cost. The importance of the cost of BOP components will increase as the stack cost is reduced. Some of the BOP components are relatively mature technologies and the potential for cost reduction is less than the stack materials.

5. Project Objective, Scope, and Approach

5.1. Objective

The cost projection developed from this effort will allow assessment of the current status of PEMFC technology relative to the 2005 DOE cost target of \$125/kW for the fuel cell stack and supporting BOP components for air, water, thermal, and fuel management. This target does not include the cost of hydrogen storage.

5.2. Scope

In this project, the scope encompassed the status of PEMFC technology in 2005 with the cost estimated for high production volumes, i.e., 500,000 units per year. Figure 15 shows the scope of the system considered. The analysis is focused on the fuel cell stack subsystem; however we also considered BOP components. We performed bottom-up costing for the major components of the fuel cell stack:

- Membrane
- Gas Diffusion Layer (GDL)
- Electrodes
- Membrane Electrode Assembly (MEA)
- Bipolar Plates
- Seals

We estimated costs for other components based on in-house expertise and discussions with vendors:

- Compressor-Expander
- Air Filtration
- Membrane Humidifier for Anode Hydrogen
- Enthalpy Wheel Humidifier for Cathode Air
- H₂ Recirculation Blower-Ejector
- Heat Exchangers
- Coolant Pumps
- Controls & Sensors

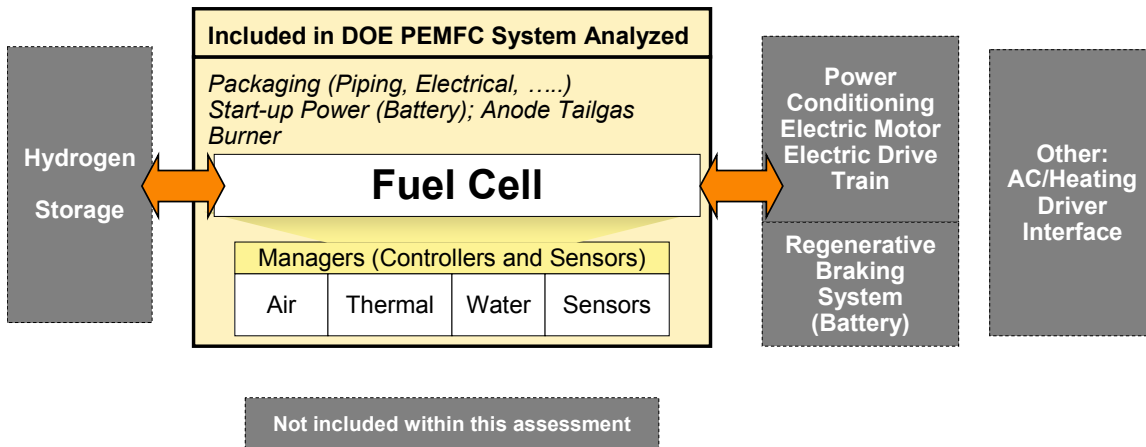


Figure 15. Scope of 2005 PEMFC Costing

5.3. Approach

This project builds on previous experience with cost analysis PEM fuel cell systems developed over the past six years and ongoing work in cost assessment of hydrogen storage technologies.

In this project, we followed a 3-step process to develop the 2005 cost projection and produce the final report, as shown in Figure 16.

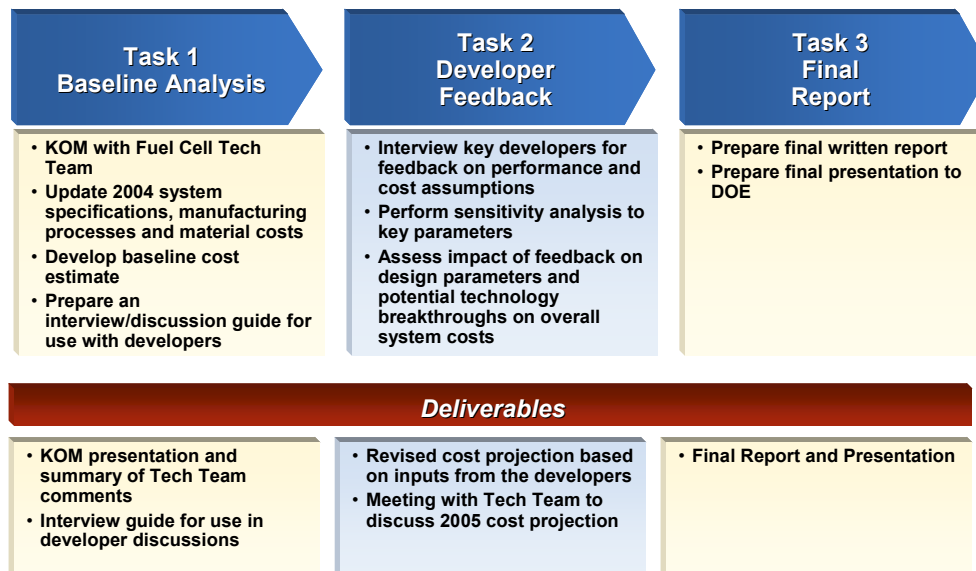


Figure 16. 2005 Cost Project Approach

6. Manufacturing Cost Model Description

6.1. Technology-Based Costing Methodology

We have applied an internally developed technology-costing methodology that uses a highly interdisciplinary approach drawing on extensive experience in the cost modeling of electrochemical and power technologies including batteries, fuel cells, and balance of plant. The model integrates a fundamental understanding of fuel cell component/system performance parameters and their interactions, with expertise in materials (e.g., polymers, inorganic materials), design, and manufacturing operations (e.g., coating, molding, automation), and extensive knowledge of process cost modeling. We used our knowledge of technology developments and our relationships with stack and subsystem developers to calibrate the cost model and perform sensitivity analyses to system operating parameters, material costs, component designs, and selection of manufacturing processes. A five-step approach for conducting manufacturing cost analysis was used.

Step 1. Product and manufacturing process definition: We started by identifying detailed product design parameters and manufacturing process options. The key elements for each component are material type and quantity, process cycle time, production equipment specifications, and direct labor requirements.

Step 2. Production process scenario definition: The production process scenario is critical for identifying realistic and credible manufacturing costs based on current manufacturing process capabilities. The key elements of a scenario include annual production volumes, plant size and location, internal and outsourced operations, and wage rates.

Step 3. Cost model development: A cost model was constructed that provides product/process costs based on the variable inputs defined in Steps 1 and 2. Cost outputs from the model were categorized by materials, labor, utilities, equipment, tooling, building, overhead labor, maintenance, and cost of capital. The structure of the model permits frequent and complex analyses of multiple inputs.

Step 4. Development of cost models for relevant competitive design options and manufacturing processes: In order to make cost comparisons of competing technologies, design options, and alternative manufacturing processes, additional models/scenarios derived from the initial customized model were developed. The structure and consistent approach of our manufacturing cost model permits accurate and rapid comparisons.

Step 5. Sensitivity, scenarios, and Monte Carlo simulation: These analyses provide an in-depth understanding of the key cost drivers in each technology and design option, the critical manufacturing processes for cost-reduction initiatives, and the economic risks associated with selected development and commercialization strategies. Figure 17 is a schematic representation of our manufacturing cost model.

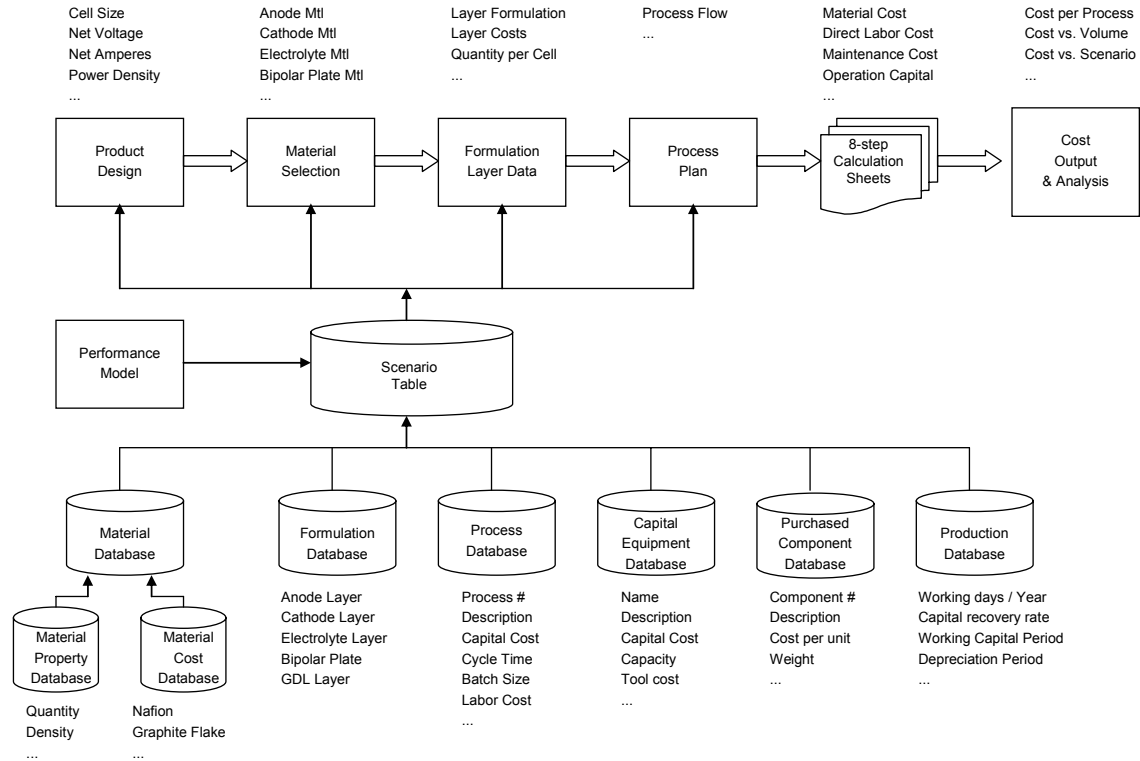


Figure 17. Manufacturing Cost Model Schematic

6.2. PEM Fuel Cell Manufacturing Cost Model

6.2.1. Overview

Our PEM fuel cell cost model is based on a bottom-up analysis of process flowcharts developed for critical components, materials, and subsystems. For this project, we worked closely with ANL to develop a stack and system configuration that would represent current fuel cell vehicle technology.

ANL then developed a model to determine the state parameters (temperature, pressure, and mass and molar flows) of the various streams and components by thermodynamic modeling. The individual reactor beds and the fuel cell stack were then scaled using available kinetic or polarization data for the assumed catalyst materials and their loadings.

We performed a bottom-up costing on the major stack components. Our manufacturing group developed production process options for key subsystems and components, and obtained raw material costs from potential suppliers. Purchased components were listed separately and suppliers were contacted regarding the availability and cost of outsourced components. An activity-based process model in Microsoft® Excel was then developed to estimate manufacturing costs using capital equipment and raw material costs, labor

rates, and throughput for 500,000 units per year. The model yields cost per kilowatt, cost by subsystems and components, and a breakdown of material and process costs.

With additional software, sensitivity and Monte Carlo analyses were performed on the base model. Our cost model assumptions and results were calibrated with feedback from the DOE, the FreedomCAR Fuel Cell Tech Team, and fuel cell suppliers and component developers. We integrated the feedback on stack and system performance parameters, manufacturing processes, and material and cost assumptions into the final cost estimate.

6.2.2. Cost Definition

As shown in Figure 18, the estimated cost includes factory costs (e.g., direct materials and labor, factory expenses, capital equipment) but excludes corporate charges for profit, sales expenses, and general services and administration.

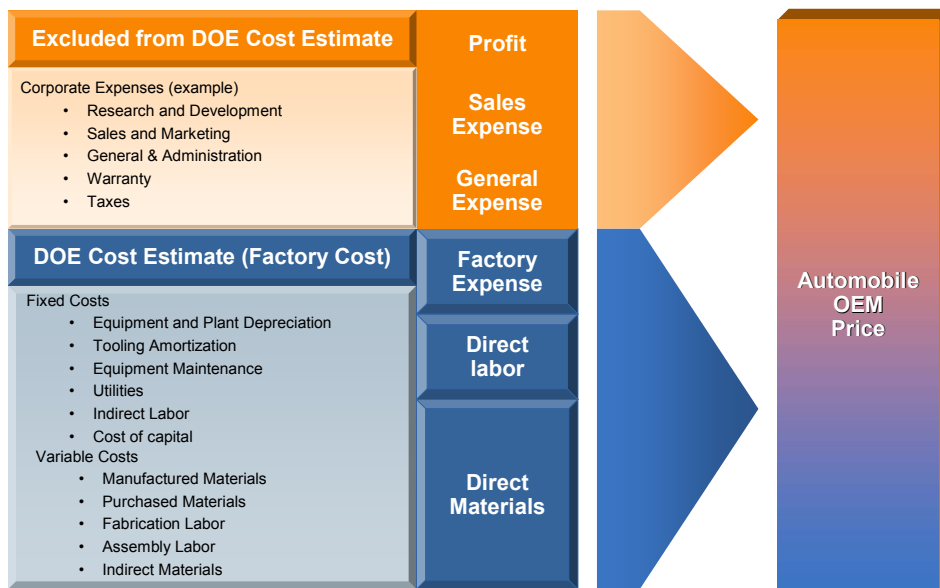


Figure 18. Cost Elements of Detailed Cost Build-up

6.2.3. Baseline Cost Model Description

Figure 19 illustrates the three essential steps we followed in developing the PEMFC system cost estimate.

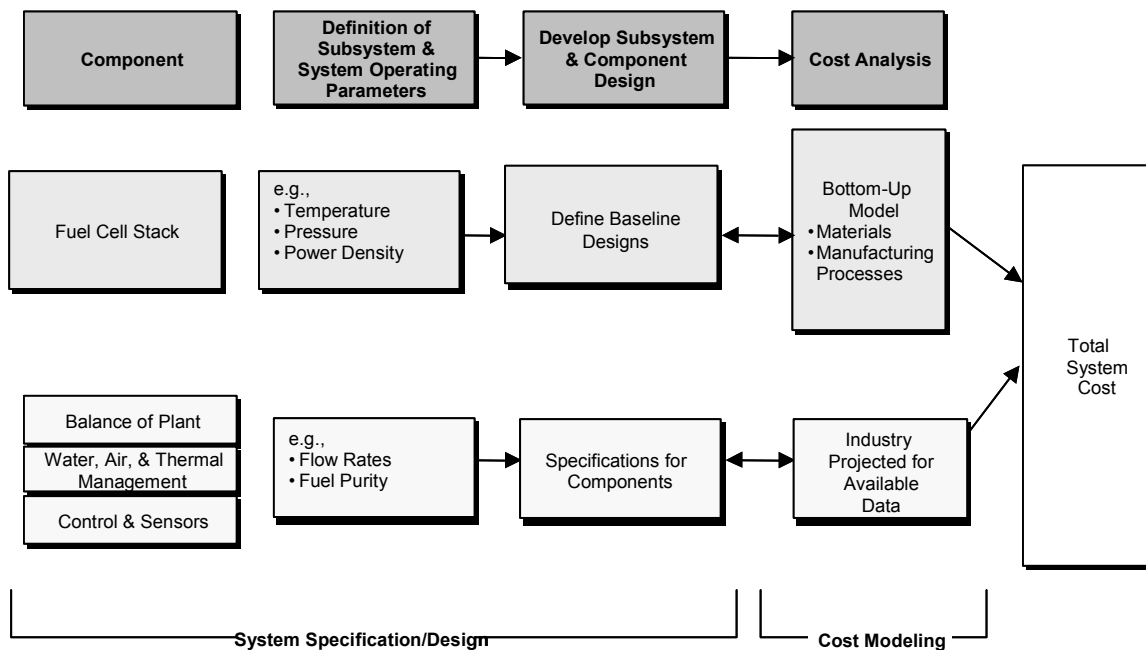


Figure 19. Approach to PEMFC System Cost Model

6.2.3.1. Definition of System Operating Parameters

Information on the system operating parameters, material selection and costs, manufacturing process selection and production capabilities were entered into the main input sheet. Data on materials and manufacturing processes were collected and evaluated in the first phase of the program. We calibrated our internal evaluation through phone interviews with leading suppliers of materials, components, and subsystems to the fuel cell system integrators. This exchange of information permitted us to refine our analysis and present a more accurate picture of the cost of state-of-the-art fuel cell designs and manufacturing processes.

6.2.3.2. Development of Subsystem and Component Design

Subsequently, incremental costs for each manufacturing process in the subsystem module sheets were estimated. For example, Figure 20 shows a flow chart of a manufacturing process for a graphite foil bipolar plate.

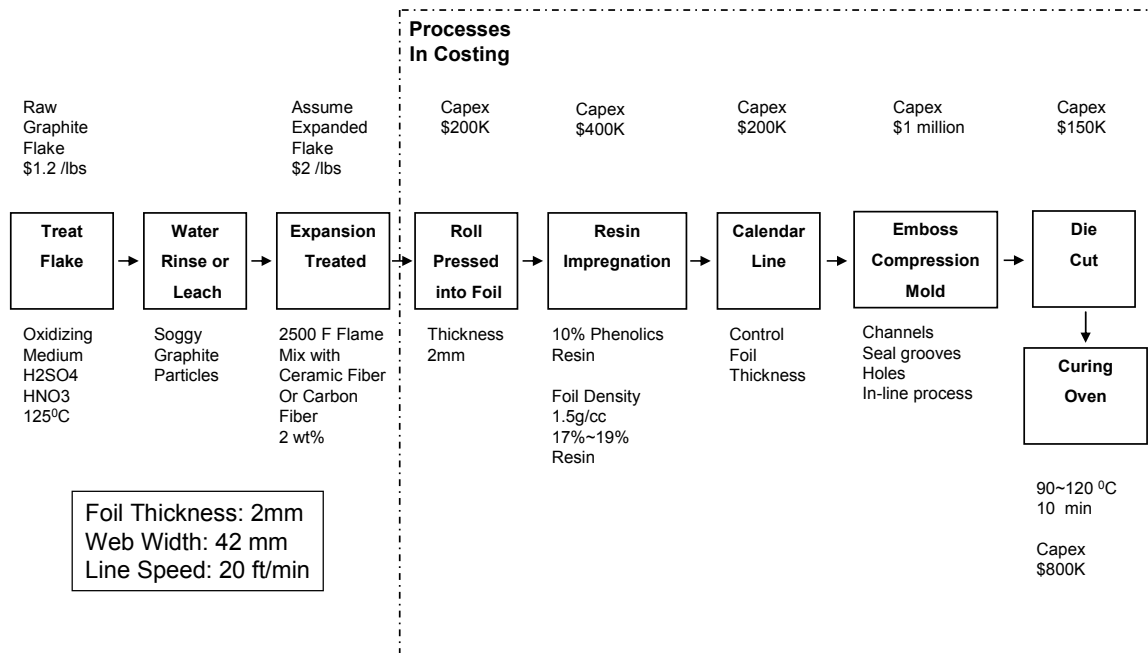


Figure 20. Graphite Foil Bipolar Plate Manufacturing Flow Chart

We defined the following assumptions for each subsystem module:

- Plant capacity scaled to market size (unit demand)
- Manufacturing process capabilities (machining, molding, coating, assembly, level of automation, etc.)
- Process and component sourcing (internal or out-sourced)
- Material volume projections for cost and availability determination
- Yield and scrap

6.2.3.3. Cost Analysis

We used a plant capacity appropriate for commercialization of PEMFC technology in the context of automotive markets (i.e., 500,000 units per year). We searched for analogies with systems in Internal Combustion (IC) engine vehicles for long-term extrapolation of costs, e.g., control and monitoring systems.

With completion of the baseline cost estimate, we visited major material and component suppliers, technology developers, and fuel cell system fabricators to present the results of our initial analysis. We used feedback from these critical interviews to refine our analysis and identify any imminent developments that would significantly impact our baseline cost estimates.

6.2.4. Sensitivity Analyses

We performed sensitivity analyses on the PEMFC system model to assess the impact of key material and manufacturing process parameters on the baseline fuel cell stack and system cost. The system cost model is a complex cost analysis tool that permits

evaluation of multiple design and operating parameters by changing selected inputs. These changes are carried throughout the model to generate revised cost estimates of selected subsystem modules as appropriate. This permits rapid and accurate comparison between design concepts, material and manufacturing developments, and system configurations. Figure 21 shows a single-variable sensitivity analysis, which depicts the impact on membrane cost, of varying one variable while holding all others constant.

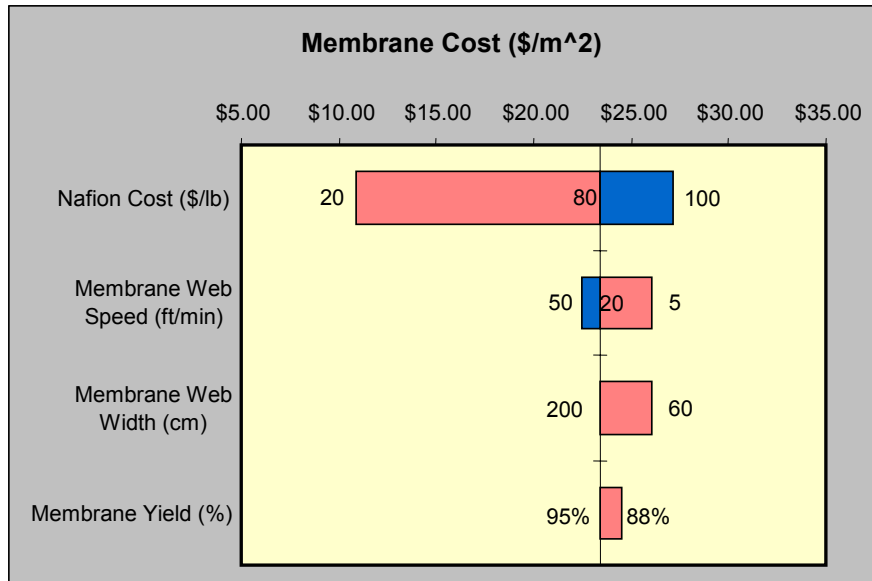


Figure 21. Example of Single Variable Sensitivity Analysis

Figure 22 shows an example of a Monte Carlo statistical analysis, in which several parameters are varied simultaneously over a specified number of trials to determine the probability distribution of the overall cost.

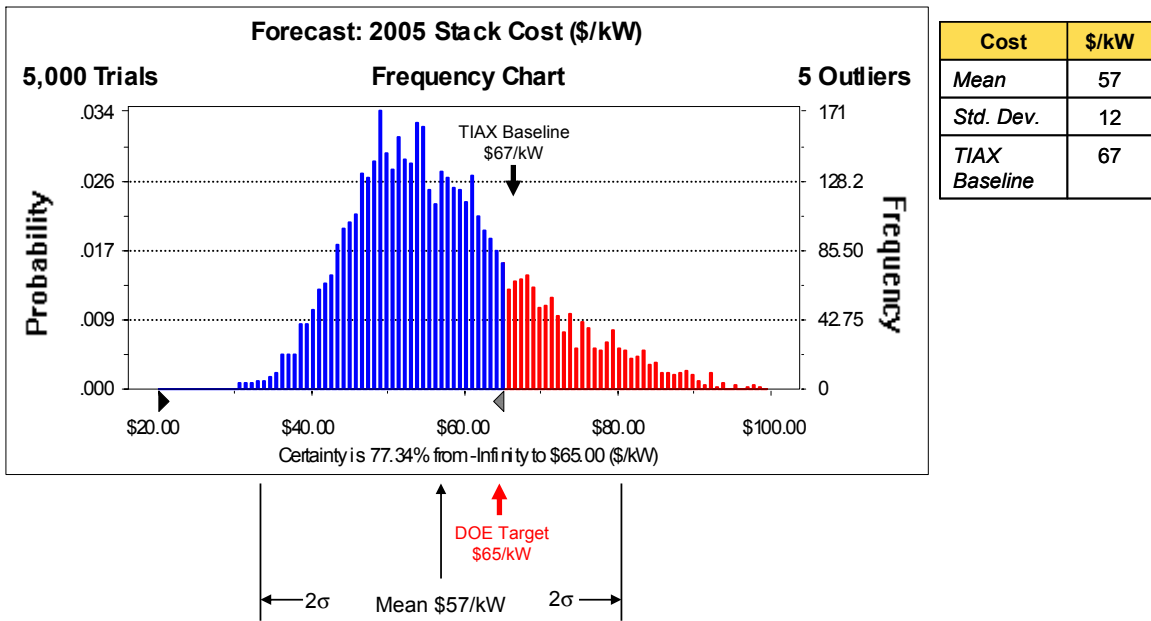


Figure 22. Example of Monte Carlo Sensitivity Analysis

Finally, the baseline costs and sensitivity results were summarized in a table using standard financial cost categories, for example: materials, labor, utilities, equipment, and tooling. Our final results include a review of system performance assumptions, material selection and performance, process flow sheets, process cycle times, and a breakdown of cost projections.

6.2.5. Supply Chain Analysis

In this project, we assume that the stack is vertically integrated and that the BOP components are purchased from suppliers. Alternatively, an OEM could assemble purchased subsystems and accept the higher cost associated with outsourcing. One of the scenarios we considered in the cost model was that the OEM would assemble the fuel cell stack using purchased MEAs and bipolar plates. Margin estimates at various levels of the supply chain are based on our experience with automotive suppliers and OEMs and on publicly available information. Figure 23 proposes a rudimentary supply chain scenario. Additionally, the MEA supplier could purchase its membrane material rather than buy the membrane or membrane precursor material (ionomer).

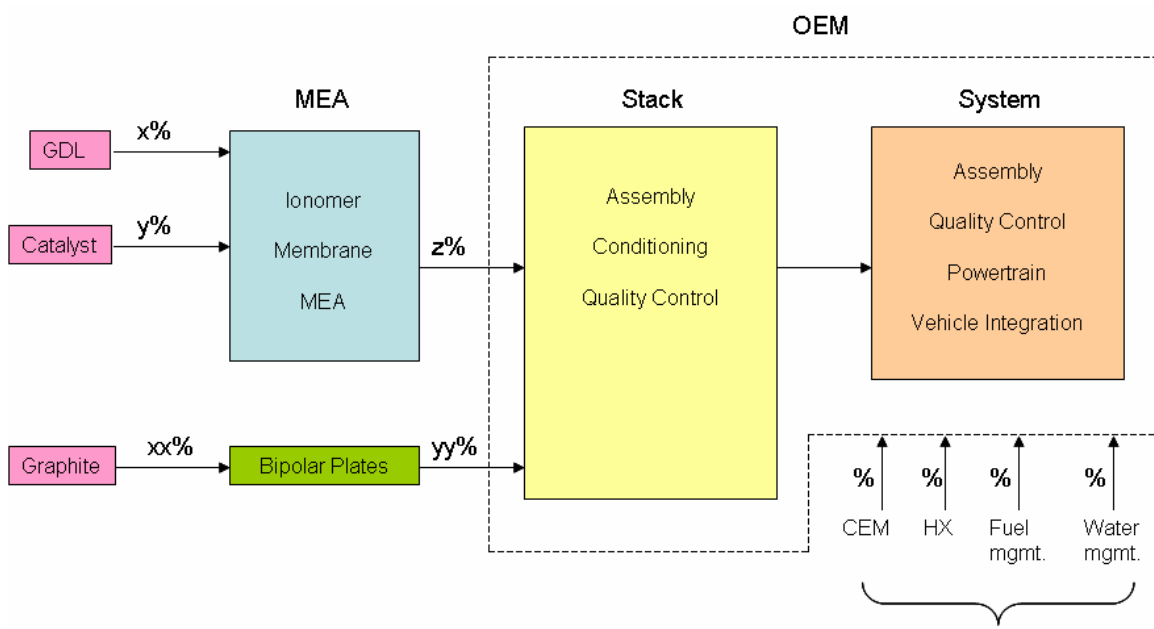


Figure 23. Illustrative Automotive PEMFC Supply Chain

7. DOE Fuel Cell System Targets

Table 10 shows the DOE targets for 80 kW_e (net) direct-hydrogen fuel cell systems for transportation applications. The cost projection developed from this effort will allow assessment of the status of PEMFC technology and cost relative to the 2005 DOE targets.

Table 10. DOE Targets

Direct Hydrogen Fuel Cell Power System		Target		
Characteristic	Units	2005	2010	2015
System Cost	\$/kW _e	125	45	30
System Efficiency @ 25% Rated Power	%	60	60	60
System Efficiency @ Rated Power	%	50	50	50
System Power Density, Specific Power	W/L, W/kg	500	650	650
Stack Cost	\$/kW _e	65	30	20
Stack Efficiency @ 25% Rated Power	%	65	65	65
Stack Efficiency @ Rated Power	%	55	55	55
Stack Power Density, Specific Power	W/L, W/kg	1500	2000	2000
MEA Cost	\$/kW _e	50	15	10
MEA Performance @ Rated Power	mW/cm ²	800	1280	1280
MEA Degradation Rate	%	10	10	10
PGM Cost	\$/kW _e	40	8	6
PGM Content	g/kW _e (peak)	2.67	0.5	0.4
PGM Loading (both electrodes)	mg/cm ²	0.7	0.3	0.2
Membrane Cost	\$/m ²	200	40	40
Bipolar Plate Cost	\$/kW _e		6	4
CEM System Cost	\$	600	400	200

Source: DOE Fuel Cell RD&D Plan Technical Targets: 80 kW_e (net) Direct-H₂ Automotive Fuel Cell Systems

8. System Analysis

8.1. Introduction

Estimating the cost of the complete system requires identifying various components, sizing the components, and estimating the parasitic loads (which affect the stack size). A thermodynamic analysis is necessary for these estimates. ANL performed the thermodynamic system analysis; similar studies by ANL are available in the public literature (6, 7). In this section we describe the system layout, explain the rationale for the various components, and summarize the key findings of the analysis. The stack operating conditions, which dictate the system configuration to a large extent, are provided in Table 11.

Table 11. Summary of the Stack Operating Conditions that Influence the System Design and Configuration of the 80 kW_e PEMFC System

Parameter	Value
Single cell voltage	0.65 V
Hydrogen consumption per pass	70%
Oxygen utilization	50%
Inlet anode and cathode RH	60%
Operating temperature	80°C
System pressure at rated power	2.5 atm

8.2. System Description

Figure 24 shows the key components of the 80 kW_e PEMFC system for transportation and the system flow schematic. The system is assumed to operate on hydrogen from a compressed hydrogen storage tank and atmospheric air. In the following sections, we briefly describe the key elements of the major subsystems.

An alternative system approach, not assessed here, is to operate at near atmospheric pressure and use in-stack water management. This approach simplifies the system design.

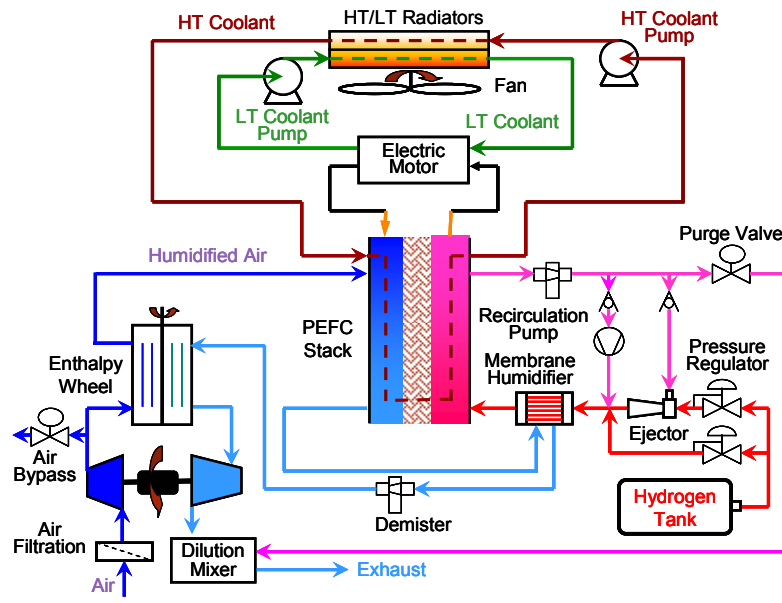
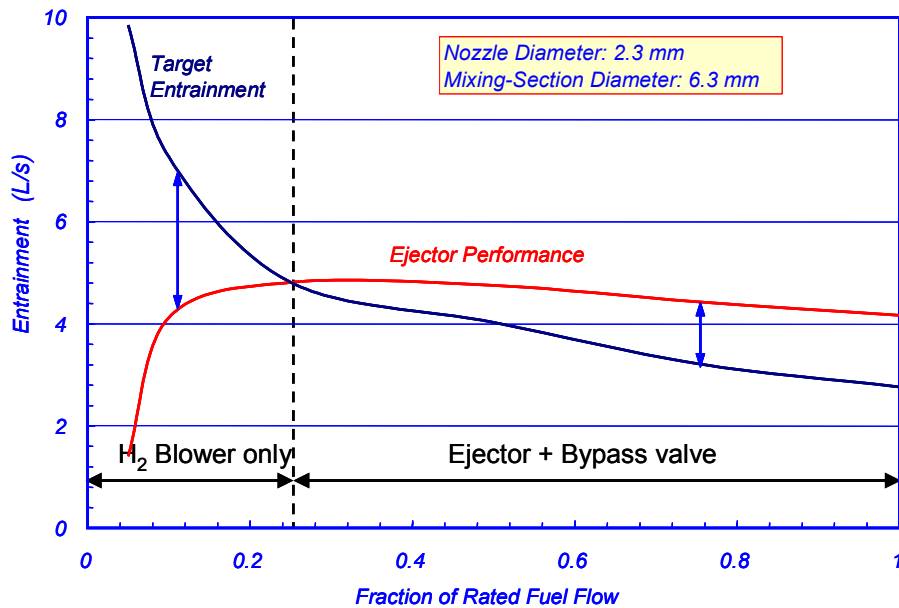


Figure 24. PEMFC System Layout

Anode hydrogen feed

Hydrogen from the compressed hydrogen tank is fed to the anode of the fuel cell via a hybrid ejector-recirculation pump. The hydrogen is humidified by air exiting the cathode through a membrane humidification unit. The humidification level in the inlet air stream is maintained at 60%.

A hybrid ejector-recirculation pump is required because of the turndown characteristics of the ejector and parasitic power requirements of the recycle blower as shown in Figure 25. For flow rates higher than 25% of rated power, the ejector designed for this application is able to supply the flow rate required. However, at less than 25% of rated power, the flow requirement is much higher than what the ejector can supply requiring the use of an active blower.



Source: Dr. Rajesh Ahluwalia of ANL

Figure 25. Comparison of the Required Flow from the Ejector versus the Actual Flow Estimated for the Chosen Ejector Design

Cathode air feed

Atmospheric air is filtered and compressed to 2.5 atm in the compressor-expander module and humidified to 60% RH at 80°C in the enthalpy wheel humidifier. The exhaust from the cathode is used for humidifying the inlet air. The pressurized air stream is expanded in the expander for energy recovery.

Stack cooling

The efficiency of the fuel cell stack under the defined operating conditions is 51.7%, implying that nearly 90 kW of heat from the stack must be rejected to maintain a constant stack temperature. A separate coolant flow-loop, the HT coolant loop in Table 24, is utilized for this purpose.

8.3. System Performance Results

The overall system efficiency is determined by the stack efficiency and the parasitic losses in the system.

8.3.1. Stack Efficiency

The stack efficiency is defined as the stack power output divided by the lower heating value of the fresh hydrogen feed. The stack efficiency accounts for the hydrogen loss through the purge of the recycle stream, the hydrogen crossover from the anode to the cathode, and the oxygen crossover from the cathode to the anode. Table 12 summarizes these factors for the baseline case. In Table 12 the hydrogen crossover is expressed as a

fraction of the fresh feed of hydrogen, and the crossover of oxygen and nitrogen are expressed as fractions of the fresh feed of the respective species to the cathode. The stack efficiency on a LHV basis was calculated as 51.7%.

Table 12. Parameters Influencing the Stack Efficiency Estimation

Parameter	Value
Hydrogen crossover ¹ (%)	0.2
Purge fraction (%)	0.6
Nitrogen crossover (%)	0.01
Oxygen crossover (%)	0.020
Hydrogen utilization (%)	99.5
Stack efficiency (% , LHV)	51.7

¹ Percentage H₂ crossover is expressed as % of fresh H₂ fed to stack, at 100% of rated power.

The purge fraction was chosen to result in optimum stack efficiency. While the crossover of the species is dictated by the properties of the membrane, the purge fraction is a parameter that is left to the designer. Figure 26 shows the impact of purge fraction on the stack efficiency. At purge fractions lower than 0.6%, the concentration of nitrogen in the anode compartment increases resulting in lower cell voltage and hence lower efficiency. At purge fractions greater than 0.6%, a greater fraction of the freshly fed hydrogen is purged out of the system without being electrochemically utilized and hence the efficiency decreases.

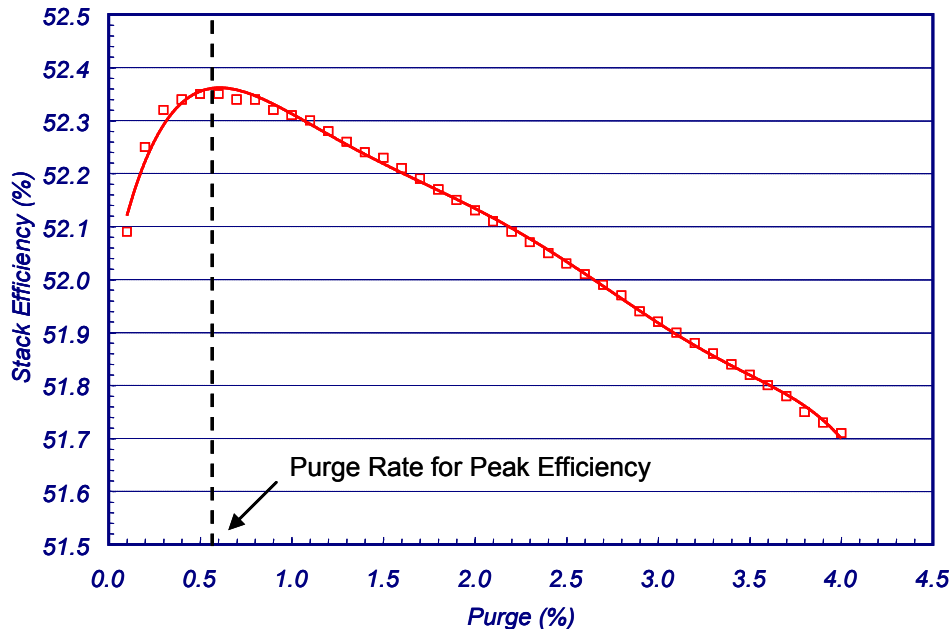


Figure 26. Stack Efficiency as a function of the purge rate from the anode recycle loop for single cell operating voltage of 0.7 V. Comparable results are obtained for 0.65 V operation.

ANL used data reported by Mittelsteadt et al. (8) to develop a correlation for nitrogen crossover in the fuel cell stack. An interesting consequence of the crossover of nitrogen into the anode compartment is that a steady state is reached for nitrogen concentration in the anode compartment. Therefore, although pure hydrogen is fed to the system, over time, hydrogen in the anode becomes diluted with nitrogen. Figure 27 shows the average concentration of nitrogen in the anode as a fraction of the rated power in of the stack. The nitrogen concentration within the stack can be as high as 15% at the stack outlet depending on the operating voltage. An important implication is that while single cell tests are often conducted on pure hydrogen, the conditions in the stack could be vastly different.

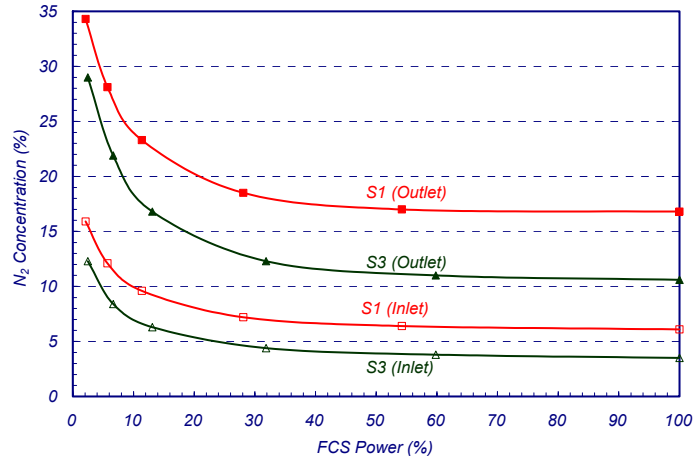


Figure 27. Nitrogen concentration in the anode stream as a function of the stack power output (which is given as a fraction of the rated power). S1 corresponds to 0.7 V single cell voltage and S3 to 0.65 V.

8.3.2. System Parasitic Power Consumption

The parasitic power consumed by the balance of plant components associated with fuel delivery, air delivery, water management, and heat management has to be supplied by the fuel cell stack, which detracts from the overall electrical power output of the stack. Table 13 summarizes the power consumption in the system. Therefore, the gross power output from the stack must equal $80 \text{ kW} + 9.5 \text{ kW} = 89.5 \text{ kW}$.

The power consumption in the compressor-expander module is the net power consumed in the module after accounting for the power recovery from the expander. At rated power, the compressor was assumed to be 78% efficient, the expander 82% efficient, the motor 92% efficient, and the controller 92% efficient. The compressor-expander was assumed to be capable of a turndown ratio of 20.

Table 13. Parasitic Power Consumption in the System

Component	Power consumption (W)
CEM (net)	5500
Enthalpy wheel motor	126
Radiator fan	2200
Coolant pump	1400

H ₂ recirculation pump	256
Total	9500

8.4. System Efficiency

For the baseline operating conditions, the system efficiency at rated power was estimated as 47% (LHV of hydrogen), as indicated in Figure 28. With decreasing power output, the system efficiency increases primarily owing to rise in the cell voltage. The peak system efficiency occurs at ~ 5% of the rated capacity or nearly 4 kW.

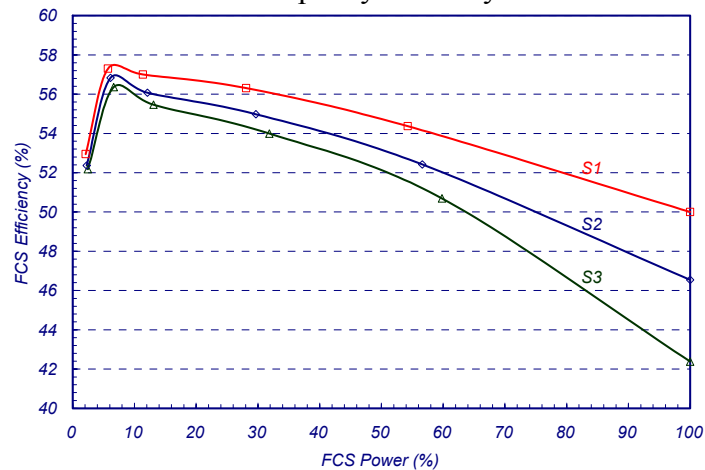


Figure 28. Efficiency of the 80 kW PEMFC system as a function of the rated power. S1 corresponds to 0.7 V single cell voltage, S2 to 0.65 V (base case) and S3 to 0.6 V.

8.5. System Component Sizing

BOP discussions, sizing, and cost are combined in Section 10.4

8.5.1. PEMFC Stack

The stack size is governed by the stack power density, which in turn is determined by the operating conditions (such as cell voltage, RH, temperature, and pressure) and the cell design parameters (such as catalyst loading and membrane thickness). The power density and cell design parameters are critical to determining the stack costs.

8.5.2. Power Density Assessment

We assumed the following for the stack power density:

- Single cell in the stack operates at 0.65 V
- Total platinum loading of 0.75 mg/cm²
- Single cell area power density of 600 mW/cm²

Based on feedback from the FreedomCAR Tech Team, we assumed an operating voltage for the single cell in the stack of 0.65 V. Based on discussions with various developers, it became clear that in stacks being evaluated in vehicles today, the catalyst loading was ~ 0.75 mg/cm² total platinum.

Data available in the literature (9) indicate that it would be possible to achieve power densities of $\sim 750 \text{ mW/cm}^2$ at these catalyst loadings and 2.5 atm operation. These measurements were made in a large single cell under idealized conditions in the laboratory. However, to translate the data to a practical stack, we assumed that the single cell lab power density would be reduced by 20%, resulting in 600 mW/cm^2 power density for the stack.

9. Cost Analysis

9.1. Introduction

In Section 2 (Summary) key assumptions and system design decisions are described, including:

- The trade-offs between designing for higher power versus efficiency are explored. Designing for higher power, e.g., 0.65 V versus 0.75 V, reduces size, weight, and cost of the stack, but decreases efficiency relative to DOE targets by approximately 5%.
- Platinum price, because of the electrode contribution to cost, has a significant impact on cost. Recent platinum prices are at all time highs (\$900/troz) while historic prices established over the last 100 years are half this value. We used the current price in the baseline analysis, but also present results for the lower price for reference. The latter is consistent with earlier cost projections.
- Power density and platinum loading are key cost drivers. With the information provided in this report, the reader can calibrate the results to their values. The cost of stack materials are provided on an area basis so the cost can be estimated for other power densities, while the impact of higher or lower platinum loadings can be estimated by factors.
- The impact of meeting life requirements has not been factored into cost, however, this was discussed with the Tech Team and developers. We did not have a relationship, i.e., between platinum loading and life, that allowed us to make this trade-off in design. For the moment, we assume that the developments that will increase the life of the stack will not involve increased platinum loadings.

The goal of this assessment is to capture the major cost contributions to the system. Within the scope of a project of this type, one cannot solve all the technical issues facing developers today. For example, we did not include system features designed to address startup in freezing conditions. As solutions to low temperature startup become public knowledge, they can be factored into the cost. The question of hydrogen purity, i.e. CO concentration, has not been factored into the system components or the assumed power density. Related to BOP, components required for purification of recovered water and sensors are not included. These BOP components are not expected to make a significant contribution now, however they may represent a larger share of the system cost in the future, as stack costs are lowered.

9.2. Stack

Stack specifications and performance assumptions are key drivers of power density and cost. Table 14 lists the stack assumptions for 2005.

Table 14. Stack Specifications and Performance Assumptions

Parameters	Units	2005 Direct-H ₂	S/C ¹	Comments
Production volume	per year	500,000	S	Same as in prev. studies
Fuel cell net power	kW _e	80	S	FreedomCAR Spec.
Fuel cell gross power	kW _e	90	C	ANL
Cell voltage @ rated power	V	0.65	S	Tech Team feedback
Stack voltage @ rated power	V	300 V @ 266 A	S	Tech Team feedback
Stack efficiency @ rated power	%	51.7%	C	ANL
Number of stacks		2	S	Same as in prev. studies
Number of cells per stack		231	C	Calculated
Cell pitch	cells/inch cells/cm	9.55, 3.76	C	Calculated
Total Pt loading	mg/cm ²	0.75	S	Tech team/developer feedback
Power density @ 0.65 V	mW/cm ²	600	S	TIAX estimates based on literature data and developer feedback
Active area per cell	cm ²	323	C	Calculated
Active area to total area	%	85	S	Developer feedback

¹ S – Specified, C – Calculated

The following material assumptions were used for the 2005 stack material cost projection. Table 15 is a summary of the stack material assumptions.

Table 15. Stack Material Assumptions

Component	Parameter	Baseline
Membrane	Material Supported	Sulfonated fluoro-polymer No
Electrodes – Cathode & Anode	Catalyst	Platinum
Gas Diffusion Layer	Material Porosity	Woven carbon fiber 70%
Bipolar Plate	Type	Expanded graphite foil
Cell Pitch	-	9.55/inch, 3.76/cm

The gasket frame seal configuration is shown in Figure 29 while Table 16 lists the stack component weight and dimensions.

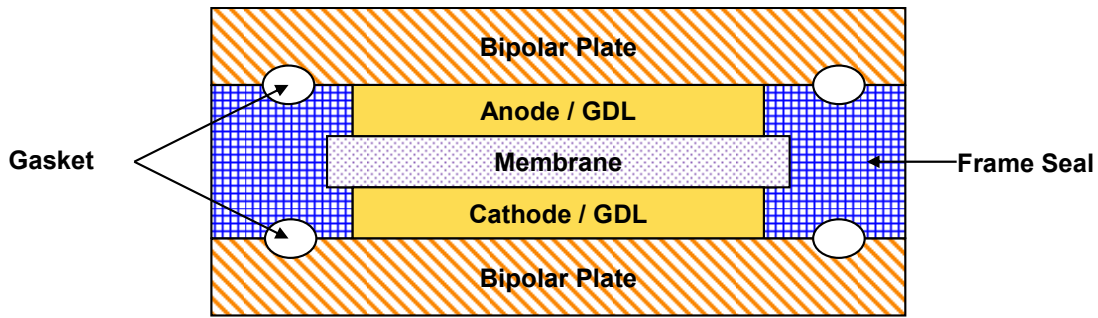


Figure 29. 2005 Stack Design

Table 16. Stack Component Weight and Dimensions

Component	Thickness (□m)	Weight (g/cell)	Weight ¹ (g/m ²)
Membrane	51	3.24	100
Anode	20	0.66	20
Anode GDL	260 ²	7.67	237
Cathode	20	0.55	17
Cathode GDL	260 ²	7.67	237
Bipolar plate (a pair)	2000	63.96	1988
Frame seal	641	2.74	85
Gasket	100	0.58	18
Total	2611	87	2702

¹ m² of active area which is 323 cm² per cell

² Thickness at 7.3 PSI (275 μm at 1 psi)

9.2.1. Membrane

9.2.1.1. Description

Introduction

A process description for fabrication of 1-2 mil thickness non-reinforced Nafion® membranes was constructed on the basis of a review of patents and publicly available literature. This process description is the basis for modeling the costs associated with membrane manufacture for PEMFCs in 2005.

Background and Information Sources

DuPont's Nafion® is the industry standard material for forming the ion permeable membranes used in PEMFCs. Nafion is composed of a highly ion-conductive polyfluorosulfonic acid (PFSA) polymer that functions as a cation exchange medium, selectively transporting protons from anode to cathode in the fuel cell.

DuPont's original patent on the Nafion material (U.S. No. 3,718,627) named Walther Grot as inventor. Following Grot's patents through time provides information on the evolution of both the Nafion material itself and its incorporation into membranes. The most recent patents on the technology are assigned to Ion Power, a business formed by Grot's son, Stephen Grot in 1999 to distribute Nafion-based products for fuel cell and electrolysis applications.

A second source of information is DuPont's 2002 Fuel Cell Seminar presentation (5). In this presentation, a road map was given describing the evolution of DuPont's membrane and dispersion products planned for 2002 to 2005.

Finally, technical bulletins available at both DuPont's and Ion Power's websites give specifications and descriptions of current Nafion products, including membranes.

The above information, along with TIAX knowledge of film and coating manufacturing processes, has been used to construct a Nafion membrane fabrication process for cost modeling.

Nafion Membranes

Non-reinforced Nafion PFSA membrane products currently available from DuPont/Ion Power include extrusion cast and dispersion cast membranes. The extrusion cast membranes (DuPont N-112, -1135, -115, -117, -1110) are melt extruded from perfluorosulfonyl fluoride resins (e.g., DuPont R-1100) followed by hydrolysis and acid exchange steps. These films are available in 2, 3.5, 5, 7, and 10 mil membrane thicknesses (EW 1100). In 2003, DuPont announced the development of a new high-volume, low-cost process for manufacture of "second generation" dispersion cast membranes. Dispersion cast films are formed directly from solutions of PFSA in water and alcohol by a coating process onto an inert PTFE backing film. These membranes are available from DuPont in 1-mil and 2-mil thicknesses at EW 1100 (NRE-211, -212). Based on available information, this dispersion casting process is the current state of the art, enabling manufacture of thin membranes with high ion conductivity, and is used as the basis for the membrane cost model. A 2-mil membrane thickness is chosen for cost modeling to be comparable to the 1999 values, in which DuPont's N-112 extruded membrane was the basis of the estimate. Further, thinner membranes (< 50 microns) need higher H₂ purge rates, can suffer from anode flooding, and higher H₂ cross-over rates.

Nafion Dispersions

Nafion Dispersions are available from both DuPont and Ion Power. The dispersions consist of PFSA polymer, water, and low-molecular weight alcohols. DuPont's product line (e.g., DE 520, DE 1020, DE 2020) includes 5%, 10%, and 20% PFSA with 34% to 90% water and 1% to 50% VOCs (n-propanol, ethanol, and mixed ethers) by weight. Dispersions are available from Ion Power in 5% and 15% wt. PFSA solutions (Liquion™ LQ-1105/1005 and LQ-1115/1015) containing 20% to 45% water and 40% to 75% isopropanol. Compared to the earlier dispersions (U.S. Patent No. 4,433,082, Grot), these dispersions (U.S. Patent No. 6,552,093, Curtin) have tighter particle size distributions and minimized VOCs in the dispersion medium. In 2003, DuPont claimed the increased uniformity in composition of these dispersions would enable more predictable coating formulations and consistent processing, contributing to improved fuel cell performance. We have based our membrane cost estimate on the use of a dispersion similar to the Liquion™ dispersion. A 40% solids content dispersion was chosen, although this is higher than the highest percentage PFSA, low VOC (40% isopropanol/45% water) dispersion available from Ion Power. The highest practical limit for polymeric colloidal dispersions with acceptable flow rheology is in the 40% to 50% solids content range. The higher weight percent PFSA dispersion is preferred for greater ease in film-forming, oven length needed and the low VOCs reduce costs involved in solvent disposal or recovery.

9.2.1.2. Manufacturing Process

Film-Forming Process

A process for fabricating non-reinforced Nafion membranes similar to DuPont's NRE-212 (EW 1100, 2 mil) was derived from U.S. Patent No. 6,552,093 (second generation dispersions, DuPont), U.S. Patent No. 6,641,862 (dispersion cast membrane electrode assemblies, Ion Power), and product bulletins from both DuPont and Ion Power.

U.S. Patent No. 6,552,093 describes a process for making films from the second generation PFSA dispersions. According to the patent, the casting of the dispersion is typically done on a polymer belt from which the film can be easily released (e.g., PTFE). A (fluorochemical) surfactant may be added to the liquid dispersion medium to lower the surface tension of the composition and promote the even distribution of the composition on the polymer belt.

The liquid dispersion medium is evaporated to form a film by heating at a temperature below the coalescence temperature, i.e., less than 100°C. The film is cured by heating to above the coalescence temperature. The Liquion product bulletin specifies solvent should be removed at 50°C for 30 minutes, followed by a curing step at 100-120°C for 15 minutes. According to the 6,552,093 patent, this two-step process is believed to fuse the polymer particles, forming a film with similar properties to those extruded in the sulfonyl fluoride (thermoplastic) form and then hydrolyzed and acid exchanged.

U.S. Patent No. 6,641,862 provides further detail on the film-forming process. In this patent, a Nafion "Web" is formed as one component of a membrane electrode assembly. A coating of "high-viscosity" Nafion ionomer dispersion is applied at a wet layer thickness of about 8 mils on a silicon-coated film of biaxially oriented polyethylene

terephthalate (PET) using a “knife over roll” wet-layer application tool. The solution was dried and cured by passing the web under infrared lamps of about 3 kW located 1 foot away and a blower moving air over the web for cooling. The web speed was about 0.25 m/min (0.8 ft/min). The resulting film was 10 microns in thickness. (Two, 10-micron ionomer layers were laminated together in the finished membrane electrode assembly.)

From DuPont’s product data bulletin, NRE-212 membranes are packaged as shown in Figure 30 below. The Nafion membrane is positioned between the two layers – a coversheet and a backing layer. The coversheet is a 0.7 mil polypropylene (PP) film, the backing sheet is a 2.0 mil silicone-treated polyester film. The composite is wound on a 6 in. ID plastic core. Standard roll widths are 12 in. (305 mm) and 24 in. (610 mm); standard lengths are 100 m.

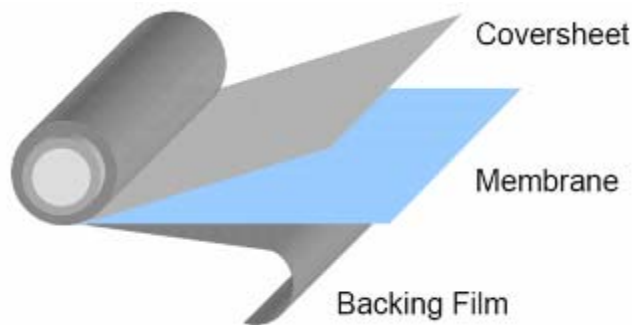


Figure 30. Nafion Membranes Structure

Ref: DuPont™ Nafion PFSA Membranes Product Information (NAE201, 2004)

The assumptions made about the cast dispersion film-forming process, based on DuPont/Ion Power information and TIAX expertise in similar processes are summarized as follows.

- Nafion dispersion of 40% by weight solids in 30% water and 30% isopropanol (somewhat higher than the Ion Power LQ-1115)
- Roll-coating process starts with 2.5 mil wet film thickness to produce 1.0 mil (25 micron) dry film thickness.
- Coating applied to a 2.0 mil silicone-treated PET (26 in. wide) backing film
- Preferred coating arrangement is “knife over roll”
- Drying process occurs in a 3-stage oven
 - Flash dry (solvent removal) is 30 minutes at 50°C
 - Full dry (curing) is 15 minutes at 110°C
 - Forced air cooling is 5 minutes at 20°C
- Line rates are in the range of 10-20 ft/minute
- 2.0 mil (50 µm) membrane is produced by a double pass (2 x 1.0 mil per pass)
- Lamination with 0.7 mil polypropylene (PP) coversheet
- Final product will be 24 in (0.61 m) wide by 328 ft (100 m) on a 6 in plastic roll core.
- Quality control stage includes pin-hole detection/web inspection
- Class 10,000 clean room environment required

Based on the assumptions above and a schematic of a coater-laminator line (10), a process flow can be laid out as shown in Figure 31.

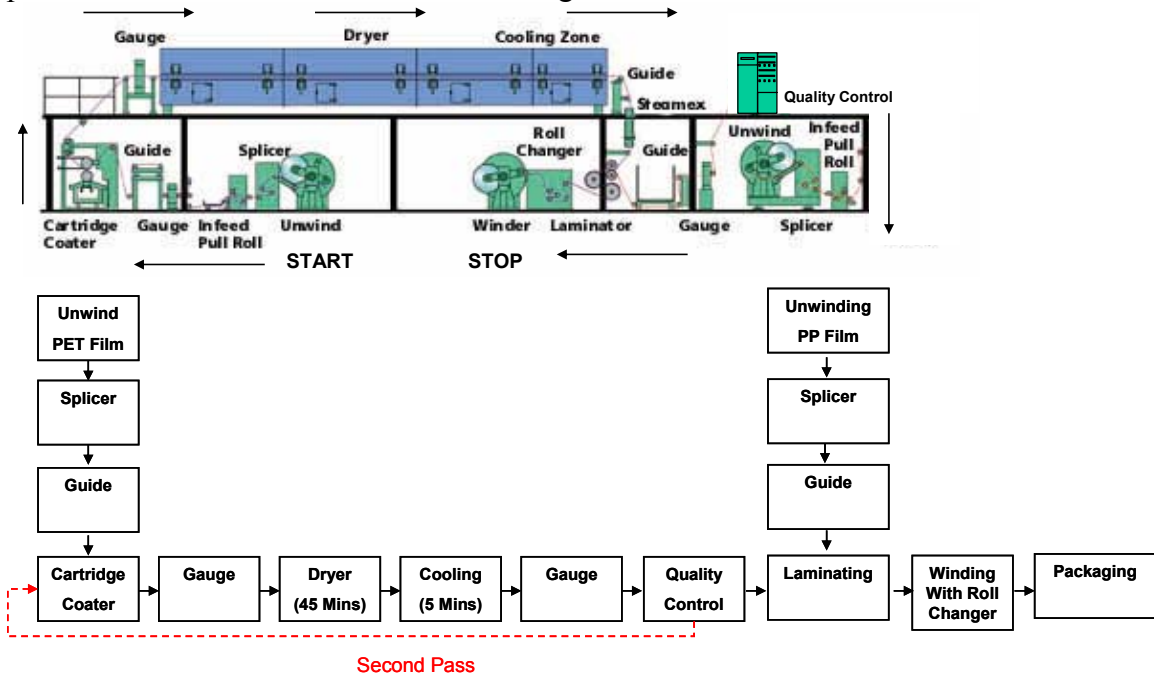


Figure 31. Membrane Manufacturing Process Flow

Ref: Black Clawson

The carrier film is approximately 2 meters wide, which is the maximum practical for this type of coating line. The coating may be done by reverse roll coating or knife over roll. The capital costs for each are quite similar, and coating quality will depend on dispersion rheology and the solvent system used in the dispersion. The oven has three sections for controlled heat-up, bake-dry, and cool-down. Wet and dry film thicknesses are monitored using convention technologies such as beta gauges. Moisture gauges monitor the water content of the film exiting the oven. Precise control of the moisture content is required to control the “plasticity” of the Nafion polymer. A second pass through the process will be run when thicker coatings are required. A laminating station adds the coversheet to the product. The edges are trimmed and the film is wound up at the last station in the line. Products may be slit to measure in-line or off-line. Rolls are bagged with metallized polyester overwrap to control the internal atmosphere.

Major Material and Process Parameters

We estimate that the raw material ionomer costs \$80/lb at high volume. Gebert et al.’s paper (11) has a lower ionomer cost of ~ \$30-50/lb. One of the major industry manufacturers indicated that \$80/lb is on the lower side. Table 17 lists the material parameters for the manufacture of the membrane.

Table 17. Membrane Material Parameters

Material List	Density (g/cc)	Cost (\$/kg)
Nafion	1.97	176
Isopropanol	0.78	1.5

The process Capital Expenses (CapEx) are based on conversations with original equipment manufacturers and the cycle time is based on a line speed of 20ft/min. U.S. Patent No. 6,641,862 shows that the membrane coating line speed is about 1 ft/min, but we assumed 20 ft/min based on industry feedback. The production line is fully automated and not labor intensive. The overall yield for the membrane process line is about 95%, based on industry feedback. Table 18 lists the process parameters for the manufacture of the membrane.

Table 18. Membrane Process Parameters

Process Description	CapEx (\$)	Labor Per Station
Unwinding	100,000	0.1
Splicer	50,000	0.1
Guiding	50,000	0.1
Cartridge Coater	350,000	0.1
Gauging	60,000	0.1
Dryer with Solvent Burner	5,000,000	0.1
Quality Control	150,000	0.1
Laminating	250,000	0.1
Winding with Roll Changer	100,000	0.1
Packaging	100,000	0.1

9.2.1.3. Membrane Costing

Baseline Cost

The estimated membrane cost is \$23/m², in which material cost represents about 90% of the total cost. Table 19 shows the membrane cost break down according to material and process.

Table 19. Membrane Material and Process Cost (on an active area basis)

Process	Material		Process	
	(\$/m ²)	(\$/kg)	(\$/m ²)	(\$/kg)
Film Handling	0.37	37.0	0.31	3.1
Coating	19.14	191.4	.61	6.1
Drying & Cooling	0.00	0.00	1.16	11.6
Quality Control	0.00	0.00	0.09	0.9
Laminating	0.00	0.00	0.07	0.7
Packaging	1.56	15.6	0.07	0.7
Subtotal	21.08	210.8	2.31	23.1
Total	23.38 (\$/m ²)			
	233.8 (\$/kg)			

Figure 32 illustrates that the material cost accounts for about 90% of the total membrane cost, while all other costs are about 10%. The capital cost and equipment and tooling cost are the second and third cost drivers. This process is not labor intensive, and labor cost is a minor fraction of total cost.

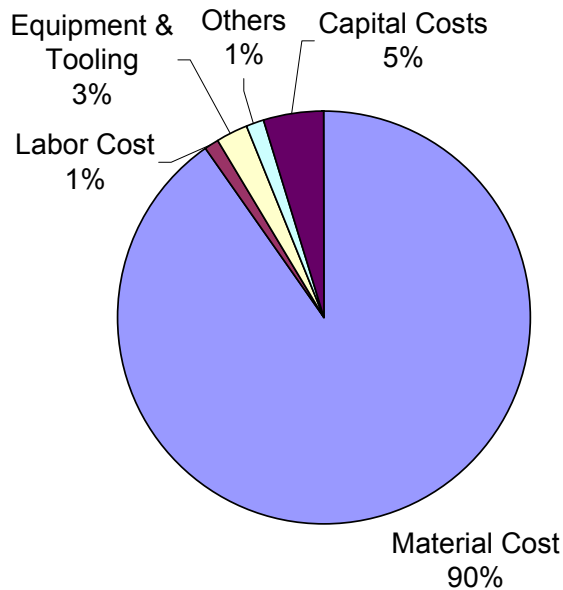


Figure 32. Membrane Cost Breakdown Pie Chart

Single Variable Sensitivity Analysis

We varied the Nafion cost, membrane web width, web coating speed, and overall membrane process yield to run single variable sensitivity analysis. This method tests each variable independently; it freezes the other variables at their baseline values when analyzing one variable. This method is also known as “one-at-a-time perturbation” or “parametric analysis.” (12)

We chose a minimum Nafion cost based on Gebert et al.’s paper (11) and a maximum cost based on industry feedback. The range of values for web width is based on TIAX experience. The minimum web speed is based on Ion Power’s patent (1ft/min) and industry feedback, while the maximum is from industry feedback. The minimum and maximum membrane yield is from industry feedback. Table 20 shows the range of values for the membrane cost sensitivity analysis.

Table 20. Membrane Single Variable Sensitivity Analysis Data Range Table

Specifications	Minimum	Most Likely	Maximum
Nafion Cost (\$/lb)	20	80	100
Web Width (cm)	60	200	200
Web Speed (ft/min)	5	20	50
Membrane Yield (%)	88%	95%	95%

The Tornado chart in Figure 33 shows that the Nafion cost has the most effect on membrane cost, which could drop to about \$10/m² when Nafion cost is \$20/lb. The membrane web speed, web width, and process yield have smaller impacts on the membrane cost for the parameter ranges assumed.

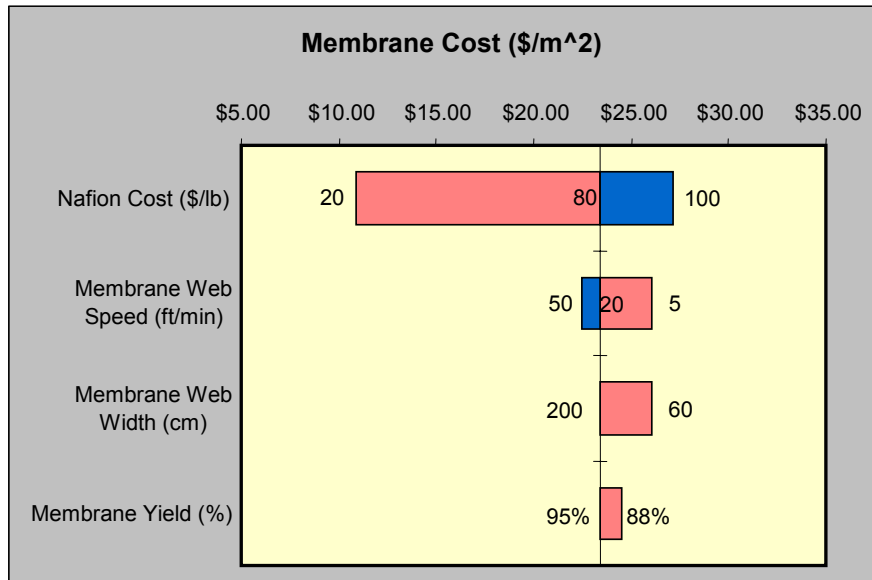


Figure 33. Membrane Single Variable Sensitivity Analysis Tornado Chart

Cost Comparison

DuPont's 2 mil non-reinforced membrane cost projection (5), GM's 1 mil non-reinforced membrane cost projection (13), and TIAX's membrane cost estimate are compared in Figure 34. DuPont's data is not available at high volume (500,000 vehicle/year). But, we can still see that TIAX's estimate is between DuPont's and GM's membrane cost projection.

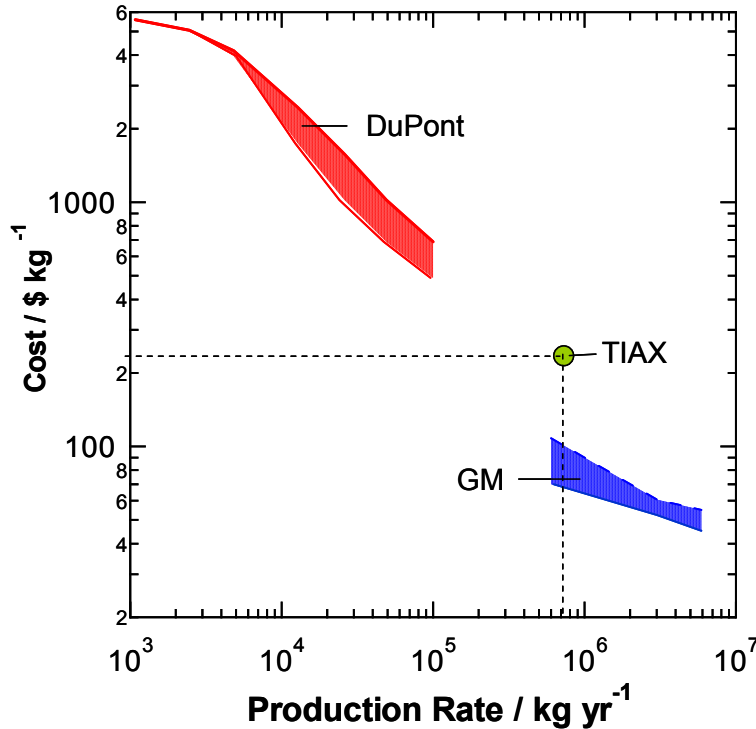


Figure 34. DuPont, GM, and TIAX Membrane Cost Comparison

Mass Production

High volume, (500,000 vehicles per year) would require 7.5 million square meters of membrane annually. A single coating line (2 mil membrane) is estimated to cost about \$6 million and a total of 3 lines would be required to meet this annual production. The total capital investment on membrane equipment is about \$20 million to meet the requirement of 500,000 vehicles annual production. The following are the assumptions:

- Stack – 90 kW gross power per stack
- Stack power density = 600 mW/cm²
- Downtime ~ 20%
- Yield assumption ~ 95%
- Operating 3 shifts (20 hours)/day, 240 days/year and production rate is ~ 4,167 stacks/day

9.2.2. Gas Diffusion Layer (GDL)

9.2.2.1. Description

Background and Information Sources

Carbon fiber-based diffusion media has high porosity and electric conductivity and is widely used as a gas diffusion layer. The woven carbon cloth and non-woven carbon paper are commercially available for fuel cell application. Woven carbon cloth does not need a binder because of its woven structure, whereas non-woven carbon paper is bonded by carbonized resin. Diffusion layers are normally made hydrophobic in order to avoid flooding. The typical treatment uses PTFE to increase hydrophobicity.

From developer discussions, we learned that the woven carbon cloths have less defects, are easier to coat, and have higher coating web speeds, but are more expensive than non-woven carbon paper. We picked woven carbon cloth-based GDLs for our baseline. The specification is based on E-TEK[®] GDL LT 1200-W, which has 275 micron thickness at 1 psi.

The above information, along with TIAX knowledge of carbon fiber and coating manufacturing processes, was used to construct a GDL fabrication process for cost modeling.

9.2.2.2. Manufacturing Process

We assume that the woven carbon cloth is available in un-coated rolls. The hydrophobic process starts with preparing the hydrophobic ink. The material parameters for the manufacture of the GDL are shown in Table 21.

Table 21. GDL Material Parameters

Material List	Loading (mg/cm ²)	Cost (\$/kg)
Woven Carbon Cloth	N/A	30
PTFE	1.75	20.75
Carbon Powder	2	3.35
Water	10	0.05

Figure 35 is a process flow chart for the manufacture of the GDL.

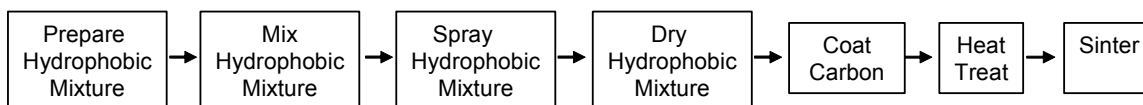


Figure 35. GDL Manufacturing Process Flow Chart

The following specific conditions and parameters were assumed:

- The hydrophobic solution, consisting primarily of PTFE and carbon powder, has a solids content of 27 wt%.

- A three-stage heat treatment oven was used for sintering
 - The first stage was at 80°C for 20 minutes to achieve uniform distribution of PTFE polymer.
 - The second stage was at 250°C for 10 minutes to allow PTFE emulsification.
 - In the third stage, the roll is heated to 350°C for 10 minutes to fix PTFE to the surface.

The process temperature and cycle time are for costing purpose only. In reality, the process step, cycle time, and firing temperature will vary.

The woven carbon cloth cost is based on the carbon fiber cost and the process cost, which includes several process steps, such as stabilization, spun yarn formation, weaving and carbonization. We assume that the PTFE is DuPont Teflon® T-30 and the carbon powder material price is a quote from Cabot®.

The CapEx process is based on conversations with industrial equipment manufacturers. The cycle time is based on a line speed of 50 ft/min. We assumed a 50% ink loss in the process of spraying the hydrophobic mixture. Table 22 lists the process parameters for the manufacture of the GDL.

Table 22. GDL Process Parameters

Process Description	CapEx (\$)	Cycle Time	Labor Per Station
Prepare Hydrophobic Material	20,000	30 Min	0.2
Mix Hydrophobic Material	50,000	300 Min	0.2
Spray Hydrophobic Material	100,000	50 Feet/Min	0.2
Dry Hydrophobic Material	400,000	20 Min	0.2
Heat Treatment	350,000	10 Min	0.2
Sinter	400,000	10 Min	0.2

9.2.2.3. Costing

Our baseline cost for the GDL is \$18.4/m², which includes both the cathode and anode side GDL layers. The material cost is about 95% of total cost, primarily because of high woven carbon cloths cost.

The developer cost estimates for a single layer GDL at high volume varies from \$5/m² to \$10/m² according to whether non-woven carbon paper or woven carbon cloth is used as the basis. Table 23 lists the material and process costs for the GDL.

Table 23. Material and Process Costs (on an active area basis)

	GDL (\$/m²)
Material	17.68
Capital Costs	0.66
Labor	0.19
Tooling	0.23
Other¹	0.13
Total	18.40

¹ Other costs include utilities, maintenance and building.

9.2.3. Bipolar plates

9.2.3.1. Description

Introduction

The bipolar plates are the largest volume and weight contributor to the PEM fuel cell stack and have a significant effect on the stack cost. There are several different technologies available to make bipolar plates. Table 24 shows four major material options.

Table 24. Bipolar Plate Material and Process Comparisons

Material	Processes	Process Layout
Graphite Polymer Composite	Compression Molding, Injection Molding, Polishing	Discrete
Carbon-Carbon Composite	Slurry Molding, Chemical Vapor Infiltration	Discrete
Flexible Graphite Foil	Expanded Flake, Rolling, Emboss Impression Molding	Roll-to-Roll Continues
Sheet Metal	Stamping, Joining, Coating	Discrete

Graphite polymer composite bipolar plates use inexpensive graphite material and a compression/injection molding process. Until this year, we used molded graphite plates as the baseline in the PEM fuel cell study. But, they may have limitations on thickness reduction and conductivity improvement.

Carbon-Carbon composite bipolar plates were developed by Oak Ridge National Laboratory (ORNL) and are being commercialized by Porvair. The bipolar plates are made by a low-cost slurry molding process to produce a carbon fiber preform and are then made hermetic through chemical vapor infiltration (CVI) with carbon. The infiltrated carbon also increases conductivity. The estimated cost is about \$26/m² at high volume, in which the CVI process cost is about 70%. The high process cost limits the application of this approach.

Metal bipolar plates can be made in thin sheets by traditional stamping processes and could be easily mass produced. But, proprietary coatings are needed for corrosion protection and stable conductivity. The coating process will be a major cost contributor.

Flexible graphite foil bipolar plates are made from expanded natural graphite flakes. They can be made thin to reduce stack volume. Graphite foil also has high electrical conductivity, low contact resistance, and low specific density, and it can be manufactured in roll-to-roll continuous process using emboss compression molding.

Figure 36 is an example process flow from the Graftech[®] company website. We selected flexible graphite foil bipolar plates as baseline in this cost study. We also assume that there are cooling channels in the middle of every bipolar plate.

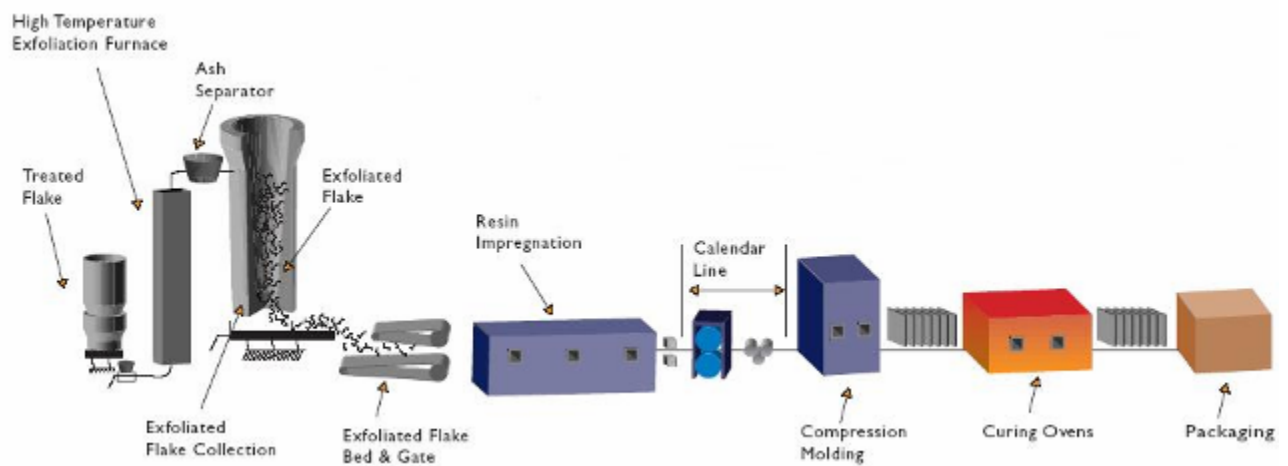
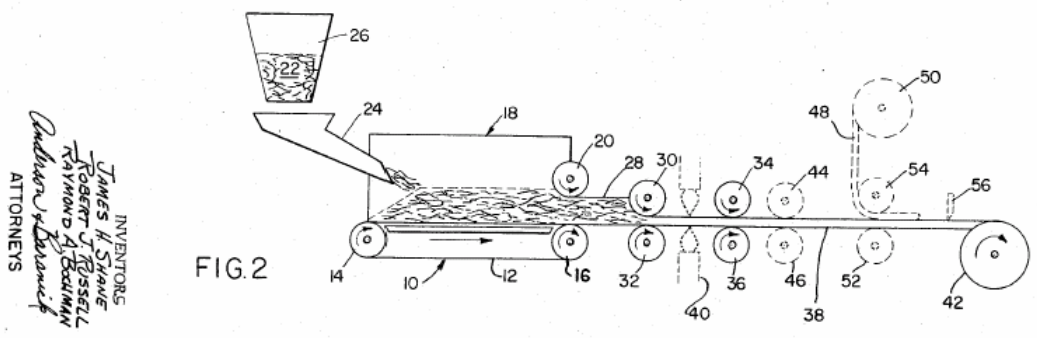
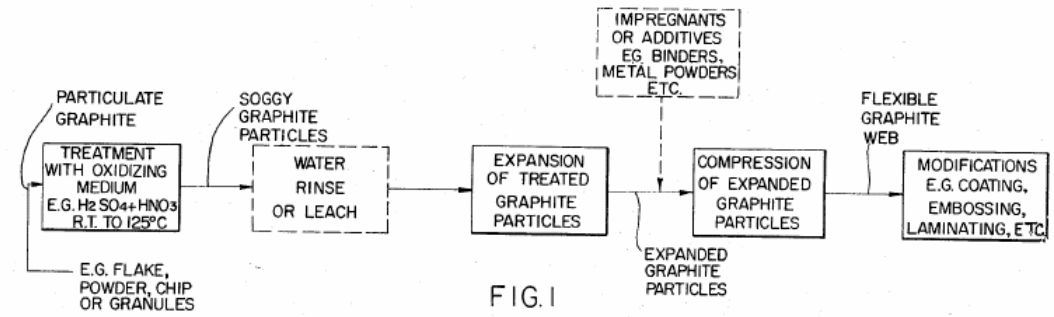


Figure 36. Grafcell[®] Production Process from GrafTech Website

9.2.3.2. Manufacturing Process

U.S. Patent No. 3,404,061 describes a process for making flexible graphite web using natural graphite flake. Figure 37 shows the process flow chart. According to the patent, the flake is cleaned by acid to remove metal impurities and then rinsed by water or leach. The cleaned flake is sintered at 1000°C to obtain expansion in the c-direction. In this process, the c-direction dimension of the expanded particles ranges from about 100 to about 300 times that of the original dimension. Next the expanded graphite particles are compressed by roll into flexible graphite web.



INVENTORS
 JAMES H. SHAW
 ROBERT J. RUSSELL
 RAYMOND A. BUSHMAN
 Attorneys
 ANDERSON & BARNHART

Figure 37. U.S. Patent 3,404,061 Flexible Graphite Web Process

U.S. Patent No. 6,663,807 provides further detail on the emboss compression molding process. In this patent, a flexible graphite sheet passes through a vessel and is impregnated with a resin system. Then, the foil is dried and calendared to dimension (0.075mm to 3.75 mm). Finally, the foil passes through the emboss roll press to form the final shape and is cured in a low temperature oven (90~120°C) for 3 to 30 min. Figure 38 is a schematic representation of the emboss compression molding of flexible graphite.

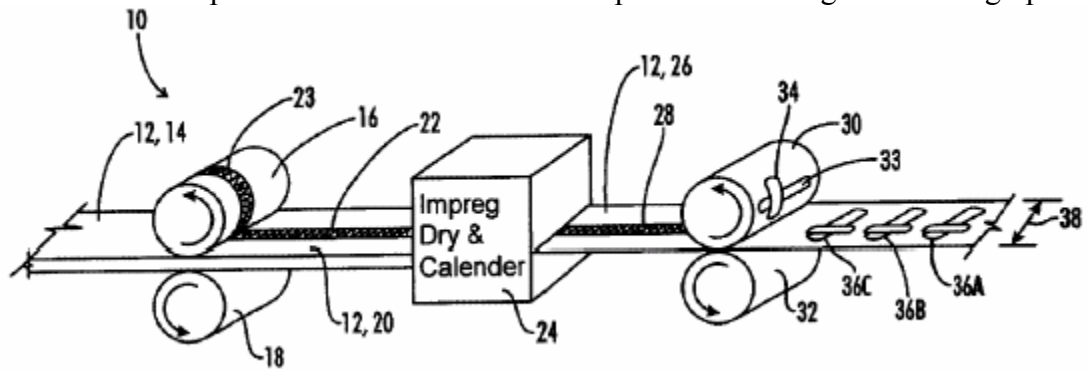


Figure 38. Embossing a Sheet of Flexible Graphite Material

The assumptions made about the embossing compression molding process are based on the patent literature, feedback from Graftech, and TIAX expertise in similar processes. The process assumptions used can be summarized as follows:

- Natural graphite flake raw material costs \$1.2/lb.
- Expanded graphite flake costs \$2.0/lb.
- Flexible graphite foil thickness is 1 mm.
- Flexible graphite foil web width is 42 mm.
- Line rates are about 20 ft/minute.
- Drying oven will be on for 3 to 30 minutes at 90 to 120°C.
- Two graphite plates are in parallel layout in the foil.
- Process line yield 95% and material scrap rate 10% (recyclable).

Figure 39 shows the flexible graphite foil bipolar plate process flow used in the cost estimation. We assumed that the expanded graphite flake is \$2/lb and we did not cost the first three process steps. Only the process steps within the dashed line frame are included in the cost model. Two plates are bonded together to form a cooling bipolar plate.

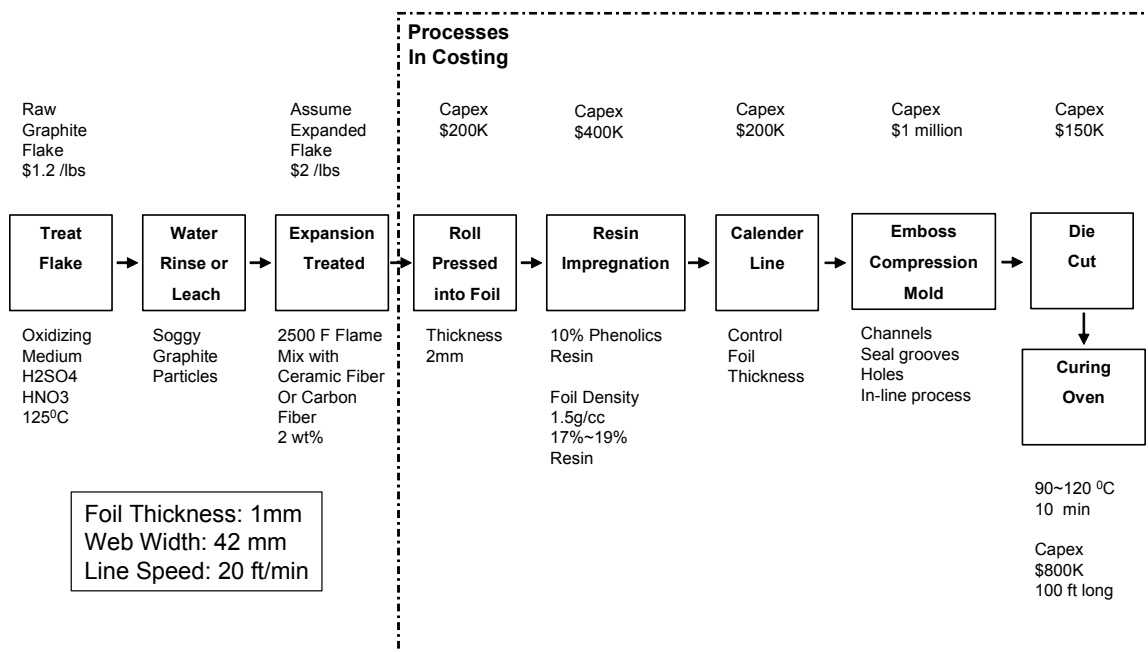


Figure 39. Graphite Foil Bipolar Plate Process Flow

Table 25 lists the material parameters and Table 26 lists the process parameters for the manufacture of the graphite foil bipolar plate.

Table 25. Graphite Foil Bipolar Plate Material Parameters

Material List	Content	Cost (\$/kg)
Expanded Graphite Flake	81%	4.40
Vinyl Ester	15%	3.73
Carbon Fiber	2%	10.00
Poly Dimethylsiloxane (SAG)	0.05%	18.50
Methyl Ethyl Ketone Peroxide	1.0%	6.66
Colbat Napthenate	0.3%	8.18

Table 26. Graphite Foil Bipolar Plate Process Parameters

Process Description	CapEx (\$)	Cycle Time	Labor Per Station
Oxidizing Graphite Flake	300,000	-	-
Water Rinse or Leach	300,000	-	-
Expansion Treatment	2,000,000	-	-
Roll Press	200,000	20 ft/min	0.2
Resin Impregnation	400,000	20 ft/min	0.2
Calender Foil	200,000	20 ft/min	0.2
Emboss Compression Mold	1,000,000	20 ft/min	0.2
Die Cut	150,000	1 plates/sec	0.2
Curing Oven	800,000	30 min	0.2

9.2.3.3. Costing

The graphite foil bipolar plate costs \$17.35/m² at high volume (500,000 vehicle/year). The material cost is about 60% and process cost is about 40% of total. Table 27 illustrates the cost breakdown.

Table 27. Graphite Foil Bipolar Plate Cost Break Down

Bipolar Plate Cost based on Active Area (\$/m ²)		
	Material	Process
Roll Form	10.23	0.90
Impregnation		1.00
Calender		0.64
Compression Molding		2.08
Die cut		0.55
Curing		1.95
Subtotal	10.23	7.12
Total	17.35	

In the process cost, the emboss compression and curing processes are the major cost contributors. Each of these steps is about 30% of the total process cost. High CapEx costs are one of the main reasons. Figure 40 shows the process cost comparison.

Major Process Costs (\$/m²)

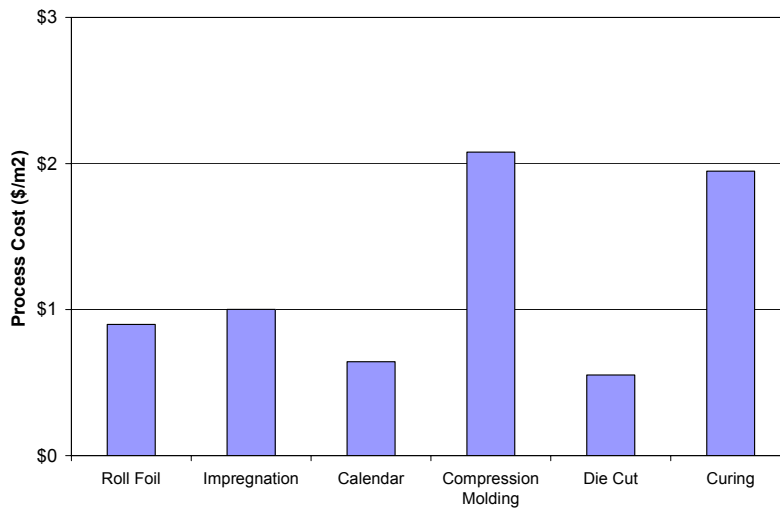


Figure 40. Graphite Foil Process Cost Bar Chart

Compression Molded Graphite Bipolar Plates

We also estimated the cost of compression molded synthetic graphite bipolar plates, which have the same geometry as the flexible graphite foil plate. The result shows the two different processes have very close costs. Figure 41 shows the compression molded plates’ process and Table 28 is the cost breakdown.

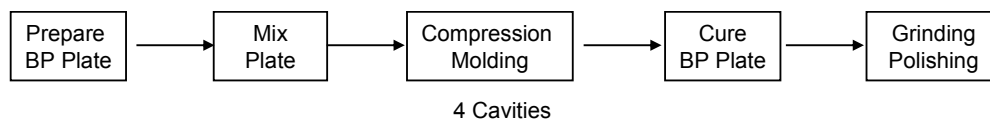


Figure 41. Compression Molded Bipolar Plate Process Flow

Table 28. Compression Molded Bipolar Plate Cost

	Bipolar Plate \$/m ²
Material	8.65
Capital Costs	3.42
Labor	2.26
Tooling	2.90
Others	1.40
Total	18.64

9.2.4. MEA

9.2.4.1. Description

Introduction

The MEA is the key stack component. A typical five-layer MEA includes anode side GDL, anode, membrane, cathode, and cathode side GDL. The platinum based catalyst can be deposited either on the GDL or the membrane. The catalyst layers are normally 3 to 20 microns thick. The thick catalyst layer is typically deposited on the GDL, while thinner catalyst layers are typically deposited on the membrane because of the GDL's rough surface.

Platinum cost and loading are major cost drivers for MEA cost. The current platinum cost is about \$850 ~ 900/troz, whereas historical prices have been about \$450/troz (14). We used \$900/troz platinum as a baseline to reflect the current price. The total platinum loading is 0.75 mg/cm² in baseline cost analysis based on feedback from the Tech Team and developers. The baseline power density is 600 mW/cm².

U.S. Patent No. 6,716,550 B1 describes an MEA using edge seals to seal reactant fluid stream passages to prevent leaks or inter-mixing of fuel and oxidant fluid streams. According to the patent, a separate framing seal engages the edge of MEA. In Figure 42, framing seal 150 comprises two sealing portions 152 and a web portion 154. The two sealing portions and the web portion are of a unitary construction. MEA 110 fits into groove 156. Figure 43 illustrates a plan view of an MEA with framing seal 150 and MEA 110. Manifold seals (165) are formed together with framing seals. The patent also provides the framing seal material, which could be silicones, ethylene propylene diene monomer (EPDM), natural rubber, etc.

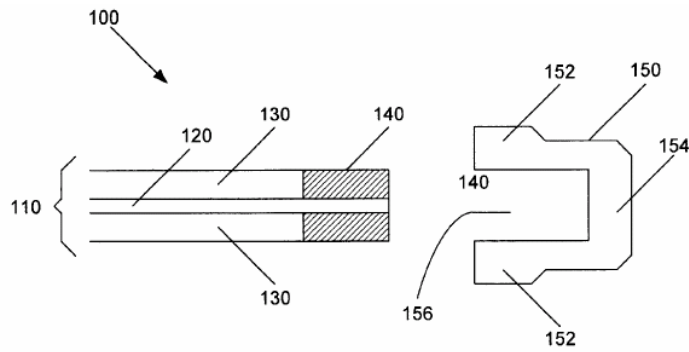


Figure 42. Framing Seal Structure (U.S. Patent No. 6,716,550)

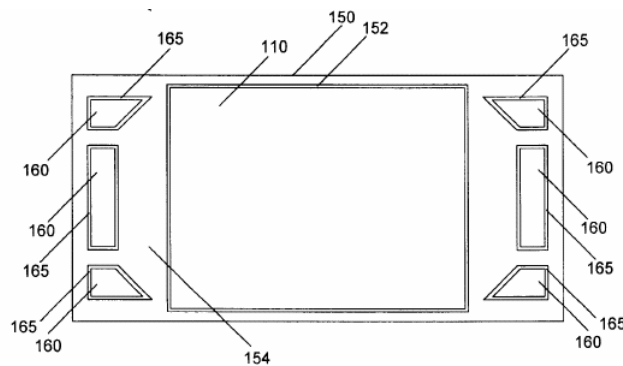


Figure 43. Framing Seals Layout (U.S. Patent No. 6,716,550)

Using the above information, along with TIAX knowledge of MEA design and analysis, we selected a baseline MEA design for cost modeling. Figure 44 illustrates the cross section of the MEA. The membrane is about 1mm larger than GDL at both sides. We have separate manifold seals for the air, fuel, and water channels.



Figure 44. MEA Structure

9.2.4.2. Manufacturing Process

Manufacturing Process

The MEA manufacturing process starts with preparation of anode and cathode layer inks. We used a gravure printing process to deposit the electrodes onto the GDLs. After the drying process, anode/GDL and cathode/GDL layers are pre-cut to size, but still connected in roll. The reason for this is that the final size of the anode/GDL and cathode/GDL layers is slightly smaller than membrane size.

Finished membrane, anode/GDL layer, and cathode /GDL layer are all in roll stock form. The five layers are assembled by hot press lamination. This roll-to-roll process improves throughput and reduces the manufacturing cost. After this, the MEA is die-cut into individual sheets. After this step, the process becomes a succession of discrete steps. Finally, the frame seals are cast into place. Figure 45 illustrates the whole MEA process.

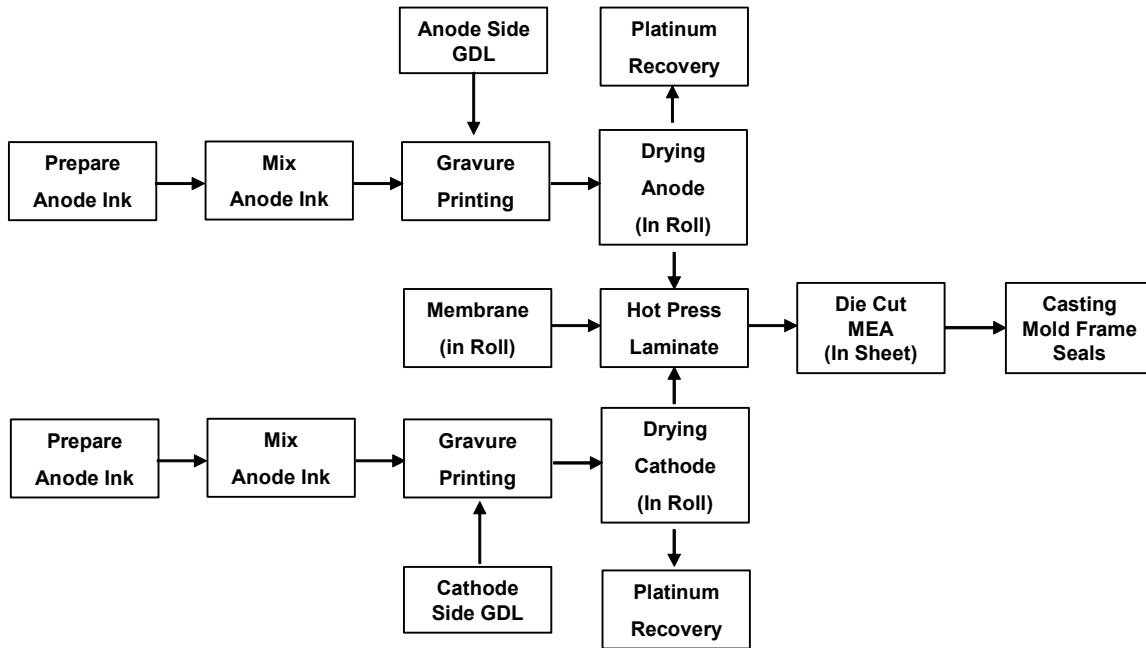


Figure 45. MEA with Frame Seals Manufacturing Process Flow

Major Material and Process Parameters

We assume that the anode catalyst loading is 0.25 mg/cm^2 , which is one third of the total platinum loading, and the cathode catalyst loading is 0.5 mg/cm^2 , which is two thirds of the total platinum loading. The assumed platinum cost is \$900/troz (\$28,936/kg). We assume there is an additional 20% of platinum cost to cover the catalyst preparation cost. The final platinum cost is \$1,080/troz (\$34,723/kg). Table 29 and Table 30 show the anode/cathode ink concentration and material costs.

Table 29. Anode Material Parameters

Material List	Content (mg/cm ²)	Cost (\$/kg)
Anode Nafion Loading	0.6	176
Anode Catalyst Support Carbon Powder	1.2	3.35
Catalyst Platinum	0.25	34,723 (added 20% process cost)
Electrode Solvent Glycerol	24	2
Nafion Solvent Alcohol	12	1.5
Water	6	0.05

Table 30. Cathode Material Parameters

Material List	Content (mg/cm ²)	Cost (\$/kg)
Cathode Nafion Loading	0.6	176
Cathode Catalyst Support Carbon Powder	10.6	3.35
Catalyst Platinum	0.5	34,723 (added 20% process cost)
Electrode Solvent Glycerol	12	2
Nafion Solvent Alcohol	12	1.5
Water	6	0.05

The fully automated roll-to-roll process has a 50 ft/min web speed and is not labor intensive. Table 31 illustrates the major process parameters.

Table 31. MEA Process Parameters

Process Description	CapEx (\$)	Cycle Time	Labor Per Station
Material Preparation (weigh)	20,000	30 min	0.2
Mixing Material	50,000	300 min	0.2
Gravure Printing	35,000	50 ft/min	0.2
Drying	300,000	30 min	0.2
Hot Press and Blank	150,000	0.17 min/cell	0.2
Mold Framing Seal	300,000	0.5 min/4 cells	0.2

9.2.4.3. Costing

The MEA costs \$325/m² with platinum loading of 0.75mg/cm². Material cost contributes about 96% and process cost contributes the balance. The electrodes dominate with about 85% of the total cost, because of the high platinum loading and high platinum cost. Table 32 shows the MEA cost breakdown.

Table 32. MEA Cost Break Down

	MEA1 (\$/m²)	Frame Seal1 (\$/m²)
Material	310.22	1.08
Membrane	-21.17	
Electrode	-271.86	
GDL	-17.18	
Capita Recovery	8.70	1.04
Labor	0.53	0.82
Tooling & Equipment	0.91	0.97
Other²	0.50	0.44
Subtotal	320.86	4.35
Total	325.21	

¹ m² of active area

² Other costs include utilities, maintenance and building

9.2.5. Gasket

9.2.5.1. Description

We assume that the MEA is sealed to the bipolar plate by an “O-ring” type gasket in a groove. The molded or form-in-place (FIP) gasket form seals around air, fuel, and water channels.

U.S. Patent No. 5,284,718 describes a gasket structure for the air, fuel, and water channels. According to the patent, the gasket grooves are molded to the bipolar plate. A SANTOPRENE brand rubber is used as gasket material, and the gasket is punched out by a metal die. Figure 46 and Figure 47 show the gasket and gasket groove structure.

We assume a similar gasket structure in our baseline model. We assume the gasket material is Nitrile Rubber (NBR) and a transfer molding process is used.

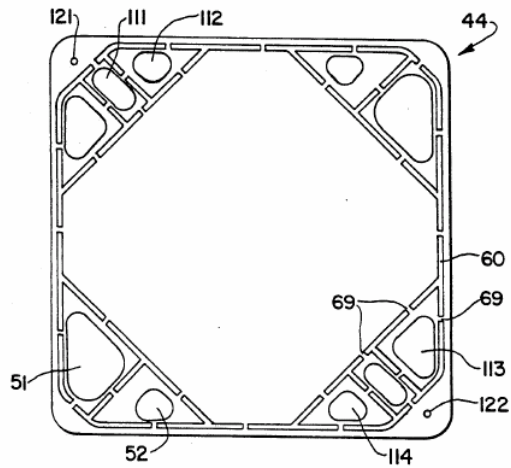


Figure 46. U.S. Patent 5,284,718, A Top View of Gasket Grooves in Bipolar Plate

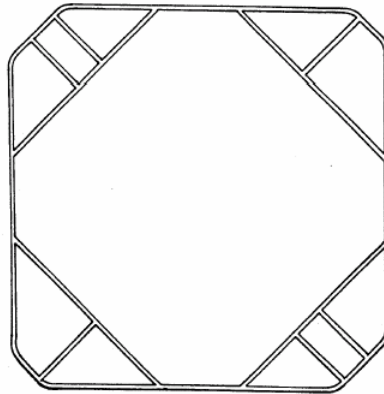


Figure 47. U.S. Patent 5,284,718, A Top View of a Sealing Gasket

9.2.5.2. Manufacturing Process

Transfer molding has a shorter cycle time than compression molding, but longer than injection molding. The bipolar plate is used as part of the “die” and the NBR gasket can be formed in place. Transfer molding has a higher material scrap rate because of the non-utilized “transfer pad.” Table 33 and Table 34 show the major material and process parameters.

Major Material and Process Parameters

Table 33. Seal Material Parameters

Material List	Density (g/cc)	Cost (\$/kg)
NBR	1.5	11.00

Table 34. Gasket Molding Process Parameters

Process Description	CapEx (\$)	Cycle Time	Labor Per Station
Transfer Molding	280,000	5 min/ 16 cavities	0.2

9.2.5.3. Costing

The gasket costs about \$1.72/m², in which material cost is about 30% and process cost is about 70%. The gasket cost is less than 1% of total stack cost. Table 35 illustrates the gasket cost break down.

Table 35. Gasket Cost Break Down

	Seal1 (\$/m2)
Material	0.49
Capital Costs	0.40
Labor	0.26
Tooling	0.39
Other ²	0.18
Total	1.72

¹m² of active area

²Other costs include utilities, maintenance and building

9.2.6. Stack Assembly

The final stack assembly integrates fully automated pick-and-place assembly robots and manual labor.

- The bipolar plates with gaskets, the MEAs with framing seals, end plates, and tie bolts are assembled by a pick-and-place robot.
- The current conductors, insulators, and outer wrap are mounted manually.
- Final stack conditioning and QC are costed separately and not included in the baseline stack cost. Figure 48 illustrates the stack assembly process flow.

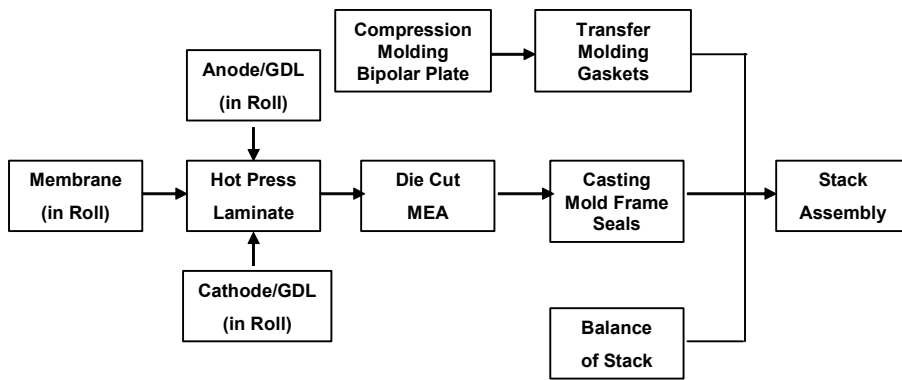


Figure 48. Stack Assembly Flow Chart

9.2.7. Stack Cost

9.2.7.1. Baseline Cost

The stack baseline cost is \$67/kW (net electric power) or \$5,360. The baseline power density assumption is 600 mW/cm². The electrodes represent approximately 77% of the fuel cell stack cost because of the increased platinum loading (0.75 mg/cm²) and platinum cost (\$900/troz). Figure 49 shows the stack cost breakdown pie chart. As a reference, the 2004 fuel cell stack cost estimate was \$72/kW with a platinum loading of 0.30 mg/cm², a power density of 350 mW/cm², and a platinum cost of \$450/troz.

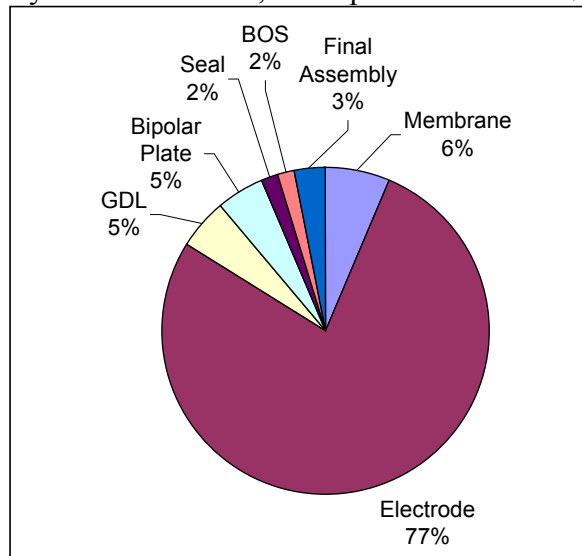


Figure 49. Stack Baseline Cost (\$/kW)

9.2.7.2. Single Variable Sensitivity Analysis

We varied the platinum cost, platinum loading, power density, membrane cost, GDL cost, and graphite material cost to perform a single variable sensitivity analysis in which each parameter is varied independently.

The minimum platinum cost corresponds to the historical price (14) and the maximum is the current price. The minimum platinum loading is from the 2004 TIAX study (15) and the maximum platinum loading is based on DOE, Tech Team, and developer feedback. The minimum power density is from the TIAX 2004 study (15) and the maximum is from literature data. The minimum membrane cost is referenced from the GM paper (13) and the maximum is from developer feedback. The minimum and maximum of GDL and graphite material costs are both from developer feedback.

Table 36. Stack Sensitivity Analysis Variable Ranges

Process Description	Units	Sensitivity Analysis		
		Min	Baseline	Max
Platinum Cost	\$/troz	450	900	900
Platinum Loading	mg/cm ²	0.30	0.75	0.75
Power Density	mW/cm ²	350	600	800
Membrane Cost	\$/m ²	10	23	50
GDL Cost	\$/m ²	10.00	18.40	20.00
Graphite Foil Material Cost	\$/lb	1.00	2.00	3.00

The Tornado chart in Figure 50 shows that the power density has the largest effect on stack cost, which could vary from \$50/kW to \$110/kW. The platinum cost and platinum loading also have a significant impact on the stack cost. In the low platinum cost case, the stack cost can drop to \$45/kW. The membrane cost, graphite material cost, and GDL cost have a smaller impact on stack cost.

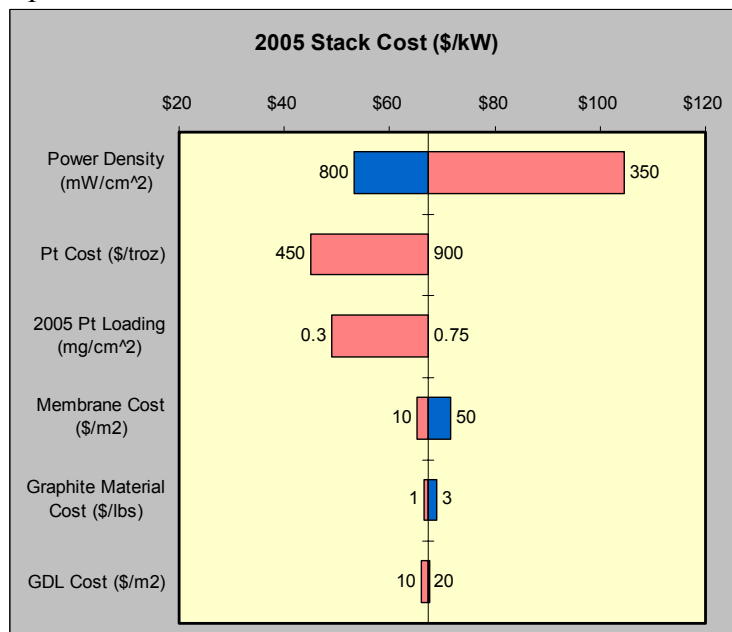


Figure 50. Single Variable Sensitivity Analysis Tornado Chart

9.2.7.3. Monte Carlo Simulation

In the sensitivity chart, the horizontal bars show magnitude and direction of sensitivity. Figure 51 illustrates again that power density has the most powerful impact on stack cost, while platinum cost and loading are in second and third position consistent with the single variable sensitivity analysis.

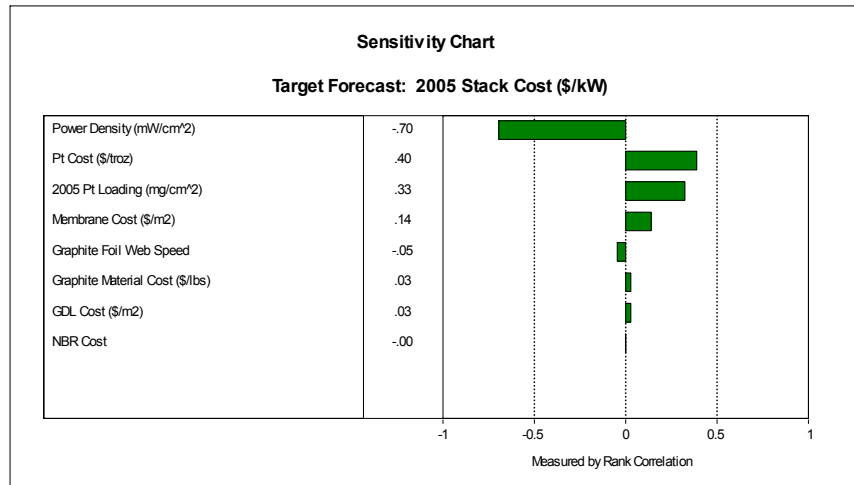


Figure 51. Stack Cost Monte Carlo Simulation Sensitivity Chart

The multi-variable sensitivity analysis in Figure 52 shows that the mean stack cost is \$57/kW at a production volume of 500,000 units per year. For the input parameters used this analysis shows a 77% certainty that the mean stack cost will be below the DOE target of \$65/kW. The TIAX baseline stack cost of \$67/kW is based on typical parameters, while the mean stack cost of \$57/kW is based on the whole set of parameters included in the sensitivity analysis.

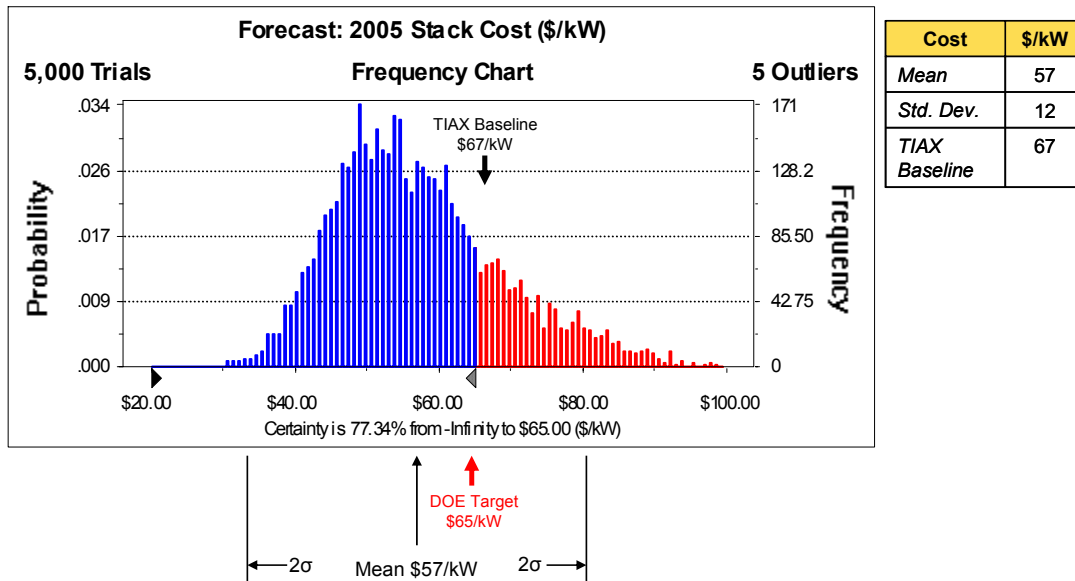


Figure 52. Stack Cost Monte Carlo Simulation Frequency Chart

9.2.7.4. Stack Cost Comparison – 2004 vs. 2005

Table 37. Stack Cost Comparison 2004 vs. 2005 (\$/m²)

Component	2004 Cost1 (\$/m ²)	2005 Cost1 (\$/m ²)	% Change
Membrane	48.85 ²	23.38	-52%
Electrode	67.19	279.02	315%
GDL	32.00	18.40	-43%
Bipolar Plate	28.10	N/A	N/A
Bipolar Plate with Cooling	27.45	17.38	-37%
Seal	7.25	6.08	-16%
BOS	6.91	6.03	-13%
Final Assembly	8.14	10.53	29%
Total	225.88	360.81	60%

The 2005 stack cost on an area basis is \$361/m², which is 60% higher than the 2004 stack cost. The following factors contributed to the changes shown in Table 37:

- Membrane: The TIAX bottom-up cost of 2 mil unsupported membranes in 2005 is \$23/m². In 2004, we assumed that the membrane was purchased at \$40/m², plus 8.85 \$/m² to condition the membrane for fuel cell use.
- Electrode: In 2005, Pt cost has increased from \$450/troz (2004) to \$900/troz. Pt loading has increased from 0.3 mg/cm² (2004) to 0.75 mg/cm² in 2005. The Pt process markup is 20%, which is the same as in 2004.
- GDL: GDL thickness decreased from 350 mm in 2004 to 260 mm in 2005 (\$8.50/m² on actual area).
- Bipolar plate: The process and material changed from molded graphite (2004) to thinner expanded graphite foil in 2005. Every plate is a cooling plate and is thinner, with less material.
- Seal/Gasket: The amount of material increased, but switched from fluoropolymer (\$30/lb) in 2004 to nitrile rubber (\$5/lb) in 2005

Table 38 illustrates the cost comparison on a net power base.

Table 38. Stack Cost Comparison 2004 vs. 2005 (\$/kW)

Component	2004 Cost1 (\$/kW2)	2005 Cost1 (\$/kW2)	% Change	2005 DOE Target (\$/kW)
Membrane	15.62	4.36	-72%	50
Electrode	21.48	52.08	142%	
GDL	10.23	3.43	-66%	
Bipolar Plate	8.98	N/A	N/A	6 (2010)
Bipolar Plate with Cooling	8.78	3.24	-63%	
Seal	2.32	1.13	-51%	
BOS	2.21	1.12	-49%	
Final Assembly	2.60	1.96	-24%	
Total	72.22	67.34	-7%	65

9.3. QC and Stack Burn-in

Stack conditioning and final quality checks, which could be significant cost contributors (e.g., 5% to 50% higher), were not included in this analysis at the recommendation of the Tech Team and DOE. Testing of the complete system with BOP would represent an additional cost.

For purposes of this analysis we assumed burn-in could take from 2 to 24 hours. Developers did not provide feedback on their burn-in parameters. However, they did confirm the importance of this step. We estimated that it would cost \$9.01/m² for 2 hours stack conditioning & QC and \$108.10/m² for 24 hours.

Table 39. Conditioning & QC Cost

	2 Hours Stack Conditioning & QC	24 Hours Stack Conditioning & QC
Number of Test Stations	521	6,250
Number of Stacks per Day	4,168	4,168
Total Equipment Cost	\$104M	\$1,250M
Cost (\$/m²)	9.01	108.10

Our cost estimates are based on the following assumptions:

- Capital cost for a test station is \$200,000
- Labor is 0.2 per station
- Yield is 100%
- Up-time is 80%
- Consumables, such as H₂ or credit for the power, are not included

Table 39 shows the capital costs and additional stack costs.

9.4. BOP

The fuel cell BOP components have been categorized into four management systems: air, water, thermal and fuel.

- The air management system includes air filtration and a compressor expander module (CEM) for air supply.
 - The water management system includes an enthalpy wheel humidifier for cathode air and a membrane humidifier for anode hydrogen.
 - The thermal management system includes high-temperature radiators and a high-temperature coolant pump.
 - The fuel management system includes a hydrogen recirculation blower and ejectors.
- BOP and ancillary components represent a significant weight/volume as well as cost contribution to the overall PEMFC system cost. As an example, Figure 53 shows a fuel cell system (16), in which the BOP appears to occupy as much as 60% of the total system volume.

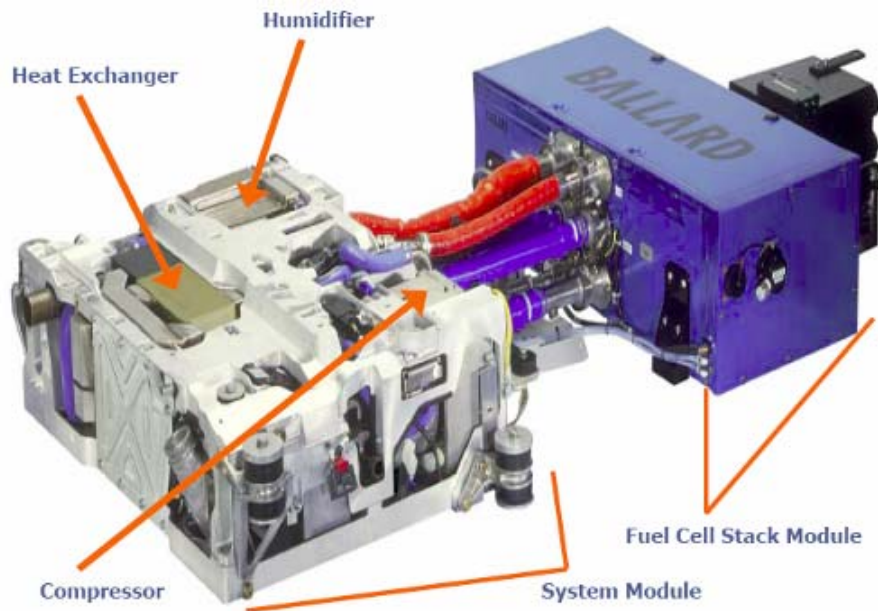


Figure 53. Fuel Cell Stack and BOP

We had discussions with several component suppliers to develop high-volume estimates of BOP component costs. In cases where these components are not produced at high volumes, we calibrated supplier cost projections by developing internal estimates based on analogies with automotive components.

9.4.1. Air Management

9.4.1.1. Air Filtration

As in IC engine vehicles, the PEMFC vehicle will require air filtration for removal of particulate matter, but will also require chemical filtration for removal of contaminants such as sulfur, salts, carbon monoxide, and hydrocarbons. We contacted Donaldson, Inc. for estimates of the air filtration systems required in PEMFC systems for transportation

applications. At high volumes of 500,000 per year, such air filtration systems are expected to represent a negligible cost, approximately \$3 per unit or less than \$0.1/kW. The filters would be an ongoing maintenance item similar to current IC engine air and oil filters.

9.4.1.2. Compressor-Expander

A CEM was chosen to supply pressurized air for the PEMFC cathode stream. The expander is included in order to recover energy from the pressurized cathode exhaust stream and thus reduce compressor motor parasitic power requirements. Honeywell, Inc. has been developing turbo-CEM equipment under contract to the DOE and serves as the basis of our cost, weight, and volume estimate. We have also benchmarked its estimate with our own, based on analogies to the automotive industry. Figure 54 (a) and Figure 54 (b) show a Honeywell CEM and motor controller (17).

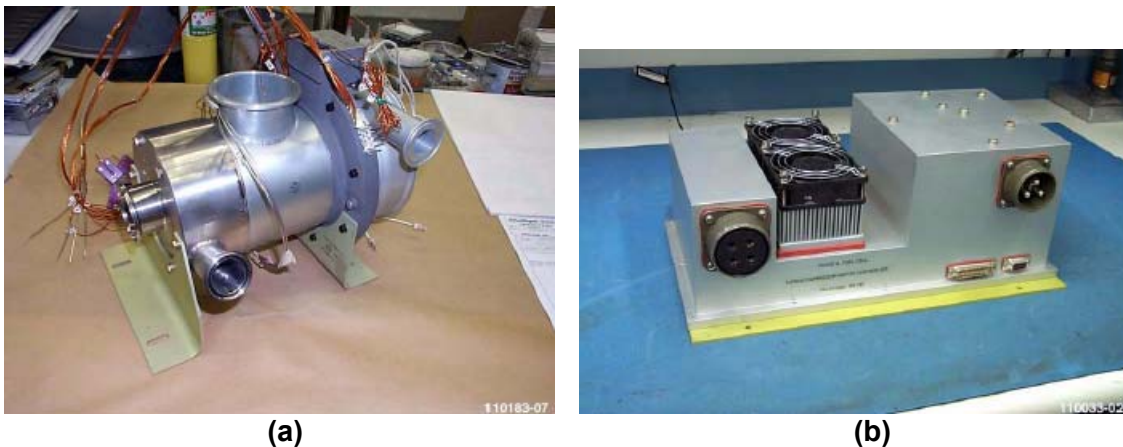


Figure 54. (a) Honeywell Fuel Cell Turbo-Compressor with Mixed-Flow Compressor and VNT® Variable Nozzle Turbine, (b) Honeywell Fuel Cell Turbo-Compressor Motor Controller

The CEM is a high-speed centrifugal machine, with a maximum speed of 110,000 rpm, and an idling speed of 36,000 rpm. It employs airfoil bearings, a mixed-flow axial compressor with 78% efficiency at rated flow, a radial inflow variable nozzle turbine with 82% maximum efficiency, and a liquid-cooled motor and motor controller with efficiency of 85%. The CEM is capable of a large turn-down ratio of 20:1. Table 40 lists some of the key parameters for the Honeywell CEM, as well as a comparison to estimates from ANL’s system model.

Table 40. Key Characteristics of Honeywell CEM

Parameter	Units	ANL1	Honeywell2
Air flow rate	g/s	98	90
Input power w/ expander	W	5.5	9.4
Input power w/o expander	W		15.7
Volume	L	16.3	15
Weight	kg	19	17.5

¹ Source: Dr. Rajesh Ahluwalia of ANL

² Source: Dr. Mark Gee of Honeywell, DOE 2005 Hydrogen Program Review

We assumed that ambient temperature is 40°C, stack temperature is 80°C, and compressor outlet pressure is 2.5 atm. Honeywell estimates the factory cost of the CEM to be \$700 for a volume of 100,000 units per year. This figure includes the turbomachinery, motor and motor controller, but does not include labor, testing, or capital expenditure. By Honeywell estimates, the cost breakout is approximately 90% for the turbomachinery, 5.5% for the motor, and 4.5% for the motor controller. We assumed that process cost represents approximately 30% or \$200 at high volumes. Finally, we included a markup of 20% to obtain an estimate of the OEM price of \$1080.

In contrast, our internal estimates, based on conventional automotive turbocharger technology, put the OEM cost of the turbomachinery at between \$200 and \$300 at large volumes. A 16 kW motor may cost between \$200 and \$250, and the motor controller another \$100 at large production volumes. This results in a total of approximately \$650, including material, process, labor, CapEx, and markup to OEM price. Table 41 compares these two cost estimates for the CEM.

Table 41. Comparison between Honeywell and TIAX Estimates for CEM Cost

Cost Contributor	Honeywell Cost	TIAX Calibrated OEM Price
Turbomachinery	\$630 (90% of \$700)	\$200-300
Motor (16 kW)	\$38 (5.5% of \$700)	~ \$200-250
Motor controller	\$32 (4.5% of \$700)	~\$100
Total material cost	\$700	
Process cost, CapEx, other	\$200 (assumed 30% process cost)	
OEM price	\$1080 (assumed 20% markup)	\$650

Another point of reference is a California Energy Commission (CEC) report (18) on the cost of hybrid-electric vehicles, which uses $\$(300+30 \times \text{kW})$ as a fit for its data on OEM motor and motor controller costs. Using a motor size of 16 kW, the CEC formula yields a motor and motor controller OEM cost of \$780. Again, using an automotive analogy for turbo-compressor OEM costs of ~\$300, we arrive at a total figure of \$1080, which is the same as our cost projections based on Honeywell technology. Therefore, we chose \$1080 as the baseline cost and used \$650 as a lower bound in a sensitivity analysis.

9.4.2. Water Management

The water management system consists of an enthalpy wheel for cathode air humidification and a membrane humidifier for anode H₂ humidification. An enthalpy wheel was chosen for cathode air humidification since it offers several advantages over a membrane humidifier, as listed below:

- Lower pressure drop and hence parasitic power usage
- Additional heat exchangers to cool the cathode air are not required
- Expander has better power recovery (lower pressure drop)

However, the enthalpy wheel humidifier was not considered for anode gas humidification since it would allow crossover of cathode exhaust gases into the hydrogen stream. We contacted Emprise for information on the enthalpy wheel technology and costs, and PermaPure for the membrane humidifier details.

9.4.2.1. Enthalpy Wheel Humidifier

The enthalpy wheel consists of a Cordierite (alumina) drum coated with a γ -alumina desiccant coating. Sensible and latent heat are exchanged between the two streams of air; warm, humid cathode exhaust air and cooler, drier inlet air. A face seal separates the exhaust and inlet air streams. Figure 55 shows a Humidicore™ enthalpy wheel humidifier from Emprise.

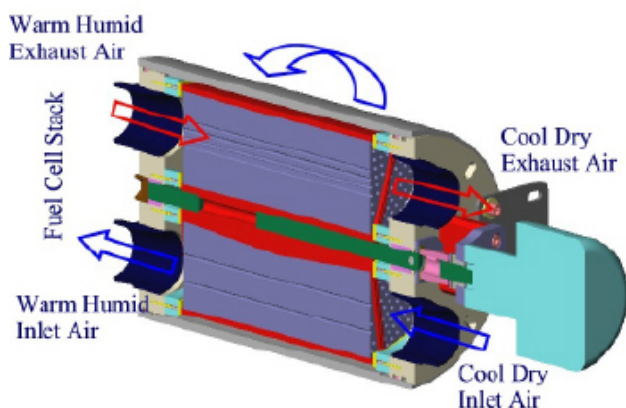


Figure 55. Humidicore Enthalpy Wheel Humidifier from Emprise

The Cordierite material is the same as that used in automotive catalytic converter monoliths and is manufactured by:

- Extrusion through a die to form the monolith
- Drying in a microwave oven
- Firing at 1200°C

A wash coat of γ -alumina is applied to the core and then fired at 1200°C. Next, it is polished or lapped to a very tight tolerance so that the face seal has a good contact surface. The polymer face seal is an injection-molded part and may be made of Delrin or glass-filled Teflon.

We used sizing data from ANL's system performance model to determine weight and volume of the enthalpy wheel and to size/cost the motor. Table 42 lists the major weight and volume parameters of the enthalpy wheel humidifier. The cartridge includes the core and packaging, but not the manifolds.

Table 42. Weight/Volume Parameters of Enthalpy Wheel Humidifier

	Units	0.65 V Case	Comments
Core	inch	7 x 7.2	Desiccant γ -alumina coated 400 cpi Cordierite monolith, 4 mil thick walls, Emprise updated core to 8"D x 6"L
Cartridge	inch	8.3 x 9.2	
Cartridge volume	L	8.0	
Cartridge weight	kg	6.8	
Motor power	W_e	110	Emprise updated motor to 25 W_e
Total volume	L	13.0	Includes 5 L motor
Total weight	kg	11.8	Includes 5 kg motor

Table 43 lists the key material costs and process costs of the Humidicore enthalpy wheel at low production volumes of 500 to 1000 per year. From discussions with Emprise, we estimate that the low-volume cost of \$750 for the enthalpy wheel humidifier could be reduced to \$260 at high volumes. At this time, the Humidicore enthalpy wheel production process is largely manual and therefore time consuming and labor intensive. Automation and use of injection molded parts could significantly lower the manufacturing cost of the humidifier.

Table 43. Materials, Processes, and Costs for Humidicore Enthalpy Wheel

Cost Contributor	Emprise Low-Volume Cost (\$)	Comment
Extruded cordierite core	40	8"D x 6"L, similar size core for automotive catalytic converter monolith ~\$10.
Plates and Seals	75	High volumes would imply a molded part with much lower cost.
Apply γ -alumina wash coat, fire @ 1200°C in oven	22	
Polishing/lapping to very tight tolerance	Not available	Manual polishing, 4 min
Face seal	6	Delrin, glass-filled Teflon, injection-molded
Manifolds	25	Injection-molded plastic, anodized Al
Motor	125	Merkle-Korff brushless DC, integrated gearbox, \$60 at high volumes

9.4.2.2. Membrane Humidifier

Figure 56 shows a typical membrane humidifier from PermaPure.

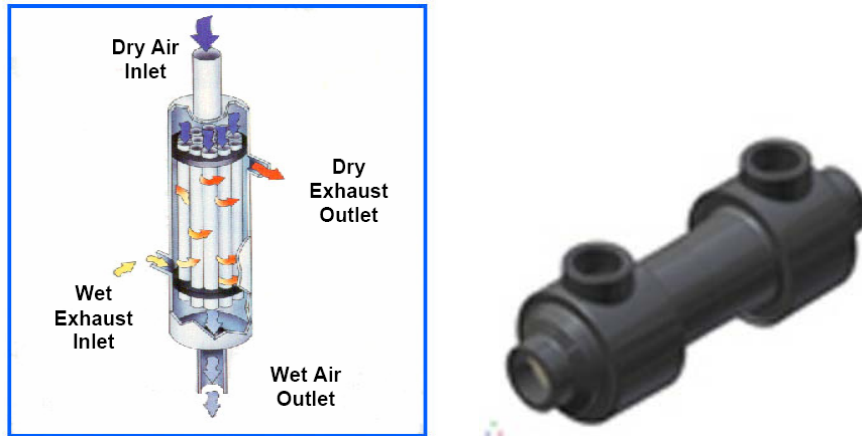


Figure 56. Membrane Humidifier from PermaPure

The humidifier consists of extruded Nafion tubes mounted in headers at each end. The headers are made of a two-part polyurethane resin. The unit is molded from glass-filled polyphenylsulfone (PPS).

We considered two PermaPure models of membrane humidifiers for the sizing and costing effort; the FC300 and the FC400 series. ANL sized a unit that is close to the FC200 series in terms of membrane area requirements. However, the unit is machined from polypropylene, which softens at temperatures above 80°C and at pressures above 12 psig. The FC300-1660-10HP would provide a 10°C approach dew point with an outlet dewpoint of 70°C for the humidified fuel stream if the cathode stream entered the humidifier saturated at 80°C. The FC400-2500-10HP provides a higher outlet dew point of 74°C for the humidified fuel stream.

We used the FC400-2500-10HP PermaPure humidifier as a basis for the cost estimation of this application. Table 44 summarizes the major weight and volume parameters for the membrane humidifier.

Table 44. Weight/Volume Parameters for Membrane Humidifier

	Units	0.65 V Case	Comments
No. of Nafion tubes		1045	ID = 1 mm, OD = 1.12 mm; used PermaPure FC400-2500-10HP unit for costing, which has 2500 tubes
Membrane area	m ²	0.65	
Core	inch	3 x 7	
Housing	inch	3.7 x 11.5	
Volume	L	2	
Weight	kg	3.0	

Source: Dr. Rajesh Ahluwalia of ANL

The membrane humidifier costs were estimated from discussions with PermaPure and calibrated with Nafion monomer cost estimates. We assumed that Nafion represents the major contribution to the material cost and that polyurethane resin and glass-filled PPS

(which make up the housing and headers) are minor contributors. Table 45 compares PermaPure and TIAX cost estimates for the FC300 and FC400 series humidifiers that were considered for this PEMFC system.

Table 45. Comparison of TIAX and PermaPure Cost Estimate for Membrane Humidifier

	Units	FC300-1660-10HP	FC400-2500-10HP
TIAX Estimate			
Average Eq. Wt. of Nafion		1015	1015
TT-040 tubing weight	g/ft	0.154	0.154
Number of Nafion tubes		1660	2500
Active length of tubing	inch	10	10
Trapped length of Nafion in headers	inch	3	3
Total length of Nafion tubing	inch	13	13
Total weight of Nafion	g	277	417
Assumed cost of Nafion	\$/lb	150	150
Material cost of Nafion tubes	\$	92	138
Assumed % process cost, other	%	50%	50%
Humidifier factory cost	\$	183	276
Assumed markup to OEM price	%	150%	150%
TIAX estimated OEM price	\$	275	414
PermaPure Price Estimate			
PermaPure estimated price	\$	350	370-400

We estimated that a membrane humidifier would cost between \$275 and \$415, while PermaPure estimates were between \$350 and \$400. Since the FC400 series humidifier is more likely to achieve the desired humidification level in the hydrogen stream, we chose the FC400-2500-10HP as the cost basis. Therefore, we assumed \$380 as the baseline cost of the membrane humidifier at production volumes of 500,000 units per year.

9.4.3. Thermal Management

We had detailed discussions with Modine, a major supplier of heat exchangers for conventional automotive and fuel cell applications. Figure 57 shows a PEMFC vehicle thermal management system consisting of three high-temperature (HT) radiators, an HT coolant pump, and a radiator fan. The main HT radiator is cooled by forced air through the radiator fan. The other two HT radiators are located in front of the wheels and are cooled by ram air. The HT main radiator looks like a conventional automotive radiator, but has enhanced heat transfer surfaces, while the HT wheelhouse radiators have a microchannel design. The HT radiators are used to cool the stack and the low-temperature (LT) radiator is used to cool the electric motor and power electronics. The LT radiator, LT coolant pump and air-conditioning condenser are not included in the scope of this costing effort.

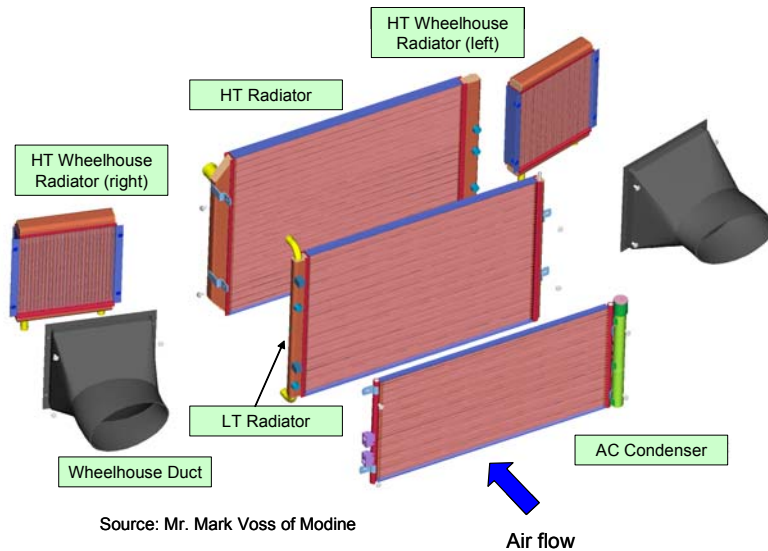


Figure 57. Typical Arrangement of Radiators in Fuel Cell Vehicle

We used a combination of ANL system performance specifications and industry input from Modine to size and cost the different components of the thermal management system. Table 46 lists some of the key characteristics of the thermal management system costed in this study.

Table 46. Key Characteristics of Thermal Management System

	Units	S2 (0.65 V)	Comments
Coolant Pump			
Flow rate	kg/s	5	$\Delta P = 13$ psi
Power	kW	1.4	34% combined pump and motor efficiency ANL estimate
Volume	L	7	
Weight	kg	7	
Radiator Fan			
Air flow rate	kg/s	3.8	55 mph @ 6.5% grade
Fan head	Pa	425	72% combined fan and motor efficiency; ANL estimate
Fan power	kWe	2.2	
Volume	L	1.5	ANL estimate
Weight	kg	2.5	ANL estimate
HT Radiators			
Heat duty	kW	80	Modine data
Surface area	m ²	0.51	Modine data
Volume	L	17	Modine data
Weight	kg	11	Modine data

Modine provided the technical information for sizing the heat exchangers at 25°C and 40°C ambient temperature, while we used the latter for specifying the radiators. The HT main radiator air inlet temperature shows the effect of the heat rejection from the LT

radiator and AC condenser. Table 47 lists these technical specifications. The coolant used is 40/60 ethylene glycol-water by volume.

Table 47. Technical Specifications of High-Temperature Radiators

General	Units		
Ambient temperature	°C	25	40
Ambient pressure	kPa	101.3	101.3
HT Main Radiator			
Air mass flow	kg/s	3.09	2.92
Air average inlet temperature	°C	34.8	48.0
Air pressure drop	Pa	335	322
Heat rejection	kW	78.9	54.6
Coolant mass flow	kg/s	2.81	2.80
Coolant pressure drop	kPa	26	25
Coolant inlet temperature	°C	80	80
HT Wheelhouse Radiators (combined)			
Air mass flow	kg/s	0.62	0.58
Air average inlet temperature	°C	25	40
Air pressure drop	Pa	372	354
Heat rejection	kW	36.7	26.3
Coolant mass flow	kg/s	0.19	0.20
Coolant pressure drop	kPa	25	25
Coolant inlet temperature	°C	80	80

By Modine estimates, the high-volume OEM cost of the high-temperature radiators plus the radiator fan would be $\$183 \pm 20\%$, when the radiator fan costs \$37. We have used \$220 as the baseline cost for the radiator and fan ($\$183 + 20\%$), and performed a sensitivity analysis with \$183 and \$260 as the bounds. Table 48 summarizes the cost, weight, and volume of the HT radiators.

Table 48. Cost of High-Temperature Radiators for 40°C Ambient Temperature

Parameter	HT Main Radiator	HT Wheelhouse Radiator	Total
Core length (mm)	692	267	
Core width (mm)	538	264	
Core depth (mm)	28	45	
Max weight (kg)	6.3	2.3	10.9
Volume (L)	10.4	6.3	23
Cost (\$)	62	42	146

9.4.4. Fuel Management

As shown in Figure 58, the fuel management system consists of a recirculating blower, venturi-ejector, fine pressure regulator, and purge valve. The hydrogen storage tank and its related cost, weight, and volume considerations are not included in the scope of this study.

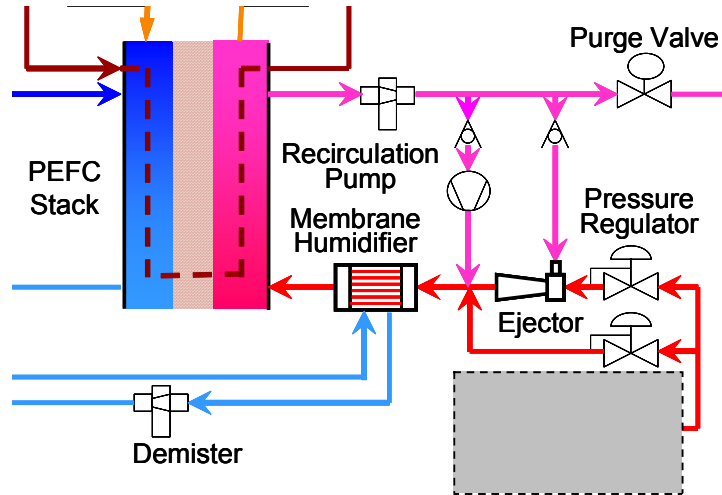
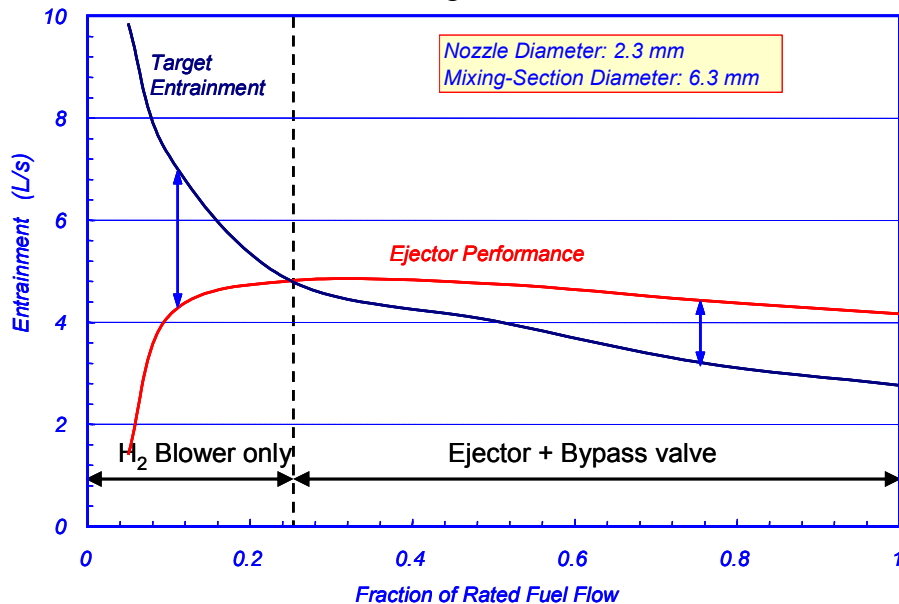


Figure 58. Fuel Management System

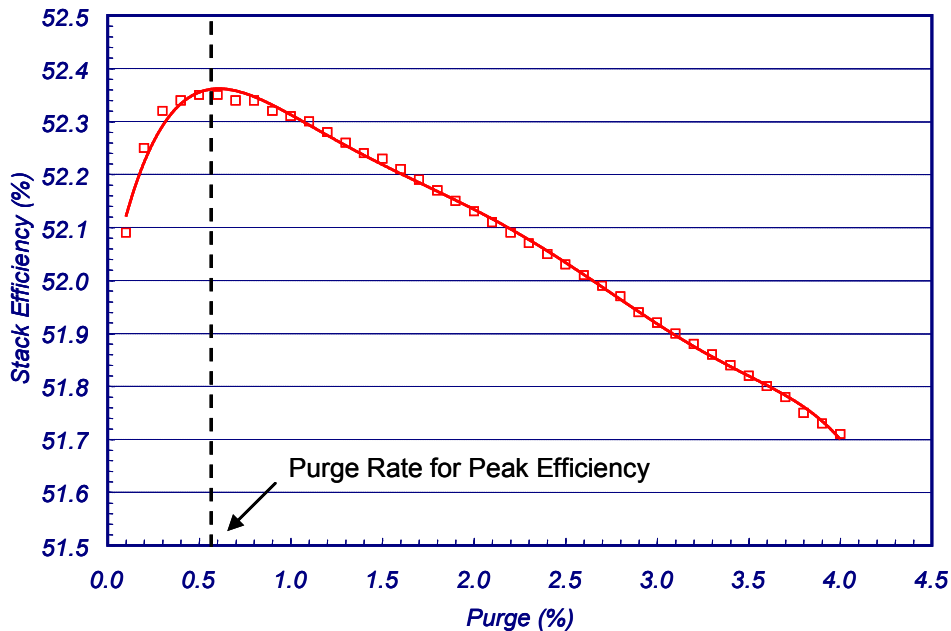
In this design, the ejector recirculates anode gases and entrains fresh H_2 for 25% to 100% of the rated flow, while the blower is utilized at flow rates below 25% of rated flow. Figure 59 is a plot of the entrainment versus fraction of rated flow. The ejector performance does not meet the target entrainment rate for flow rates below 25% of rated flow, and hence the blower is used in this region.



Source: Dr. Rajesh Ahluwalia of ANL

Figure 59. Zones of Operation of the Blower and Ejector

However, at flow rates greater than 25% of rated capacity, the ejector performance exceeds the target entrainment rate, and some H₂ must bypass the ejector. The purge valve continuously vents the built-up H₂, N₂, and H₂O stream to minimize the dilution effects of N₂ crossover. The purged H₂ is diluted by mixing with cathode exhaust air to percentages safe for discharge. From system efficiency modeling performed by ANL, the optimum purge rate is 0.6%. This assumes pure hydrogen feed and 70% hydrogen consumption per pass. At lower purge rates, the stack efficiency decreases because of lower cell voltage due to build-up of N₂, while at higher purge rates, the stack efficiency decreases because of lower effective H₂ utilization. Figure 60 shows this relationship between stack efficiency and purge rate for a cell voltage of 0.7 V.



Source: Dr. Rajesh Ahluwalia of ANL

Figure 60. Optimum Purge Rate for Cell Voltage of 0.7 V

The ejector design is based on the ejector-venturi principle and uses the pressure energy in the high-pressure hydrogen tank (regulated to a desired pressure below 5000 psi) as the motive force to recirculate anode gases, as well as deliver a fresh feed of hydrogen. The high-pressure hydrogen issuing through an expanding nozzle has its pressure energy converted to velocity energy. A vacuum is created, and the anode gases (H₂, N₂, H₂O) are entrained. The mixture of gases enters the venturi diffuser where its velocity energy is converted into pressure sufficient to discharge against a predetermined back-pressure. Figure 61 below depicts the operating principle of the ejector-venturi.

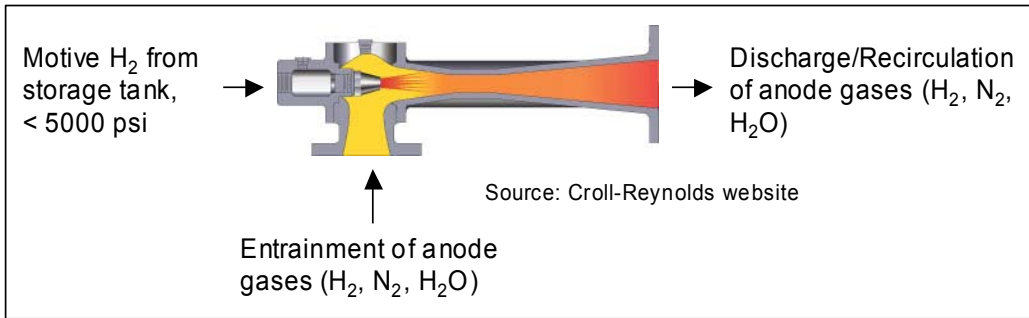


Figure 61. Ejector-Venturi Operating Principle

In some situations, more than one ejector with solenoid controls would be required to provide the necessary range of recirculation flows. Figure 62 (a) and Figure 62 (b) show some pictures of typical ejectors.

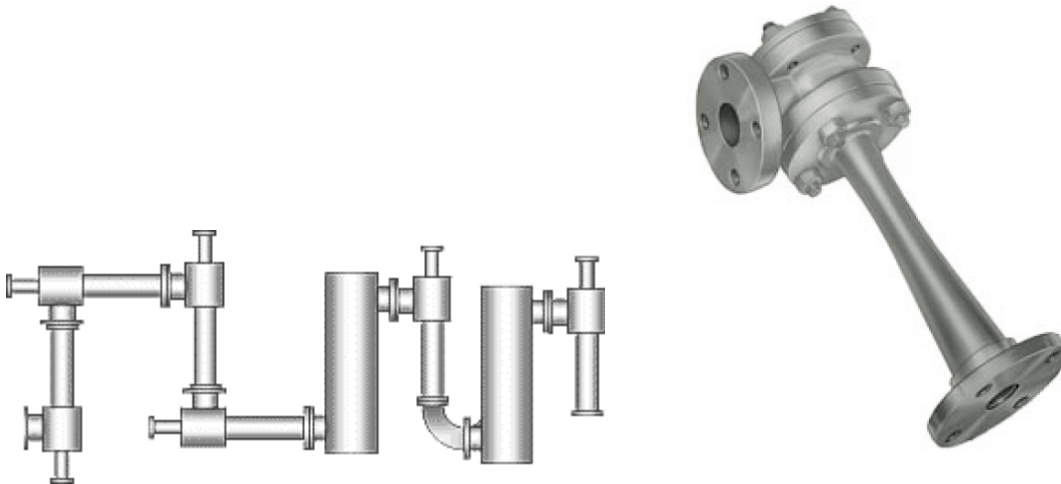


Figure 62. (a) Croll-Reynolds' Schematic of Multiple Ejectors in Series, (b) Ejector from Elmridge

We have assumed that two ejectors would satisfy the range of flows between 25% and 100% of rated flow. Discussions with Elmridge, a manufacturer of ejectors, indicate that current prices for such an ejector at low volumes would be approximately \$300 per ejector. However, significant savings would be achieved with automated production lines and appropriate tooling, and we believe the cost of the ejector component could be approximately \$20 at high-volume production. Table 49 lists key characteristics of the ejector.

Table 49. Characteristics of H₂ Ejector

	Units	Value	Comment
Volume	L	3.5	Includes air-cooled controller; (24 or 42 V)
Weight	kg	1.8	
Cost	\$	40	2 ejectors assumed

We found only one supplier for the hydrogen recirculation blower, H₂ Systems Inc., although others may exist. We used the drawing available on H₂ Systems' website as the basis to develop a high-volume cost estimate of such a blower. Figure 63 shows a schematic drawing of the HRB-L blower with dimensions in mm, while Table 50 lists key characteristics of the blower assembly.

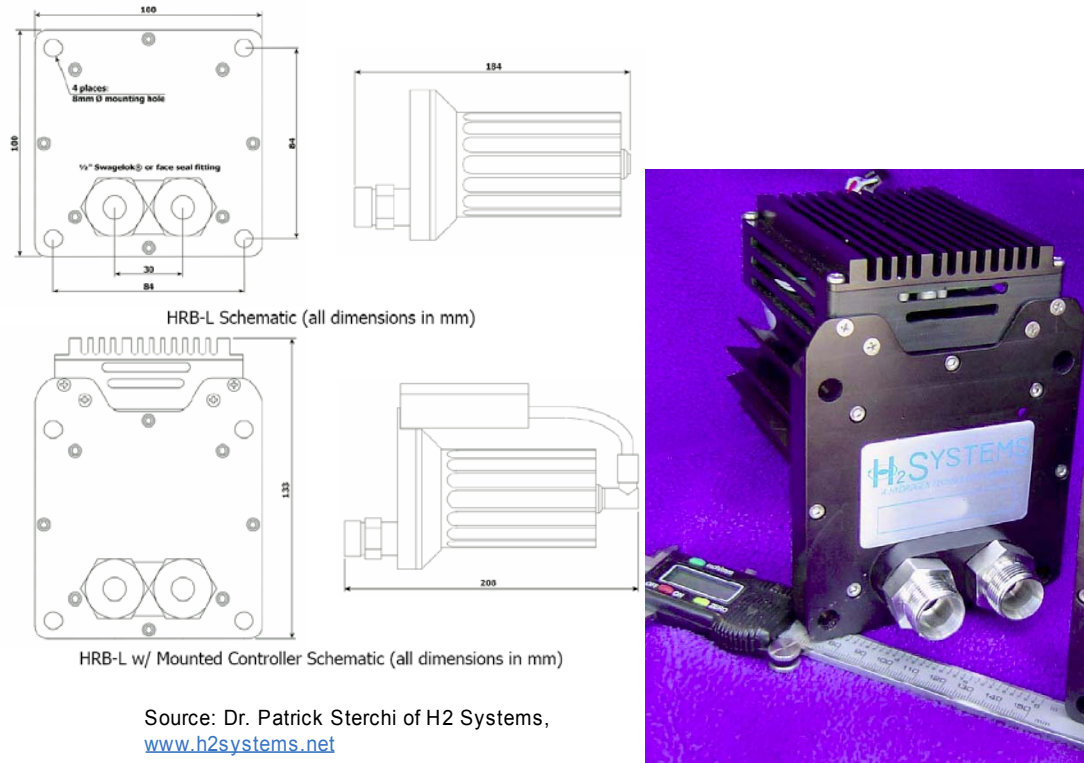


Figure 63. Hydrogen Recirculating Blower from H₂ Systems, Inc.

TIAX internal estimates project a blower cost of \$85 and motor and motor controller costs of \$200, with a heat sink cost of \$15 at high volumes. Therefore, the total cost of the unit would be approximately \$300 at high volumes. The motor is expensive due to the fact that it is a high-rpm motor. H₂ Systems provides a total weight estimate of 1.5 kg and a volume of 2.7 L for the blower.

Table 50. Characteristics of Recirculating Blower Assembly

	Cost (\$)	Comments
Blower assembly w/ seals	85	Thermoplastic impeller, 14% to 20% peak efficiency
Motor	150	4-5 A continuous current @ 24 V; 25,000-30,000 rpm, 87% to 89% efficiency; TIAX cost estimate \$50 to \$100
Motor controller	50	TIAX estimate \$30 to \$50
Heat sink	15	Motor heat rejection, air cooled, finned
Total	300	H₂ Systems' cost estimate \$500

9.5. System Cost

The overall cost of the PEM fuel cell system is \$108/kW, with the stack contributing 63% (\$67/kW) and the BOP and assembly contributing 37% (\$41/kW). Figure 64 shows the breakout between stack and BOP contribution to the 2005 PEMFC system cost.

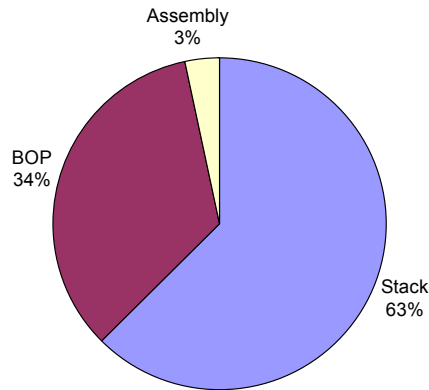


Figure 64. Stack and BOP Contributions to System Cost

Relative to past analyses, the BOP cost represents a larger percentage of the system cost. In 2004, TIAX analyses estimated the stack cost to be \$72/kW and the BOP cost to be \$25/kW, resulting in a system cost of \$97/kW. Table 51 is a comparison of 2005 system cost with 2004 system cost for an 80 kW net PEMFC system for transportation applications.

Table 51. Comparison Between 2004 and 2005 System Costs

Cost Contributor	2004 Cost (\$/kW)	2005 Cost (\$/kW)	2005 DOE Target (\$/kW)
80 kW _e Net Stack	72	67	65
BOP & Assembly	25	41	60
PEMFC System	97	108	125

The air management system is the largest share of the BOP cost, with the CEM and air filtration representing \$13.5/kW, or 13%, of the overall system cost. The water management systems comprised of the enthalpy wheel and membrane humidifier represent the next largest contributors to the BOP cost at \$8/kW, or 7%, of the overall system cost. The fuel management system and thermal management system each contribute \$4.3/kW, or 4%, of the overall system cost. Figure 65 shows a detailed breakout of the contributors to the system cost.

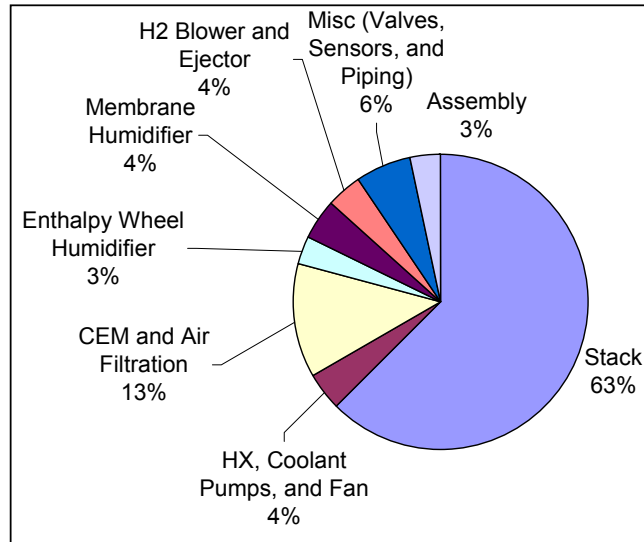


Figure 65. Detailed Breakout of System Cost

A multi-variable sensitivity analysis was performed on the overall system cost. Power density, platinum cost, platinum loading, Nafion cost, graphite cost, carbon cloth cost, nitrile rubber cost, CEM cost, hydrogen blower cost, and radiator cost were varied simultaneously to obtain a mean system cost. Table 52 shows the parameter values selected for the system cost sensitivity analysis.

Table 52. Parameter Values for the System Cost Sensitivity Analysis

Parameter	Units	Minimum	Baseline	Maximum
Power density	mW/cm ²	350	600	800
Pt cost	\$/troz	450	900	900
Pt loading	mg/cm ²	0.45	0.75	0.75
Nafion cost	\$/kg	44	176	220
Graphite cost	\$/lb	1	2	4
Carbon cloth cost	\$/kg	15	30	60
Nitrile rubber cost	\$/lb	3	5	8
CEM cost	\$/unit	700	1080	1200
H ₂ blower cost	\$/unit	200	300	500
Radiator cost	\$/unit	183	220	260

Figure 66 shows the relative impact of the different parameters on system cost. Consistent with the stack being the largest cost in the system, power density, platinum cost, and platinum loading are the top three drivers for the system cost. A group of seven parameters, including BOP component costs and stack material costs, are secondary drivers of system cost.

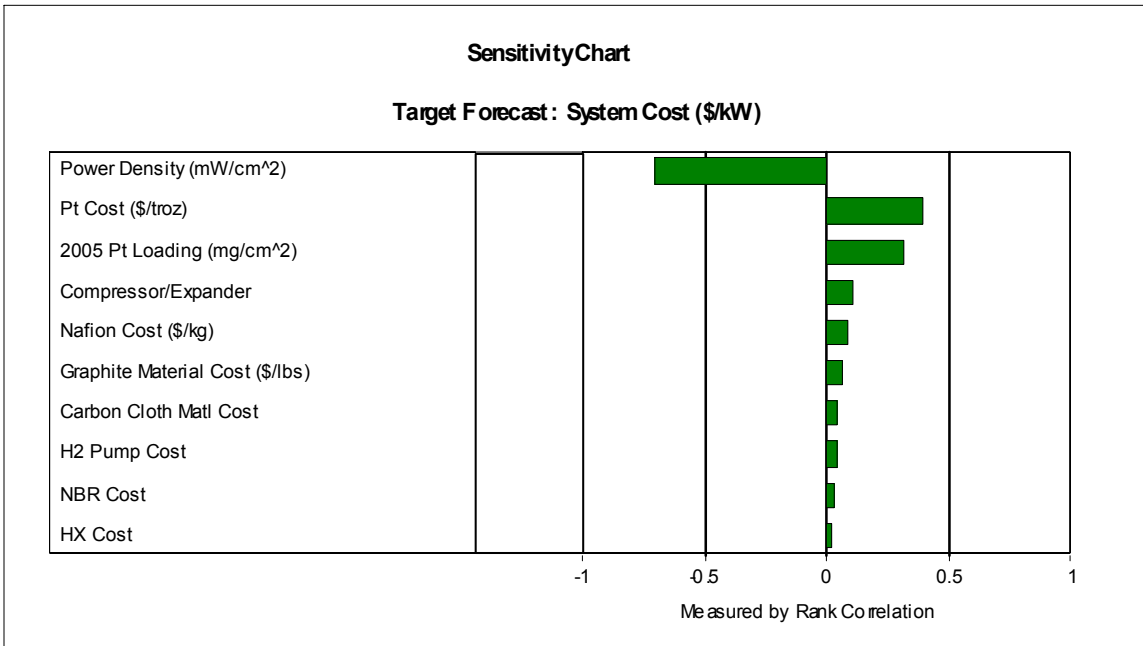


Figure 66. Parametric Studies on System Cost

Figure 67 shows the results of a Monte Carlo analysis for the same variation of input parameters with the mean system cost at \$97/kW and with a standard deviation of \$12/kW at a production volume of 500,000 units per year. For the chosen set of input parameters, there is a 98% probability that the mean system cost will be below the DOE target of \$125/kW.

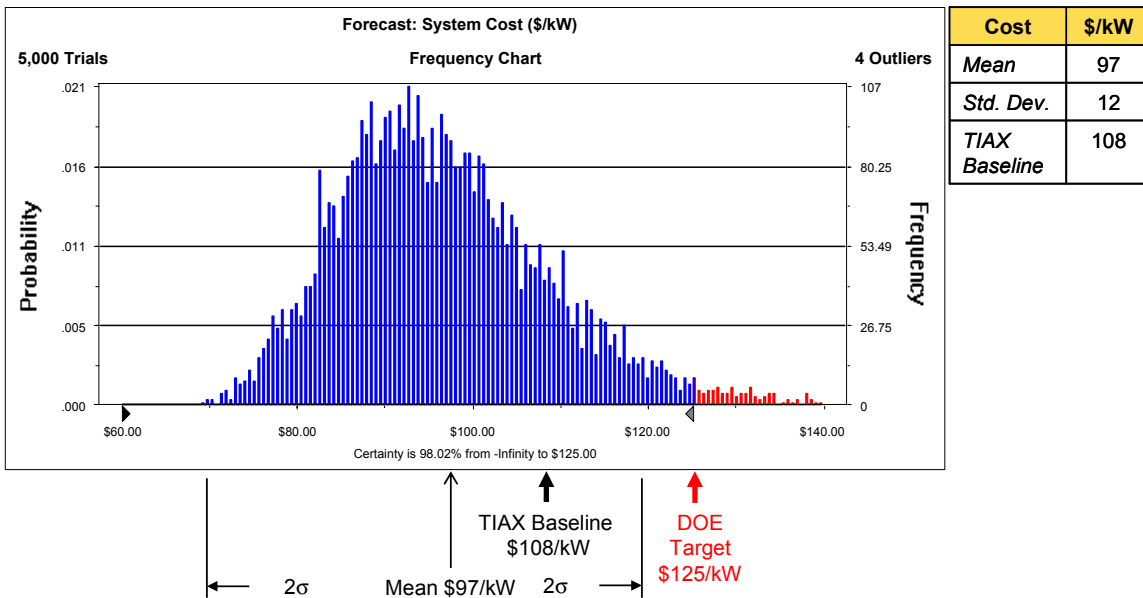


Figure 67. Monte Carlo Analysis on System Cost

9.6. Scenarios

9.6.1. Lower Platinum Price

We also costed a low platinum price scenario in which the platinum price is \$450/troz with a 40% catalyst process mark-up. The analysis shows that the stack cost is \$48/kW and the system cost is \$88/kW. Compared with the baseline costs, the stack cost is about 30% lower and the system cost is about 20% lower. The lower platinum cost only changes the electrode cost, which decreases by 40% from \$52/kW to \$32/kW. Table 53 compares the \$450/troz and \$900/troz platinum price scenarios.

Table 53. Low Platinum Price Scenario

	Platinum Price (\$/troz)	
	450	900
Stack Cost (\$/kW)	47.64	67.34
System Cost (\$/kW)	87.89	107.59
Stack % of System Cost	54%	63%
Electrode % of Stack Cost	68%	77%
Catalyst Mark-up Over LME Platinum Price (%)	40%	20%

9.6.2. Inclusion of Value Chain Costs

In the baseline analysis, we assumed that the stack manufacture is vertically integrated, and the BOP components are purchased from suppliers. Alternatively, an OEM could also assemble purchased subsystems and accept the higher cost associated with outsourcing. One of the scenarios we considered in the cost model was that the OEM would assemble the fuel cell stack using purchased MEAs and bipolar plates.

For the purpose of this analysis, we used margins of 30% on the various stack components. It should be noted that the BOP components are outsourced/purchased parts in the baseline analysis as well. If the OEM is assumed to be the stack integrator, the margin allocations may look as shown in Figure 68.

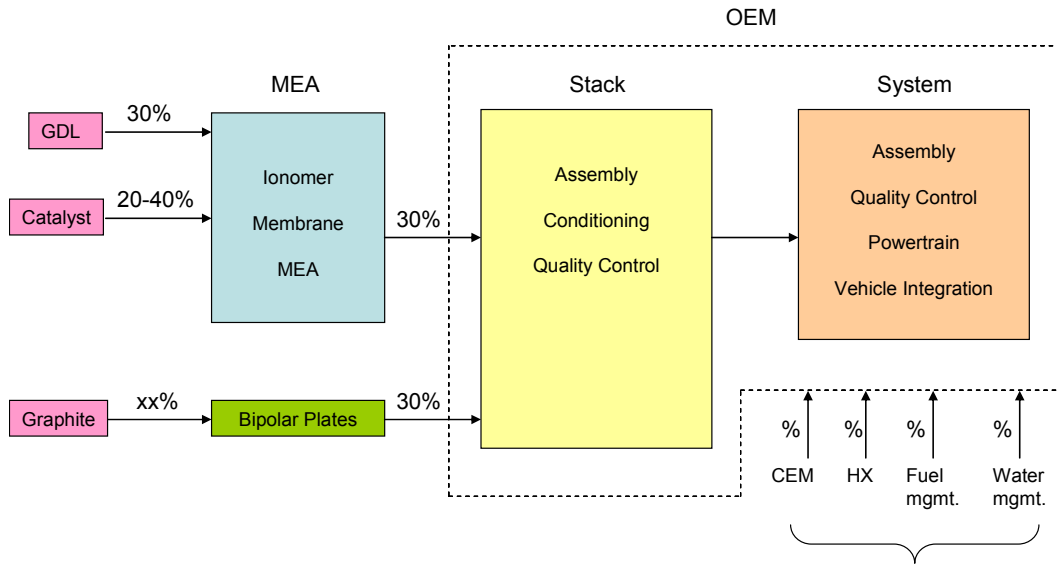


Figure 68. Illustrative Automotive PEMFC Supply Chain

A sample calculation is outlined in Table 54 below. If value chain costs are included, our analyses show a 31% increase in the stack cost, from \$67/kW to \$88/kW, and a 19% increase in the system cost from \$108/kW to \$129/kW.

Table 54. Value Chain Cost Calculation

Component	Vertically Integrated Stack		Supply Chain Scenario	
		Cost (\$/kW)	% margin	Cost (\$/kW)
Stack				
Membrane		4.36	-	4.36
Electrodes		52.08	-	52.08
GDL		3.43	30%	4.46
Seals		1.13	-	1.13
MEA sub-total		61	30%	81
Bipolar Plates		3.24	30%	4.21
Balance-of-Stack		1.12	-	1.12
Stack Assembly		1.96	-	1.96
Stack sub-total		67	-	88
System				
Balance-of-Plant		41	-	41
System total		108	-	129

9.7. Study Results Relative to DOE Targets

The 2005 PEM fuel cell system meets the DOE targets for cost and specific power, but falls short of the DOE efficiency targets by five percentage points. The latter results from the decision to use a cell design voltage of 0.65V rather than 0.7 V. Table 55 summarizes

the volume, weight, and cost of the various fuel cell subsystems and compares them to relevant DOE targets.

Table 55. Summary of 2005 PEMFC System Results

Subsystem	Volume (L)	Weight (kg)	Cost (\$/kW)	DOE 2005 Target
Stack	51	58	67	65 \$/kW
Stack power density (W_e/L)	1569			1500 W_e/L
Stack specific power (W_e/kg)	1379			1500 W_e/kg
Air management system (CEM, air filter)	15	17.5	13.5	
Fuel management system (blower, ejectors)	5.1	6.2	4.25	
Thermal management system (HT radiators, fan, coolant pump)	25.5	20.5	4.25	
Water management system (enthalpy wheel, membrane humidifier)	15	15	8	
Other components & Assembly	19	21	11	
BOP Subtotal	80	80	41	
Total	131	138	108	125 \$/kW
FC system power density (W_e/L)	610			500 W_e/L
FC system specific power (W_e/kg)	580			500 W_e/kg
FC system efficiency @ rated power	46%			50%
FC system efficiency @ 25% rated power	55%			60%

It should be noted that the volume estimates do not include a packing factor, which would lower the volumetric power density. If a packing factor is included, the 2005 system will not meet the DOE targets for fuel cell system power density.

At the stack level, the stack cost is slightly higher than the DOE target of \$65/kW. However, the stack meets the DOE target of 1500 W_e/kg for specific power and is close to the DOE target of 1500 W_e/L for stack power density. Decreased bipolar plate thickness and higher power density were the main drivers for increased stack power density.

The fuel cell system efficiency falls short of the DOE system efficiency target of 46% at rated power. This is primarily because of the choice of cell voltage of 0.65 V, which results in a stack efficiency of 51.7% at rated power. For a cell voltage of 0.7 V, the stack efficiency is 55.3% at rated power, and fuel cell system efficiency is 49.8% at rated power.

The baseline system contains 1.4 grams platinum per kilowatt. FreedomCAR and DOE roadmaps show values of 1.1 and 1.3 g Pt/kW respectively for the 2004 stack status similar to the baseline value from this study.

10. Conclusions and Recommendations

10.1. Key Drivers

The summary at the front of the report provides an overview of the key findings. Additional discussion on the key drivers (power density, platinum price, and platinum loading) and BOP follows.

The question of stack performance and platinum loading are key technical inputs into the cost projection and are also closely held data within the industry. We have provided the basis for our selection of parameters and tried to account for the impact of the uncertainty in these values on cost with the sensitivity analyses. Consideration of single cell current-voltage data, performance degradation of the MEA, de-rating of the single cell performance in the stack to avoid hot-spots, and life are factors in selecting operating points and platinum loading. Additional industry input is needed to strengthen the basis for selection of these parameters. The ongoing Hydrogen Infrastructure and Fuel Cell vehicle technology validation effort between industry and the DOE may provide data on performance, life, and grams platinum per kW across a range of demonstration vehicles representative of current technology, however, low cost is probably a secondary consideration in this project.

In this study, our primary focus was on technology advances such as power density, platinum loading, component design parameters (e.g., dimensions, sizing parameters), and material costs. Our projections for these parameters have been calibrated against industry estimates. However, of all the materials considered, the already high price of platinum (\$/kg) is very sensitive to the existing supply/demand relationship and econometric factors including political events and growth in emerging economies such as China and India. The current high price of platinum is largely driven by strong demand from emerging economies (both for vehicle emissions control and jewelry) and the difficulties with expanding mining output in South Africa. We have tried to address the issue of platinum pricing by assuming today's high cost for the baseline projection while using the historic price (\$450/troz) as the minimum in the sensitivity analysis. In comparing the 2005 projection with earlier values, the reader should separate the changes in performance metrics (i.e., power density and platinum loading) from the econometric factors (i.e., platinum price). Historical data suggest the latter will come down, however, this will be an ongoing concern.

10.2. Other Factors

We started the cost project in 1998/1999 using a vertically integrated production process to project the stack manufacturing cost. This provides a minimum cost projection, but may not represent the reality of a fuel cell powertrain manufacturing value chain. We have included a value chain scenario to illustrate the potential impact of including supplier margins on the stack cost. Of course the assumed margins will be highly dependent on the competitive intensity for that component, the state of the technology of each developer, premiums for performance, and component demand relative to production capacity. The impact of value chain margins on stack cost could be on the order of 20% to 50% depending on these factors.

Quality control technology, its implementation in production lines, and its reliability will have a significant impact on the yield of the stack process and product reliability. Fuel cells with their bipolar design, have many cells (hundreds) in series, consequently performance and reliability will be highly dependent on obtaining uniform material properties and eliminating point defects. Existing techniques (electrostatic, dielectric, and optical) may be used to monitor pinholes and thickness of the membrane, however, measuring the uniformity of electrochemical performance using methods that depend on many parameters including uniformity of catalyst loading and surface treatments, thickness of electrode layers, porosity, and pore size distribution of layers require development. At this time, these processes are proprietary and we have not included them in the stack cost.

The cost of burn-in was considered as part of quality control on the stack. The cost of burn-in will depend on the time and equipment required for this step. This is also a proprietary topic and we were not able to obtain direction on which parameters to use. Currently, burn-in processes are not well understood, and developers indicated that this should be an area of research because it will impact manufacturing cost and product reliability of stacks. Engine tests are currently used to reduce product warranty costs in cars.

Use of advanced hydrogen storage technologies will add hardware for thermal integration of the stack with the storage system. On a total system basis, this could lower cost, but it might make the stack subsystem more expensive.

10.3. Recommendations

As a result of our discussions with developers and our analysis the following areas may be the subject of future assessments:

- A more in-depth look at BOP components including humidification and fuel management might be needed. The level of product design, manufacturing methods, and number of developer options were found to be at a much earlier stage of development than the stack.

- What technology, material, design, and manufacturing advances are required in stack and BOP components to achieve the 2015 target of \$30/kW for the fuel cell subsystem? In a materials intensive technology, increases in performance (kW/kg) and reductions in material cost (\$/kg) are required to lower overall cost. Simultaneously, simplification of design will reduce components.
- We have only considered a high-production volume scenario (500,000 units per year), while the cost as production volume ramps up to achieve economies of scale will be important to the commercialization process. Assessment of cost at lower production volumes will be important to estimating the incentives needed to introduce early products.
- A more detailed look at the Quality Control requirements and technologies needed for high yields and reliable products would be important to the success of fuel cell powertrains.

11. Acknowledgements

We appreciated the support from NREL and the DOE in conducting this project. As in previous analyses, ANL's system modeling support and experience in specification of fuel cell systems has been valuable in developing our results.

Furthermore, the input and feedback from the FreedomCAR Fuel Cell Technical Team, stack component developers, stack developers, and BOP component developers has been very important to the development of input assumptions and designs that are representative of 2005 technology, while still protecting proprietary information.

The Principal Investigator's name appears on project reports and summaries, however, this report represents the efforts of a dedicated project team including Yong Yang (manufacturing cost model), Suresh Sriramulu (fuel cell technology), Jayanti Sinha (BOP), Peter Kopf (polymer processing), and Cathryn Firenze (administration and report preparation).

12. Appendix

12.1. \$450/troz Baseline Cost Scenario

The following figures provide cost breakdowns for the low-priced platinum scenario.

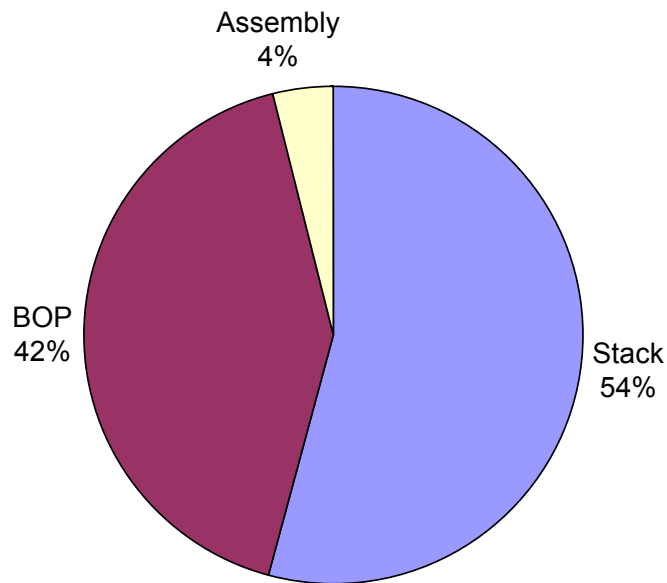


Figure 69. Breakdown of System Cost for an 80 kW Direct Hydrogen Fuel Cell System (88 \$/kW, \$450/troz platinum price) Produced at 500,000 Units per Year

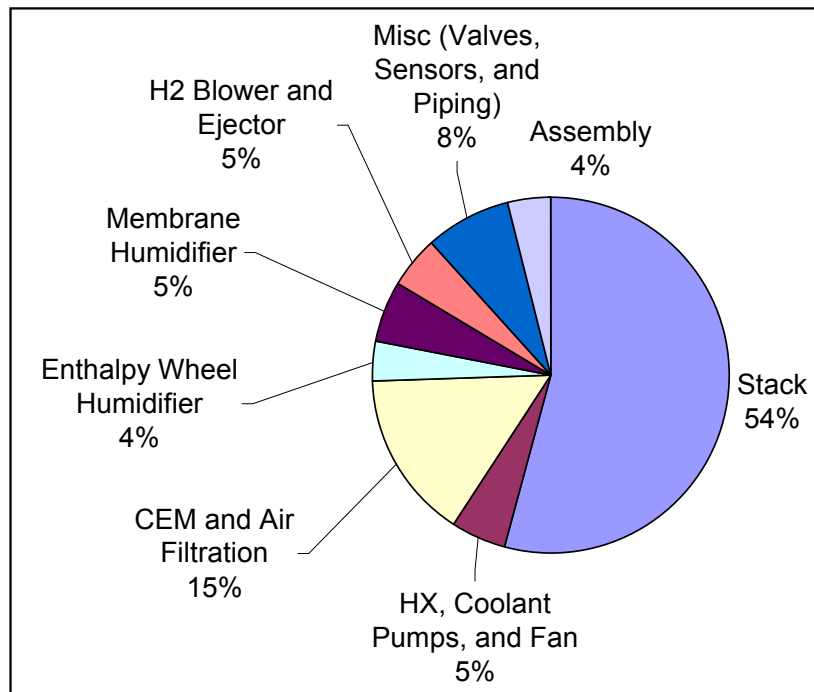


Figure 70. Breakdown in Stack and BOP Component Cost Contributions for an 80 kW Direct Hydrogen Fuel Cell System (\$88/kW, \$450/troz platinum price)

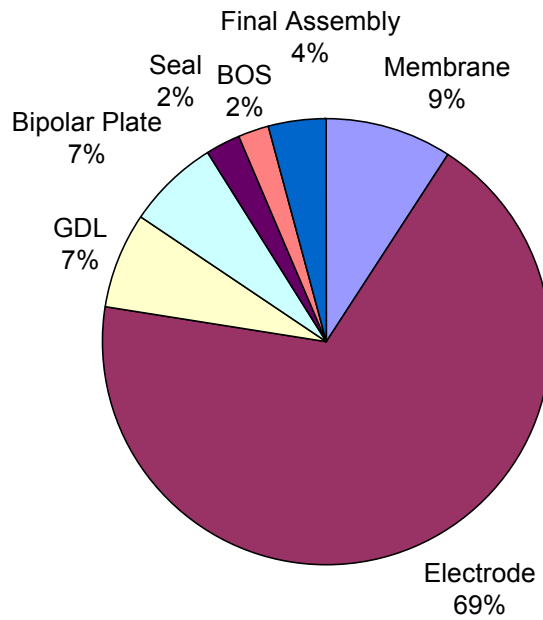


Figure 71. Cost Breakdown for 2005 80 kW Direct Hydrogen Stack (\$48/kW, \$450/troz platinum price)

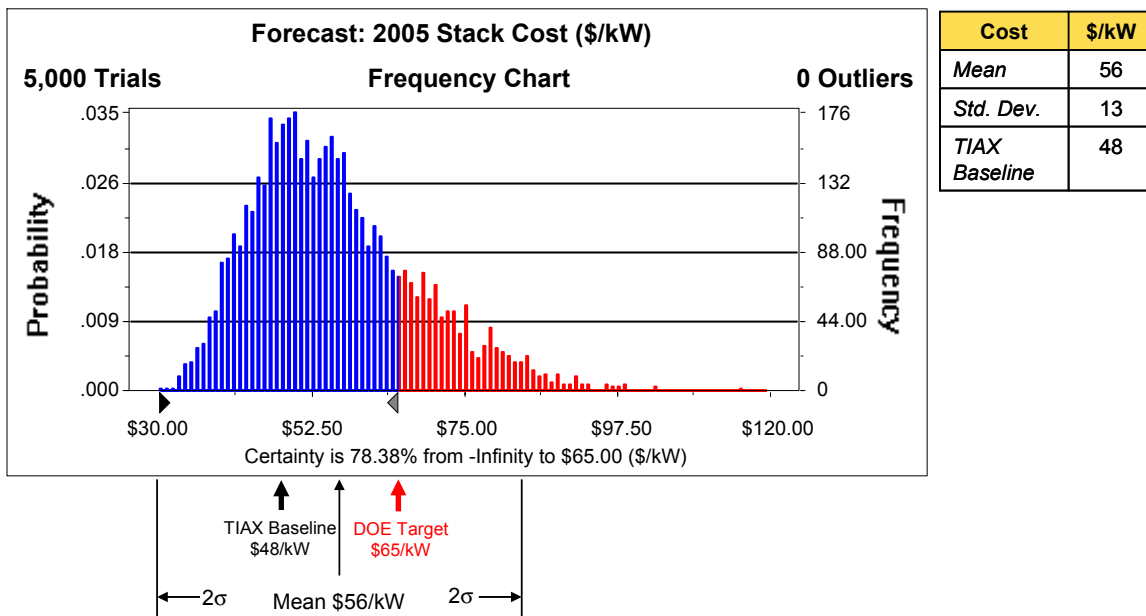
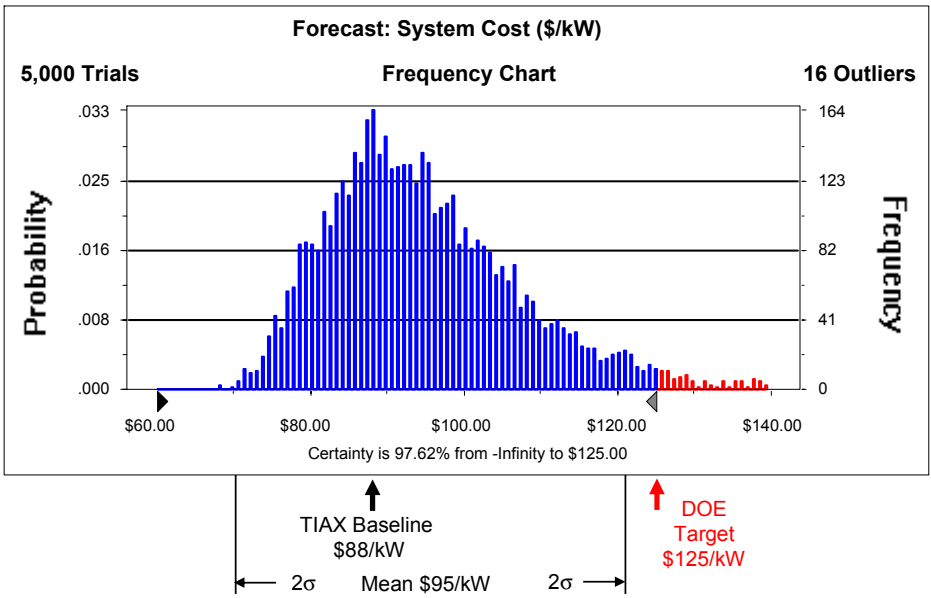


Figure 72. Range in Stack Cost due to Uncertainty in Input Parameters (\$450/troz platinum price)



Cost	\$/kW
Mean	95
Std. Dev.	13
TIAX Baseline	88

Figure 73. Range in System Cost due to Uncertainty in Input Parameters (\$450/troz platinum price)

13. References

1. Carlson, E., "Cost Analyses of Fuel Cell Stacks/Systems," for the Department of Energy, DOE Program Manager –Garland, N.; Prime Contract No. DE-FC02-99EE50587.
2. Carlson, E.; Thijssen, J.; Lasher, S.; Sriramulu, S.; Stevens, G.; Garland, N., "Cost Modeling of PEM Fuel Cell Systems for Automobiles", Future Car Congress, Paper 2002-01-1930, Society of Automotive Engineers (2002).
3. Ahluwalia, R.K. and Wang, X., "Direct Hydrogen Fuel Cell Systems for Hybrid Vehicles," Journal of Power Sources, in print now.
4. Ahluwalia, R.K.; Wang, X. and Rousseau, A., "Fuel Economy of Hybrid Fuel Cell Vehicles," 2004 Fuel Cell Seminar, San Antonio, TX, Nov. 2-5, 2004.
5. Curtin, D.E. and Watkins, M.A., "High Volume, Low Cost Manufacturing Process for Nafion® Membranes," 2002 Fuel Cell Seminar, Palm Springs (November 2002)
6. Ahluwalia, R.K.; Wang, X.; Doss, E.D.; and Kumar, R., "Fuel Cell Systems Analysis." 2005 USDOE Hydrogen, Fuel Cells & Infrastructure Technologies Program Review, Crystal City VA, May 2005.
7. Ahluwalia, R.K.; Wang, X.; Doss, E.D.; and Kumar, R., "Transportation Systems and Balance of Plant Components," DOE Hydrogen Program, FY 2004 Progress Report, pp. 511-515.
8. Mittelsteadt, C. and Umbrell, M. of Giner Electrochem, "Gas Permeability in Perfluorinated Sulfonic Acid Polymer Electrolyte Membranes," 207th ECS Meeting, Quebec City, CA, May 2005.
9. Cleghorn, S. of DuPont, "A Portfolio of Cost Effective MEA Products," Grove Seminar Presentation, London, September 2003.
10. <http://www.bcconverting.com/content/2prodline/coatingtapelbl.htm>
11. Gebert, M.; Hohlein, B. et al., "Benchmark Cost Analysis of Main PEFC-Ionomer Membrane Solutions." Trans. of the ASME, Journal of Fuel Cell Science and Technology, Vol. 1, pp. 56-60, Nov. 2004.
12. "Crystal Ball User's Manual," Version 4.0, Decisioneering, Inc., 1999.

13. Mathias, M.; Gasteiger, H., et al. of General Motors Corp., "Can Available Membranes and Catalysts Meet Automotive Polymer Electrolyte Fuel Cell Requirements?" Am. Chem. Soc. Preprints, Div. Fuel Chem., 49 (2), 471, 2004.
14. Carlson, E; Huang, Y.; and Noordzij, M., "Precious Metal Availability and Economic Analysis for PEMFC Vehicle Commercialization," 2003 Fuel Cell Seminar, Miami Beach (November 2003).

Carlson, E., "Precious Metal Availability and Cost Analysis for PEMFC," Commercialization Project for the Department of Energy, DOE Program Manager –Anderson, A., Prime Contract No. DE-FC04-01AL67601

Final report reference DOE web-site:
http://www.eere.energy.gov/hydrogenandfuelcells/pdfs/tiax_platinum.pdf
15. Carlson, E., "DOE Hydrogen Program FY2004 Progress Report, V.I.4 Cost Analyses of Fuel Cell Stacks/Systems, Discussion of Cost Assessment of Compressed Hydrogen Storage Tank Costs," DOE Program Manager – Garland, N., Prime Contract No. DE-FC02-99EE50587.
16. Gangi, J., "Fuel Cells in Transportation Applications," Fuel Cells 2000, Hydrogen Technology Forum, Washington DC, June 2004
17. Gee, M. of Honeywell, "Cost and Performance Enhancements for a PEM Fuel Cell System," DOE Hydrogen Program, FY 2004 Progress Report, pp. 531-533.
18. Energy & Environmental Analysis Inc., "Analysis and Forecast of the Performance and Cost of Conventional and Electric-Hybrid Vehicles," Prepared for the California Energy Commission (CEC), P600-02-13CR, March 2002.

REPORT DOCUMENTATION PAGE

Form Approved
OMB No. 0704-0188

The public reporting burden for this collection of information is estimated to average 1 hour per response, including the time for reviewing instructions, searching existing data sources, gathering and maintaining the data needed, and completing and reviewing the collection of information. Send comments regarding this burden estimate or any other aspect of this collection of information, including suggestions for reducing the burden, to Department of Defense, Executive Services and Communications Directorate (0704-0188). Respondents should be aware that notwithstanding any other provision of law, no person shall be subject to any penalty for failing to comply with a collection of information if it does not display a currently valid OMB control number.

PLEASE DO NOT RETURN YOUR FORM TO THE ABOVE ORGANIZATION.

1. REPORT DATE (DD-MM-YYYY) December 2005		2. REPORT TYPE Subcontract Report		3. DATES COVERED (From - To) through September 30, 2005	
4. TITLE AND SUBTITLE Cost Analysis of PEM Fuel Cell Systems for Transportation				5a. CONTRACT NUMBER DE-AC36-99-GO10337	
				5b. GRANT NUMBER	
				5c. PROGRAM ELEMENT NUMBER	
6. AUTHOR(S) E.J. Carlson, P. Kopf, J. Sinha, S. Sriramulu, and Y. Yang				5d. PROJECT NUMBER NREL/SR-560-39104	
				5e. TASK NUMBER HF55.8100	
				5f. WORK UNIT NUMBER	
7. PERFORMING ORGANIZATION NAME(S) AND ADDRESS(ES) TIAX LLC 15 Acorn Park Cambridge, Massachusetts 02140-2390				8. PERFORMING ORGANIZATION REPORT NUMBER KACX-5-44452-00	
9. SPONSORING/MONITORING AGENCY NAME(S) AND ADDRESS(ES) National Renewable Energy Laboratory 1617 Cole Blvd. Golden, CO 80401-3393				10. SPONSOR/MONITOR'S ACRONYM(S) NREL	
				11. SPONSORING/MONITORING AGENCY REPORT NUMBER NREL/SR-560-39104	
12. DISTRIBUTION AVAILABILITY STATEMENT National Technical Information Service U.S. Department of Commerce 5285 Port Royal Road Springfield, VA 22161					
13. SUPPLEMENTARY NOTES NREL Technical Monitor: Keith Wipke					
14. ABSTRACT (Maximum 200 Words) The results of sensitivity and Monte Carlo analyses on PEM fuel cell components and the overall system are presented including the most important cost factors and the effects of selected scenarios.					
15. SUBJECT TERMS PEMFC; fuel cell; cost analyses					
16. SECURITY CLASSIFICATION OF:			17. LIMITATION OF ABSTRACT UL	18. NUMBER OF PAGES	19a. NAME OF RESPONSIBLE PERSON
a. REPORT Unclassified	b. ABSTRACT Unclassified	c. THIS PAGE Unclassified			19b. TELEPHONE NUMBER (Include area code)

Standard Form 298 (Rev. 8/98)
Prescribed by ANSI Std. Z39.18